

UCSF

UC San Francisco Electronic Theses and Dissertations

Title

Role of cyclic nucleotide-gated channels in the transduction and adaptation of vertebrate rod and cone photoreceptor cells

Permalink

<https://escholarship.org/uc/item/1024b453>

Author

Hackos, David H.

Publication Date

1998

Peer reviewed|Thesis/dissertation

Role of Cyclic Nucleotide-Gated Channels in the Transduction
and Adaptation of Vertebrate Rod and Cone Photoreceptor Cells

by

David H Hackos

DISSERTATION

Submitted in partial satisfaction of the requirements for the degree of

DOCTOR OF PHILOSOPHY

in

Biophysics

in the

GRADUATE DIVISION

of the

UNIVERSITY OF CALIFORNIA

San Francisco



UCSF LIBRARY

Copyright 1998

by

David H Hackos

To my beloved Christine

UCSF LIBRARY

Acknowledgements

I dedicate this thesis and the rest of my life to my wife Christine, who's tragic death prevented her from seeing the completion of this dissertation. We fell in love with each other during our second year of graduate school, and passion was our bond. She was a very special person, and I felt extremely lucky that she had chosen me to spend her life with. She was everything to me, and I would have done anything in the world for her. We helped each other through all the difficult parts of graduate school, and celebrated our triumphs together. While our relationship lasted for almost 7 years, we were married for only a little over one year. In this time, we traveled the world together, contemplated life together, and loved each other to the fullest extent possible. Her absence from my life cuts deeply into me like a savage knife, leaving me wounded and bleeding – in unimaginable pain. My only hope is that I can someday find some sort of fulfillment in life again with the knowledge that it will never be the same again.

I would like to thank my advisor, Juan Korenbrot. After a depressing failed attempt to solve the crystal structure of the $\beta\gamma$ subunit of transducin, I knew I needed to find a lab that would develop my love and passion for science if I were to succeed as a scientist. I chose well. Juan is everything a great mentor should be: he is passionate about the research, he spends quality time with each person in the lab, he is an excellent writer and presenter, and he has an uncanny ability to make even impossible experiments work. My relationship with Juan is a very special one. We have a bond that goes deeper than the ordinary advisor-student relationship. He has been there for me almost like a father – supporting me at an emotional as well as scientific level. I am especially grateful that he was there for me in Washington DC when Christine was killed – I don't know how I would have survived without him. While I am ready now to leave his lab and start a new page of my life, I will miss Juan greatly.

I would also like to mention a number of faculty members who have helped me through the graduate school experience and with whom I have made special friendships.

UCSF LIBRARY

Bruce Alberts and Marc Tessier-Lavigne, Christine's mentors at UCSF, were there for me in Washington DC when I needed them, and have worked very hard to comfort me during these very difficult times – for which I am forever grateful. Robert Fletterick, my previous mentor, has been extremely helpful to me throughout graduate school as a PI, as the chair of my orals committee, and as a friend. I owe incredible gratitude to Julie Schnapf and Roger Cooke, the members of my thesis committee, for helping me put together this thesis. Julie especially has become a real friend in recent times – she is someone I have incredible respect for as a person and a scientist and someone with whom I always have such great discussions. I would like to thank Martin Shettlar, who is one of my favorite members of the UCSF faculty simply because I have so very much enjoyed all of our interactions together. Also I thank Ira Herskowitz, who many years ago inspired me to enter the world of functional, as opposed to structural, biology with his excellent Genetics course. In addition, he and his lab have helped me tremendously in my recent work with yeast and have been there for me after Christine's death. Finally, I would like to thank Kenton Swartz, who will soon be my mentor as I become a postdoctoral researcher at the NIH. I am always surprised at the generosity and friendship he has shown toward me, especially during these very difficult times, and before I have become a member of his lab.

I would like to thank the students and postdocs of Juan's lab that have helped make my stay so enjoyable. All of these people have been there for me and have truly cared for me during my recent crisis after Christine's loss. David Julian, who always had something pleasant to say, was fun having around since we shared an interest in building and designing various gadgets. Arturo Picones, who taught me the delicate art of patching the cone outer segment membrane, always had some great stories to tell about his days as a scientist in Mexico. Tania Rebrik, the feminine side of the lab, fascinated us by telling us all about Russia and Russian culture. And Andrew Olson, who loves to talk endlessly about his daughter, and more recently his newborn son, and has really become a

UCSF LIBRARY

great friend. These people generate the truly enjoyable atmosphere of the lab, which I will surely miss.

While working at UCSF, I have made numerous friends among my fellow students, each of which has made my life here so much more enjoyable. There are so many, in fact, that I don't have room to mention them all here, but I would like to give special thanks to a few. I originally met Richard Wagner at Yale when we were visiting graduate schools. We later became very good friends and roommates. He has always struck me as someone who thinks very deeply about the world – I have enjoyed his company greatly. I met Nira Pollock through Christine and Mike, and over the years we have become very close friends. I have enjoyed every second of time I have had the opportunity to spend with Nira, and I hope we will be able to keep up a great friendship despite being on opposite sides of the country. Peter Follette and I had a special friendship during the first few years of graduate school, when we would hang out together, sometimes at Colma to see a movie, sometimes sailing together in the bay. Women got in the way of our friendship, but it eventually was revived and will hopefully continue for a long time in the future. And I would also like to thank the countless other friends that have made my graduate school experience so much fun.

My parents deserve extra special thanks. They have truly supported me through graduate school and through Christine's death. Certainly, without their dedication in making sure I had every opportunity in the world, I wouldn't be here today. I hope I will be able to do as well with my own children someday.

Finally, I would like to thank the Howard Hughes Medical Institute for funding me for five years as a predoctoral fellow, and the ARCS Foundation for funding my final year. Chapter II has been previously published in the *Journal of General Physiology* and is reproduced with permission (see page viii) from The Rockefeller University Press.

A Poem

So suddenly you are gone
It seems like just yesterday
That I was visiting you in DC
Walking in the park
Sitting in the café.

I remember telling the Suppershuttle driver
“Wait, stop! – I’ve forgotten something”
Only to give you one last hug
One last kiss
Not knowing the truth.

Now I have your clothing
Your beautiful wedding dress
The dozens of shoes that were never enough
The socks that I used to take off
So I could tickle your feet.
I have your jewelry
Your furniture
Your plants that are growing brown under my care
I have nothing.

Now I am an old man
An empty shell
A painful image of the past
Living life to live life
Nothing more.

The Rockefeller
University Press

1114 First Avenue, 4th Floor
New York, New York 10021
(212) 327-7938
Fax (212) 327-8587

11 August 1998

Dr. David H. Hackos
Department of Physiology
University of California-San Francisco
San Francisco, CA.

Dear Dr. Hackos:

We shall be glad to grant you permission for the reproduction of the material referred to in your letter of 31 July 1998.*

Our only requirements are that you also obtain permission from the author(s) and give suitable acknowledgment to the source in the following manner: Reproduced from **The Journal of General Physiology** by copyright permission of The Rockefeller University Press.

Sincerely yours,

THE JOURNAL OF
GENERAL PHYSIOLOGY



Iris Vallecilla
Permissions Coordinator

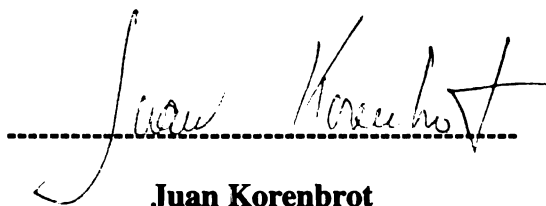
*JGP-vol:110,515,28,1997 - article for thesis.

UCSF LIBRARY

Role of Cyclic Nucleotide-Gated Channels in the Transduction and Adaptation of Vertebrate Rod and Cone Photoreceptor Cells

by

David H Hackos

A handwritten signature in black ink, reading "Juan Korenbrot", is written over a horizontal dashed line. The signature is fluid and cursive.

Juan Korenbrot

Chair, Thesis Committee

Abstract

In both rod and cone photoreceptor cells, absorption of a photon by the visual pigment rhodopsin leads to activation of a phosphodiesterase and the consequent closure of cGMP-activated ion channels in the outer segment membrane. Since the channel is the sole entrance pathway of Ca^{++} into the outer segment, channel closure causes a decline in the intracellular free Ca^{++} concentration, which in turn alters the gain and sensitivity of the photoresponse, leading to adaptation. In this thesis work, I have sought to characterize the properties of the rod and cone photoreceptor cGMP-gated channels to determine what role they play in adaptation and in defining the physiological differences between rods and cones.

I have found that the cone channel, like to rod channel, is modulated by Ca^{++} in the presence of a calmodulin-like factor. However, unlike the rod channel, the cone

channel is sensitive to physiological Ca^{++} concentrations. This indicates that Ca^{++} modulation of the channel is much more important for adaptation in cones than in rods.

I have found that the Ca^{++} permeability of photoreceptor cGMP-gated channels is a function of the cGMP concentration. Thus, in these channels selectivity is linked with the gating machinery, indicative of gating-dependent structural changes within the pore. Taking this observation into account, I have found that in the presence of physiological cGMP concentrations, cone channels are nearly 10-fold more permeable to Ca^{++} than rod channels, significantly greater than previously measured at much higher nonphysiological concentrations of cGMP.

While differences in Ca^{++} permeability between rod and cone channels suggest a role the channel might play in defining rod-cone differences, the critical quantity that must be measured is the actual fractional Ca^{++} current through the channels. Using a fluorescence technique, I have made the first direct measurements of fractional Ca^{++} current through the rod and cone channels. I find that in rods, only about 25% of the current is carried by Ca^{++} , whereas the cone channel is essentially a Ca^{++} channel. These channel differences should give rise to differences in adaptation features, and possibly some of the differences between rods and cones.

UCSF LIBRARY

Table of Contents

Chapter I: Introduction.....	1
The dark adapted state.....	2
The activation cascade.....	4
The feedback pathway and adaptation.....	7
Rod-cone differences.....	10
Cyclic nucleotide gated channels.....	11
References.....	18
Chapter II: Calcium modulation of ligand affinity in the cGMP-gated ion channels of cone photoreceptors.....	25
Abstract.....	26
Introduction.....	27
Materials and Methods.....	30
Results.....	35
Discussion.....	52
Reference List.....	60
Chapter III: Divalent cation permeability is a function of gating in native and recombinant photoreceptor cyclic nucleotide gating channels....	65
Abstract.....	66
Introduction.....	68
Materials and Methods.....	71
Results.....	77
Discussion.....	100
Reference List.....	109
Chapter IV: Direct measurement of fractional calcium current through rod and cone photoreceptor cGMP-gated channels.....	113
Abstract.....	114
Introduction.....	115
Materials and Methods.....	118
Results.....	123
Discussion.....	135
Reference List.....	140
Chapter V: Summary and conclusions.....	145
References.....	149

List of Figures

Chapter II

Figure 1. Modulation of cGMP-dependent currents in detached membrane patches.....	36
Figure 2. Modulation of 8-Br-cGMP-dependent currents in membrane patches detached from cone outer segments.....	39
Figure 3. I-V curves measured in the same membrane patch detached from cone outer segments before and after exposure to the EDTA/EGTA solution.....	41
Figure 4. I-V curves measured in the same membrane patch detached from a cone outer segment before and after exposure to the EDTA/EGTA solution.....	43
Figure 5. Ca ⁺⁺ -dependence of current amplitude in the presence of the endogenous modulator in a cone outer segment patch.....	45
Figure 6. Effect of calmodulin on modulation of cGMP-dependent currents in detached membrane patches.....	47
Figure 7. Competition between calmodulin and the endogenous modulator in a cone outer segment membrane patch.....	49
Figure 8. Ca ⁺⁺ -dependence of the effect of calmodulin on rod and cone membrane patches.....	51
Figure 9. The effect of Ca ⁺⁺ modulation of ligand affinity on current amplitude as a function of cGMP concentration.....	55

Chapter III

Figure 1. Effect of 10mM Ca ⁺⁺ on the I-V curve recorded from the retinal rod channel.....	78
Figure 2. Method for rapidly obtaining large numbers of I-V curves at different cGMP concentrations.....	79
Figure 3. Relative Ca ⁺⁺ -permeability as a function of cGMP concentration.....	81
Figure 4. Reversal potential as a function of cGMP in symmetric 150mM NaCl conditions.....	83
Figure 5. Relative permeability for Sr ⁺⁺ as a function of cGMP concentration.....	85
Figure 6. Selectivities of Cs ⁺ and NH ₄ ⁺ relative to Na ⁺ as a function of cGMP concentration.....	87
Figure 7. Selectivities for methyammonium and dimethyammonium relative to Na ⁺ as a function of cGMP concentration.....	88
Figure 8. Calcium block as a function of cGMP concentration.....	90
Figure 9. Permeability for Ca ⁺⁺ relative to Na ⁺ as a function of cGMP concentration in cone channels.....	92
Figure 10. Relative permeability for Cs ⁺ and NH ₄ ⁺ with respect to Na ⁺ as a function of cGMP concentration in cone channels.....	94

Figure 11. Calcium block of recombinantly expressed rod α and $\alpha\beta$ channels.....	95
Figure 12. Relative Ca^{++} permeability as a function of cGMP in expressed rod α and $\alpha\beta$ channels.....	97
Figure 13. Relative permeability for Cs^+ and NH_4^+ with respect to Na^+ as a function of cGMP concentration in recombinant α and $\alpha\beta$ channels.....	98
Figure 14. Intermediate state model.....	104

Chapter IV

Figure 1. Schematic illustration of single cell microfluorimeter.....	120
Figure 2. Measurement of Ca^{++} flux (f) through rod cGMP-gated channels.....	124
Figure 3. Calibration of the Ca^{++} flux measurement in rods.....	127
Figure 4. Dependence of Pf on flash intensity (cGMP concentration).....	129
Figure 5. Measurement of Ca^{++} flux (f) through cone cGMP-gated channels.....	131
Figure 6. Calibration of the Ca^{++} flux measurements in cones.....	132
Figure 7. Dependence of Pf on flash intensity in cone photoreceptors.....	134
Figure 8. Average fractional calcium currents (Pf) through the cGMP-gated channel measured in either rod or cone photoreceptor cells at different flash intensities.....	138

Chapter I
Introduction

UCSF LIBRARY

The vertebrate retina has the remarkable property of being able to accurately detect contrast differences in a visual image despite ranges of background light intensity of over 12 orders of magnitude. This is due partially to the adaptation process within the photoreceptor cells and partially to the presence of two types of photoreceptor cells in the retina; rods, which specialize at low intensity light detection, and cones, that can work under conditions of bright background light. While the light detection process in rods is well understood, adaptation is still poorly understood in both rods and cones and is currently an area of intense research. The goal of the research described in this thesis is to better understand the process of adaptation at the molecular level and to understand, at least in part, the molecular differences between rods and cones that give rise to differences in their adaptation abilities.

The process of phototransduction in vertebrates can be divided into two separate enzymatic pathways, the activation cascade and the feedback pathway. The cGMP-gated ion channel present in the outer segment membrane plays a central role in phototransduction by linking these two pathways together as well as by generating the electrical signal in response to light. This central role makes the channel an ideal target for the process of adaptation as well as in defining rod-cone differences. However, before introducing the cGMP-gated channel, it is first important to understand the environment in which the channel is situated, both in the dark adapted state and during the response to light.

The dark adapted state

Before a photoreceptor is presented with a light stimulus, about 1-5% of the cGMP-gated ion channels in the outer segment membrane are open (Cobbs et al., 1985). This gives rise to a membrane current referred to as the dark current, which in rods is about 50-100pA and in cones is about 30-60pA. To maintain this current, a small amount of cGMP must be present in the dark. This particular concentration of cGMP is held

UCSF LIBRARY

constant by the opposing activities of two enzymes, guanylyl cyclase, which synthesizes cGMP, and cGMP phosphodiesterase (PDE), which hydrolyses it. The rate of PDE in the dark is dependent only on the cGMP concentration, and since $[cGMP] \ll K_m$ (for the PDE) under these conditions, the rate of PDE increases essentially linearly with $[cGMP]$. In contrast, the cyclase activity is controlled by the calcium concentration (see feedback pathway), and therefore calcium sets the balance between these two enzymes and determines the value of the cGMP concentration.

The intracellular calcium concentration is in turn maintained by the balance between calcium influx through cGMP-gated channels and calcium efflux through the Na-Ca,K exchange pump (also in the outer segment membrane). The exchange pump has a rate that is essentially linear with calcium concentration. Therefore, the channel controls the balance of these two processes, and therefore controls the calcium concentration. Thus, the concentration of cGMP in the dark (and therefore the dark current) is controlled by a feedback process, where the number of open channels controls the calcium concentration, which in turn controls (by controlling cyclase activity) the number of open channels.

Therefore, there is a defined relationship between the cGMP and calcium concentration. In general, if $[cGMP]$ decreases, so will $[Ca^{++}]$, and vice versa. However, changes in $[cGMP]$ will not instantaneously affect $[Ca^{++}]$. This delay is caused in part by the finite rates of calcium influx and efflux, but also by the presence of cytoplasmic calcium buffers. The calcium buffer is likely made up of several different components, each with different kinetic properties, as seen by the multiexponential decay of free calcium concentration following a rapid decline in $[cGMP]$. It is believed that in the dark adapted state, about 1 in 100 Ca^{++} ions are free (Lagnado et al., 1992). Buffers for cGMP are also known to be present in the outer segment, most likely due to high concentrations of PDE (Cote and Brunnock, 1993).

The activation cascade, which results in a transient rise in the PDE activity, upsets the balance of the dark adapted state, resulting in the photoresponse. This light

dependent decrease in [cGMP] results in a decrease in [Ca⁺⁺] as well, which initiates the feedback process and adaptation. The molecules that define these two processes are outlined below.

The activation cascade

Rhodopsin

The first part of the activation cascade is rhodopsin, the visual pigment of photoreceptor cells. Rhodopsin is an integral membrane protein situated in disk membranes stacked inside the rod outer segment (or in the disk membrane-like invaginations of the outer segment membrane in cones). Like all proteins in the class of G-protein coupled receptors, it contains seven transmembrane helices, which in the case of rhodopsin, harbor the chromophore 11-cis-retinal covalently linked to Lys-296 via a protonated Schiff base (Bownds, 1967; Dratz and Hargrave, 1983; Oseroff and Callender, 1974). Light catalyzes a cis-to-trans photoisomerization of 11-cis-retinal resulting in all-trans-retinal, which induces a series of structural transitions in rhodopsin eventually giving rise to the active state Metarhodopsin II (also called Rh*).

Just as important as the activation mechanism of rhodopsin is its inactivation mechanism. This is initiated by rhodopsin kinase, which binds to Meta-II and phosphorylates up to eight or nine serines and threonines near the carboxy terminus (Wilden and Kuhn, 1982; Aton et al., 1984). Arrestin recognizes phosphorylated rhodopsin and binds to it tightly, preventing activated rhodopsin from interacting with transducin. The time-course of these inactivation reactions is not entirely clear, but it most likely involves many steps, each of which decay exponentially without any one being rate limiting (Rieke and Baylor, 1996).

Transducin

The heterotrimeric G-protein transducin binds to the Meta-II state of rhodopsin, which catalyzes the exchange of GDP for GTP in transducin (Fung et al., 1981; Stryer et al.,

UCSF LIBRARY

1981). The binding of GTP causes a structural change in transducin that results in the release of the G-protein beta-gamma subunit. The alpha subunit of transducin is then able to bind to the cGMP phosphodiesterase (PDE) gamma subunit, preventing the gamma subunit from interacting with, and inhibiting, the PDE holoenzyme. In addition to their signaling roles, G-proteins are enzymes with GTPase activity. The hydrolysis of GTP to GDP allows the beta-gamma subunit to rebind the transducin alpha subunit, bringing it back to the inactive state and providing an elegant inactivation mechanism. However, the intrinsic GTPase activity (about 1/sec) is many times too slow to account for the inactivation time-course that must be present in the photoreceptor cell. This fact has revealed the presence of a GTPase activating protein (GAP) in the outer segment that has recently been identified as RGS9 (He et al., 1998), which in the presence of PDE gamma, increases the rate of GTP hydrolysis by a factor of 100. This inactivation time-course is thought to be dominated by a single exponential process, which accounts for the phenomenon of recovery translation invariance in rods (Nikonov et al., 1998).

cGMP phosphodiesterase(PDE)

The photoreceptor PDE consists of two nonidentical ~90 kDa catalytic subunits (alpha and beta) and two identical ~11 kDa inhibitory subunits (gamma) (Deterre et al., 1986). In a dark adapted photoreceptor cell, there is a small amount of active PDE present, referred to as the dark PDE activity. While it is not clear from where this arises (it may be due to a slight excess in the outer segment concentration of catalytic subunits over inhibitory subunits), it is essential to photoreceptor function. The enzyme becomes half-activated by the removal of one PDE gamma subunit, and fully active upon removal of both gamma subunits. The function of this enzyme is to catalyze the hydrolysis of cGMP to GMP. In this way, the concentration of cGMP decreases during the photoresponse, which results in the closure of cGMP-gated ion channels in the outer segment membrane.

UCSF LIBRARY

Guanylyl cyclase

The guanylyl cyclase (GC) of the outer segment is responsible for the synthesis of cGMP from GTP. Since the activity of this enzyme is inhibited by calcium (see feedback pathway), its activity is relatively low in the dark (when the calcium concentration is high) compared to during the light response (when the calcium concentration drops). This enzyme is thus functions to maintain the dark current before the light response and to speed the recovery of the photoreceptor cell following the light response.

cGMP-gated channel and Na-Ca,K exchanger

The cGMP-gated channel is responsible for converting light dependent changes in the concentration of cGMP to changes in membrane voltage. In the dark, a the photoreceptor outer segment membrane has a resting potential of approximately -40mV. The channel itself has a reversal potential near 0mV since the channel is relatively nonselective for cations. Thus, when channels close due to light dependent changes in [cGMP], the membrane becomes more hyperpolarized, resulting in a closure of Ca^{++} channels at the synaptic pedicule. This results in a decrease in the rate of neurotransmitter secretion, transferring the signal to the other cells of the retina.

While the cGMP-gated channel does not select Na^+ over K^+ , it is significantly more permeable to Ca^{++} than the other physiologically relevant cations. This allows a substantial amount of Ca^{++} to enter the outer segment through the channel even though the extracellular Ca^{++} concentration may be as low as 1mM (compared with the >100mM extracellular Na^+ concentration). Calcium leaves the cytoplasm through the Na,Ca-K exchange pump, which is an electrogenic exchanger with a stiochiometry of 4 Na^+ for every 1 Ca^{++} and 1 K^+ . Under physiological conditions, the rate of the exchanger is essentially entirely dependent of the intracellular Ca^{++} concentration, which indicates that this protein does not regulate intracellular calcium, it only clears it out of the outer segment with well-defined kinetics. Thus the channel has the sole responsibility of setting the cytoplasmic Ca^{++} concentration.

The Feedback Pathway and Adaptation

Adaptation

Adaptation is often defined as the reduction in sensitivity to light when a photoreceptor is presented with a steady background light. However, this is actually opposite to the motivation of the process of adaptation - the photoreceptor should work to maintain sensitivity, not reduce it. Even without the process of Ca^{++} -dependent adaptation, a photoreceptor becomes less sensitive to light due to a process called *amplitude compression*, which is caused by the fact that cGMP-gated channels cannot close any farther than fully closed. Thus, adaptation should be defined as the light-dependent *increase* in sensitivity that counteracts decreases in sensitivity due to amplitude compression. This allows photoreceptors to remain responsive to light over a much larger range of background light intensities than they would have without this active process.

Adaptation (as I have now defined it) has been found experimentally to require changes in intracellular Ca^{++} concentration (Matthews et al., 1988; Fain et al., 1989). If calcium is not allowed to change, either by altering the extracellular Ca^{++} concentration or by injecting the cell with a high concentration of a Ca^{++} buffer, adaptation fails to occur and the cell decreases in sensitivity with background light as would be predicted from amplitude compression. It is this calcium-dependent process which I refer to as the feedback pathway, as is described below.

Feedback Pathway

When calcium enters the outer segment cytoplasm through cGMP-gated channels, it binds to a number of calcium-binding proteins, which in turn alter the behavior of specific proteins involved in phototransduction. The following list are the Ca^{++} dependent processes so far known to exist in rod phototransduction.

UCSF LIBRARY

1. GCAP

GCAP (Guanylyl Cyclase Activating Protein) and its interaction with guanylyl cyclase was the first Ca^{++} dependent process discovered to exist in rods (Lolley and Racz, 1982; Koch and Stryer, 1988), though the identity of the GCAP protein itself was only recently established (Palczewski et al., 1994; Dizhoor et al., 1995). GCAP binds to cyclase in a calcium-dependent manner and acts to inhibit its activity. Thus, when the intracellular Ca^{++} concentration drops during the photoresponse or during exposure to background illumination, GCAP is no longer able to inhibit cyclase, and the cyclase activity increases. This results in an increase in the rate of cGMP synthesis, and an increase in the number of open channels. Adaptation results because more channels are open than would have been if the cyclase activity were not Ca^{++} dependent. More open channels means that the cell can give larger responses under bright light conditions than it would have without adaptation. It is known that this process is relatively fast with a $K_i = 100\text{nM}$, well within the range of physiological Ca^{++} concentrations (Calvert et al., 1998).

2. Recoverin

Recoverin was originally purified with the intention of finding GCAP (Dizhoor et al., 1991; Ray et al., 1992). It was soon discovered, however, that recoverin (also known as S-modulin) does not interact with cyclase, but rather interacts with rhodopsin kinase in a Ca^{++} dependent manner (Hurley et al., 1993; Kawamura et al., 1993). Recoverin is now known to inhibit the activity of rhodopsin kinase, increasing the lifetime of activated rhodopsin. Thus, when the calcium concentration declines during the light response, recoverin dissociates from rhodopsin kinase, resulting in an increase in the kinase activity, shortening the lifetime of activated rhodopsin. This decreases the gain of the activation cascade, resulting in adaptation. However, recent experiments (still unpublished) with recoverin knock-out mice seem to indicate that recoverin does not play a physiologically significant role in rods. Whether or not it plays an important role in cones is still under investigation.

3. Calmodulin

Calmodulin was found to bind to the cGMP-gated channel, leading to an increase in the channel's sensitivity to cGMP (Hsu and Molday, 1993, 1994). In rod channel patches, the $K_{1/2}$ for the channel can increase by a factor of 1.5-2 when Ca^{++} -calmodulin binds to the channel. An increase in sensitivity to cGMP will allow more channels to open under conditions of steady background light than would have opened without this effect, resulting in adaptation. Experiments done in a partially intact truncated rod preparation have shown that under physiological conditions, the K_i for the Ca^{++} dependence of channel $K_{1/2}$ is about 20nM (Nakatani et al., 1995), which is lower than the minimum value of Ca^{++} concentration (about 30-50nM). This low K_i indicates that at least in rods, this effect may not be important, except perhaps under very bright conditions (Koutalos and Yau, 1996). There is still no conclusive evidence that calmodulin is in fact the physiologically relevant modulator of the channel. Experiments with excised photoreceptor patches have shown small differences between the endogenous modulator and bovine calmodulin (Gordon et al., 1995; Hackos and Korenbrot, 1997; this thesis, chapter II), suggesting that perhaps a protein similar to but distinct from calmodulin is involved.

4. Other Ca^{++} dependent processes

Evidence for a fourth Ca^{++} binding regulatory protein that alters the gain of the activation cascade has been found (Lagnado and Baylor, 1994). When the calcium concentration decreases during the light response, this protein, which has not yet been identified, apparently acts upstream of recoverin and somehow reduces the activity of light-activated rhodopsin. The K_i for this calcium-dependent process has been measured to be 35nM, which indicates that this process may not be important except at very bright light intensities.

It has also been demonstrated that protein kinase C is present in the outer segment and can phosphorylate rhodopsin in a calcium dependent manner (Newton and Williams, 1993). However, recent experiments seem to indicate that protein kinase C has no functional role in phototransduction (Xiong et al., 1997).

5. Noncatalytic cGMP binding sites on PDE

In addition to Ca^{++} , cGMP itself may play a role in the feedback pathway in rods. It has been found that cGMP regulates the duration of PDE activation by transducin (Arshavsky et al., 1991, 1992; Arshavsky and Bownds, 1992; Cote et al., 1994). When cGMP binds to the noncatalytic site on PDE, the GTPase activity of transducin is found to be much slower than when these sites are not occupied. This means that during the light response, when the cGMP concentration drops, these noncatalytic site no longer contain bound cGMP, and therefore the inactivation rate of transducin increases. The effect of this process is to decrease the gain of the activation cascade, resulting in adaptation.

Rod-Cone Differences

Cone photoreceptors are in general less sensitive to light (about 10-fold), have much faster kinetics, and have more robust adaptation abilities than rod photoreceptors (Miller and Korenbrot, 1992). The molecular differences that give rise to these physiological differences are not yet known. It has been suggested, however, that some of the difference is due to differences in calcium homeostasis (Miller and Korenbrot, 1994; Miller et al., 1994). In particular, it is known that the cGMP-gated channels have a greater Ca^{++} permeability in cones than in rods (Perry and McNaughton, 1991; Picones and Korenbrot, 1990; Perry and McNaughton, 1991) and also a much faster rate of Ca^{++} efflux through the exchange pump (Nakatani and Yau, 1989; Hestrin and Korenbrot, 1990; Perry and McNaughton, 1991). In this thesis, I will show that the differences in Ca^{++} permeability between the two channel types is in fact significantly greater than has been previously thought. In chapter III, I will show there is a 7.5-fold difference in Ca^{++}

permeability, and in chapter IV, I will show that this leads to a 4-fold difference in Ca^{++} flux, making the cone channel effectively a Ca^{++} channel. A much faster rate of Ca^{++} influx and efflux in cones should give rise to faster and larger changes in intracellular Ca^{++} concentration, leading partially to the expected differences in the physiological properties of rods and cones. The elements that respond to Ca^{++} , such as GCAP, recoverin, and calmodulin, may be able to respond better to physiological Ca^{++} concentrations than their rod counterparts. In chapter II of this thesis (see also Hackos and Korenbrot, 1997; Rebrik and Korenbrot, 1997), I will show that the cone channel, as opposed to the rod channel, is modulated by physiological levels of Ca^{++} . Thus in cones, changes in intracellular Ca^{++} concentration may lead to larger changes in the activity of the Ca^{++} response elements of the feedback pathway. However, mathematical modeling of the photoresponse shows that differences in Ca^{++} dynamics cannot be the full explanation for the rod-cone differences. In fact, many other properties, such as the inactivation rate of the PDE, must be faster in cones to account for the observed physiological behavior. A full analysis of the activity of the cone PDE and other enzymes will require a biochemical preparation of cone outer segments, which is not yet technically feasible.

Cyclic Nucleotide Gated Channels

The cGMP-gated ion channel of the photoreceptor outer segment membrane is central to phototransduction, both in its generation of the electrical signal to light and in its control of the cytoplasmic Ca^{++} concentration, which is required for adaptation. Thus, it is of interest to investigate the role that these channels play in adaptation and the role that differences between the rod and cone channels play in the functional differences between these two cell types.

Photoreceptor cGMP-gated channels are members of the class of cyclic nucleotide gated (CNG) channels. Three members of this family have been identified in vertebrates; the rod, cone, and olfactory channels. CNG channels have also been found in numerous

other tissues, but their importance is not as clear as it is for photoreceptors and olfactory neurons.

The cloning and sequencing of the CNG channels have revealed that they are members of the voltage gated channel superfamily (Kaupp et al., 1989; Jan and Jan, 1990). These channels form tetrameric structures (Liu et al., 1996), where each subunit passes through the membrane six times. The six membrane spanning helices are labeled S1-S6. Between S5 and S6 is the pore region (P region), which is thought to line most of the ion permeable pathway through the channel. In CNG channels, there is an additional large C-terminal domain that includes a cyclic nucleotide binding domain similar in sequence to the cAMP binding domains of catabolite-activating protein (CAP), a bacterial transcription factor, and cAMP- and cGMP-dependent protein kinase. There is also a smaller N-terminal domain, which includes a highly charged portion that may be proteolytically removed from the channel during processing (Molday et al., 1991).

The cloned rod, cone, and olfactory channels form active CNG channels when expressed in either *Xenopus* oocytes or HEK293 cells (Kaupp et al., 1989; Bonigk et al., 1993; Dhallan et al., 1990). However, it was noticed early on that these channels did not display the same single channel kinetics, binding affinity to cGMP or cAMP, sensitivity to l-cis-diltiazem and Ca^{++} block, and modulation by calmodulin as was seen in the native channel. At least part of this discrepancy has been found to be due to the presence of a second subunit of the channel, referred to as the beta subunit (Chen et al., 1993; Korschen et al., 1995). When this is coexpressed with the alpha subunit, the resulting channels have the correct kinetics, l-cis-diltiazem and Ca^{++} block sensitivity, and calmodulin modulation, but still have a lower affinity for cyclic nucleotide when compared with the native channel. Furthermore, while the rod beta subunit has been cloned, it remains to be determined whether the cone channel also has a beta subunit (it is known that the rod beta subunit is not expressed in cones). A beta subunit has been reported for the olfactory channel, but it is still not clear whether this is in fact the physiological beta subunit (Bradley et al., 1994; Liman and Buck, 1994).

UCSF LIBRARY

The CNG channel pore is quite complex. While the pore is essentially nonselective for small monovalent cations such as Li^+ , Na^+ , and K^+ , it is significantly more permeable to divalent cations, especially Ca^{++} (for review, see Yau and Baylor, 1989; Menini, 1995). The permeability for NH_4^+ is much larger than the other monovalent cations, but the channel is completely impermeable to tetramethylammonium (TMA). Ions of intermediate sizes such as methylammonium and dimethylammonium are partially permeable and have been used to determine the effective diameter of the pores of rod and olfactory channel (Picco and Menini, 1993; Goulding et al., 1993). The greater permeability for divalent cations has been shown to be due in large part to the presence of a conserved glutamate residue (E363) in the pore - when this is changed to an unchanged amino acid, the divalent cation permeability is greatly reduced (Root and Mackinnon, 1993; Eismann et al., 1994). As is the case for calcium channels, divalent cations block the pore in addition to permeating. The block is significantly different depending on which side of the membrane divalent cations are placed; (for Ca^{++} block) externally, $K_i = 10\mu\text{M}$, and internally, $K_i = 1\text{mM}$. All of this behavior can be easily explained by postulating the presence of a divalent cation binding site in the pore (perhaps E363) that is asymmetrically located within the electric field across the membrane. Both one and two well Eyring rate models have used this idea to successfully predict much of the current-voltage relationship in the absence and presence of divalent cations for both rod and cone channels (Zimmerman and Baylor, 1992; Haynes, 1995; Wells and Tanaka, 1997).

The actual amount of calcium that flows into the outer segment per pA of cGMP-dependent current has not been measured directly, but it has been estimated that calcium carries 10-15% of the dark current in rods (Nakatani and Yau, 1988; Lagnado et al., 1991) and 21% in cones (Perry and McNaughton, 1991). These numbers were obtained by measuring the decay of the electrogenic Na-Ca,K exchange current following a bright light stimulus (which rapidly causes all of the cGMP-gated channels to close). By fitting the exchange current with a single or double exponential, it is possible to extrapolate

back to the point when half of the channels have closed. This allows an estimation of the exchange current in the dark. Since the exchanger has a defined stoichiometry (one calcium ion per charge carried), this gives an estimation of the amount of calcium efflux in the dark. Since at equilibrium, calcium influx and efflux must be the same, dividing the calcium efflux with the measured total dark current provides the percentage of the dark current carried by calcium. However, this method is prone to error for many reasons. Perhaps the most important is the fact that the exchange current consists of multiple exponential timecourses probably as a result of the presence of different calcium buffers in the outer segment cytoplasm, each with different kinetics (McCarthy et al., 1996). As a result, it is difficult to distinguish the closure rate of the channel from the fast exponential decay timecourses of the exchange current (especially in cones, where the exchanger rate is extremely fast). Large errors in the calcium flux can potentially occur by missing the fast decay processes in the exchange current. The method is also limited because the measurement of important trends, such as the dependence of calcium flux on [cGMP], voltage, and extracellular calcium cannot be easily measured. In chapter IV of this thesis, I have made the first direct measurements of fractional Ca^{++} current through both the rod and cone channels.

Several other studies have measured the permeability ratio between calcium and sodium (or potassium) by determining the channel's reversal potential under a variety of bi-ionic or semi bi-ionic conditions (Picones and Korenbrot, 1995; Frings et al., 1995; Haynes, 1995). While the permeability ratio (PCa/PNa) can be directly measured in excised patch recordings, it is not straight forward to calculate calcium fluxes from PCa/PNa measurements. However, the observed trends between rods and cones are consistent with the exchange current measurements. The cone PCa/PNa (or PCa/PK) is found to be about 3 times larger than the same value in rods.

The mechanism by which the cGMP binding domain actually gates the channel is still a mystery, but many intriguing observations have been made. X-ray crystal structures of the cAMP binding domains of CAP (Weber and Steitz, 1987) and PKA have

provided insights into the cGMP binding site of the channel, and the local structural changes that occur upon binding (Kumar and Weber, 1992). One interesting question that has been answered based on this information as well as with mutagenesis experiments is the molecular basis for cyclic nucleotide selectivity. The rod channel is much more sensitive to cGMP than to cAMP by about a factor of 20-50 (Kaupp et al., 1989; Goulding et al., 1994), while the olfactory channel interacts equally well with either cAMP or cGMP (Nakamura and Gold, 1987; Zufall et al., 1994). By making chimeric channels in which various sections of the rod and olfactory channels were exchanged, it was determined that a particular helix (called the C-helix) within the cyclic nucleotide binding domain completely determined the nucleotide selectivity (Goulding et al., 1994). This was further refined to show that aspartate residue 604 (in the C-helix) was intimately involved in nucleotide selectivity (Varnum et al., 1995).

Further experiments have shown that there is an interaction between the N-terminal and cyclic nucleotide binding domains. This interaction seems to be autoexcitatory – i.e. the N-terminal domain increases the binding domain's affinity for cyclic nucleotide (Gordon et al., 1997; Varnum and Zagotta, 1997). It was further shown that calmodulin (at least for the olfactory channel) decreases the sensitivity of the channel to cAMP by specifically blocking this domain interaction. However, it is still unknown how the cyclic nucleotide binding domain alters the structure of the channel, affecting open probability.

Several pieces of evidence point to structural changes in the pore during the gating process. The local anesthetic tetracaine has been found to block the channel in a state-dependent manner (Fodor et al., 1997a, 1997b). Analysis of this state-dependence has revealed that tetracaine binds to the pore only when the channel is in the closed state. Furthermore, it was found that the block was not state-dependent when tetracaine was applied to the E363G mutant channel. This implies that E363, which is known to be part of the selectivity filter in the pore, is undergoing conformational changes during the gating process. Structural changes in the pore have also been revealed by looking at the

affects of sulfhydryl-specific reagents on channels containing cysteine substitutions within the pore (Sun et al., 1996). When such a cysteine reacts with a methanethiosulfonate (MTS) reagent, the pore becomes blocked or altered, which can be detected electrophysiologically. Sun et al., 1996, found 3 residues that were accessible from both sides of the membrane despite the fact that the MTS reagents tested could not permeate the channel. It was further shown that MTS reagents can react with these cysteines from both sides of the membrane even when the channel is in the closed state. These data have been interpreted to show that there is not a "gate" in front of the pore on either side of the membrane, but rather the pore itself acts as the gate. Therefore, the pore can change structure to form either a closed gate (representing the closed state of the channel), or the selectivity filter (when the channel is open). Surprisingly, this is not the case in K^+ channels, which would be predicted to have similar pore structures based on the high degree of sequence similarity on this part of the channel (Liu et al., 1997; Holmgren et al., 1997). One possible caveat of the Sun et al., 1996 experiments is that the MTS reagents may not be as membrane-impermeant as was assumed (Holmgren et al., 1996).

Another interesting aspect of CNG channel gating is the presence of gating-dependent subconductance states. These subconductance states were described soon after the channel was discovered. Depending on the investigator, either one (Haynes et al., 1986; Zimmerman and Baylor, 1986; Tanaka et al., 1987) or two (Hanke et al., 1988; Bennett et al., 1989) subconductance states could be observed. Ildefonse and Bennett (1991) presented evidence for the presence of three subconductance states (which are present only at low cGMP concentrations) in addition to the fully open state, and therefore argued that the channel has four cGMP-binding sites, where each binding state represents one of the subconductance states. Recently, however, elegant experiments by Ruiz and Karpen (1997) have shown that there is not a one-to-one relationship between the number of cGMP molecules bound to the channel and the channel's occupancy of one particular subconductance state. Using a photo-crosslinkable cGMP analog, there were

able to determine the number of cGMP molecules bound to a single channel and record its electrophysiological behavior. This revealed that the channel samples each of the conductance states under all conditions – only the probability of occupying a particular state is dependent on the number of bound cGMP molecules. This also reveals that the average conformational state of the pore is dependent on cGMP concentration. The fact that the pore exists in different conformations depending on [cGMP] opens the possibility that important pore properties (such as ion selectivity) might be dependent on [cGMP] as well. In chapter IV of this thesis, I provide evidence that the ion selectivity of rod and cone cGMP-gated channels is indeed dependent on cGMP concentration, suggesting that the subconductance states represent states of the channel with altered pore structure.

UCSF LIBRARY

References

- Arshavsky, V. Y. u.; Gray-Keller, M. P., and Bownds, M. D. (1991) cGMP suppresses GTPase activity of a portion of transducin equimolar to phosphodiesterase in frog rod outer segments. Light-induced cGMP decreases as a putative feedback mechanism of the photoresponse. *J Biol Chem* 266: 18530-7
- Arshavsky, V. Y. and Bownds, M. D. (1992) Regulation of deactivation of photoreceptor G protein by its target enzyme and cGMP. *Nature* 357: 416-417
- Arshavsky, V. Y.; Dumke, C. L., and Bownds, M. D. (1992) Non-catalytic cGMP binding sites of amphibian rod cGMP phosphodiesterase control interaction with its inhibitory gamma-subunits-a putative regulatory mechanism of the rod photoresponse. *J. Biol. Chem* 267: 24501-24507
- Aton, B. R.; Litman, B. J., and Jackson, M. L. (1984) Isolation and identification of the phosphorylated species of rhodopsin. *Biochem* 23: 1737-41
- Bennett, N.; Ildefonse, M.; Crouzy, S.; Chapron, Y., and Clerc, A. (1989) Direct activation of cGMP-dependent channels of retinal rods by the cGMP phosphodiesterase. *Proc Nat Acad Sci USA* 86: 3634-8
- Bonigk, W.; Altenhofen, W.; Muller, F.; Dose, A.; Illing, M.; Molday, R. S., and Kaupp, U. B. (1993) Rod and cone photoreceptor cells express distinct genes for cGMP-gated channels. *Neuron* 10: 865-77
- Bownds, D. (1967) Site of attachment of retinal in rhodopsin. *Nature* 216: 1178-81
- Bradley, J.; Li, J.; Davidson, N.; Lester, H. A., and Zinn, K. (1994) Heteromeric olfactory cyclic nucleotide-gated channels: a subunit that confers increased sensitivity to cAMP. *Proc Nat Acad Sci USA* 91: 8890-4
- Calvert P. D.; Ho T. W.; LeFebvre Y. M.; Arshavsky V. Y. (1998) Onset of feedback reactions underlying vertebrate rod photoreceptor light adaptation. *J Gen Physiol* 111: 39-51
- Chen, T. Y.; Peng, Y. W.; Dhallan, R. S.; Ahamed, B.; Reed, R. R., and Yau, K. W. (1993) A new subunit of the cyclic nucleotide-gated cation channel in retinal rods. *Nature* 362: 764-767
- Cobbs, W. H., A. E. Barkdoll III and E. N. Pugh Jr. (1985) Cyclic GMP increases photocurrent and light sensitivity of retinal cones. *Nature*. 317:64-66
- Cote, R. H. and Brunnock M. A. (1993) Intracellular cGMP concentration in rod photoreceptors is regulated by binding to high and moderate affinity cGMP binding sites. *J Biol Chem* 268: 17190-8

UCSF LIBRARY

- Cote, R. H.; Bownds, M. D., and Arshavsky, V. Y. (1994) cGMP binding sites on photoreceptor phosphodiesterase: role in feedback regulation of visual transduction. *Proc Nat Acad Sci USA* 91: 4845-9
- Deterre, P.; Bigay, J.; Robert, M.; Pfister, C.; Kuhn, H., and Chabre, M. (1986) Activation of retinal rod cyclic GMP-phosphodiesterase by transducin: characterization of the complex formed by phosphodiesterase inhibitor and transducin alpha-subunit. *Proteins* 1: 188-93
- Dhallan, R. S.; Yau, K. W.; Schrader, K. A., and Reed, R. R. (1990) Primary structure and functional expression of a cyclic nucleotide-activated channel from olfactory neurons. *Nature* 347: 184-7
- Dizhoor, A. M.; Ray, S.; Kumar, S.; Niemi, G.; Spencer, M.; Brolley, D.; Walsh, K. A.; Philipov, P. P.; Hurley, J. B., and Stryer, L. (1991) Recoverin: a calcium sensitive activator of retinal rod guanylate cyclase. *Science* 251, 915-8
- Dizhoor, A. M.; Olshevskaya, E. V.; Henzel, W. J.; Wong, S. C.; Stults, J. T.; Ankoudinova, I., and Hurley, J. B. (1995) Cloning, sequencing, and expression of a 24-kDa Ca²⁺-binding protein activating photoreceptor guanylyl cyclase. *J Biol Chem* 270: 25200-6
- Dratz, E. A. and Hargrave, P.A. (1993) *Trends Biochem Sci* 8: 128-135
- Eismann, E.; Muller, F.; Heinemann, S. H., and Kaupp, U. B. (1994) A single negative charge within the pore region of a cGMP-gated channel controls rectification, Ca²⁺ blockage, and ionic selectivity. *Proc Nat Acad Sci USA* 91: 1109-13
- Fain, G. L.; Lamb, T. D.; Matthews, H. R., and Murphy, R. L. (1989) Cytoplasmic calcium as the messenger for light adaptation in salamander rods. *J Physiol* 416: 215-43
- Fodor, A. A.; Gordon, S. E.; Zagotta, W. N. (1997a) Mechanism of tetracaine block of cyclic nucleotide-gated channels. *J Gen Physiol* 109: 3-14
- Fodor, A. A.; Black, K. D., and Zagotta, W. N. (1997b) Tetracaine reports a conformational change in the pore of cyclic nucleotide-gated channels. *J Gen Physiol* 110: 591-600
- Frings, S.; Seifert, R.; Godde, M., and Kaupp, U. B. (1995) Profoundly different calcium permeation and blockage determine the specific function of distinct cyclic nucleotide-gated channels. *Neuron* 15: 169-79
- Fung, B. K.; Hurley, J. B., and Stryer, L. (1981) Flow of information in the light-triggered cyclic nucleotide cascade of vision. *Proc Nat Acad Sci USA* 78, 152-6

- Gordon, S. E.; Downing-Park, J., and Zimmerman, A. L. (1995) Modulation of the cGMP-gated ion channel in frog rods by calmodulin and an endogenous inhibitory factor. *J Physiol* 486: 533-46
- Gordon, S. E.; Varnum, M. D., and Zagotta, W. N. (1997) Direct interaction between amino- and carboxyl-terminal domains of cyclic nucleotide-gated channels. *Neuron* 19: 431-41.
- Goulding, E. H.; Tibbs, G. R.; Liu, D., and Siegelbaum, S. A. (1993) Role of H5 domain in determining pore diameter and ion permeation through cyclic nucleotide-gated channels. *Nature* 364: 61-4
- Goulding, E. H.; Tibbs, G. R., and Siegelbaum, S. A. (1994) Molecular mechanism of cyclic-nucleotide-gated channel activation. *Nature* 372: 369-74
- Hackos, D. H. and Korenbrot, J. I. (1997) Calcium modulation of ligand affinity in the cyclic GMP-gated ion channels of cone photoreceptors. *J Gen Physiol* 110: 515-528
- Hanke, W.; Cook, N. J., and Kaupp, U. B. (1988) cGMP-dependent channel protein from photoreceptor membranes: single-channel activity of the purified and reconstituted protein. *Proc Nat Acad Sci USA* 85: 94-8
- Haynes, L. W.; Kay, A. R., and Yau, K. W. (1986) Single cyclic GMP-activated channel activity in excised patches of rod outer segment membrane. *Nature* 321: 66-70
- Haynes, L. W. (1995) Permeation and block by internal and external divalent cations of the catfish cone photoreceptor cGMP-gated channel. *J Gen Physiol*; 106: 507-23
- He, W.; Cowan, C. W., and Wensel, T. G. (1998) RGS9, a GTPase accelerator for phototransduction. *Neuron* 20: 95-102
- Hestrin, S. and Korenbrot, J. I. (1990) Activation kinetics of retinal cones and rods: response to intense flashes of light. *J Neurosci* 10: 1967-73
- Holmgren, M.; Liu, Y.; Xu, Y., and Yellen, G. (1996) On the use of thiol-modifying agents to determine channel topology. *Neuropharm* 35: 797-804
- Holmgren, M.; Smith, P. L., and Yellen, G. (1997) Trapping of organic blockers by closing of voltage-dependent K⁺ channels: evidence for a trap door mechanism of activation gating. *J Gen Physiol* 109: 527-35
- Hsu, Y. T. and Molday, R. S. (1993) Modulation of the cGMP-gated channel of rod photoreceptor cells by calmodulin. *Nature* 361: 76-9

UCSF LIBRARY

- Hsu, Y. T. and Molday, R. S. (1994) Interaction of calmodulin with the cyclic GMP-gated channel of rod photoreceptor cells. Modulation of activity, affinity purification, and localization. *J Biol Chem* 269: 29765-70
- Hurley, J. B.; Dizhoor, A. M.; Ray, S., and Stryer, L. (1993) Recoverin's role: conclusion withdrawn. *Science* 260: 740.
- Ildelfonse, M. and Bennett, N. (1991) Single-channel study of the cGMP-dependent conductance of retinal rods from incorporation of native vesicles into planar lipid bilayers. *J Membr Biol* 123: 133-47
- Jan, L. Y. and Jan, Y. N. (1990) A superfamily of ion channels. *Nature* 345: 672.
- Kaupp, U. B.; Niidome, T.; Tanabe, T.; Terada, S.; Bonigk, W.; Stuhmer, W.; Cook, N. J.; Kangawa, K.; Matsuo, H.; Hirose, T., and et, al. (1989) Primary structure and functional expression from complementary DNA of the rod photoreceptor cyclic GMP-gated channel. *Nature* 342: 762-6.
- Kawamura, S. (1993) Rhodopsin phosphorylation as a mechanism of cyclic GMP phosphodiesterase regulation by S-modulin. *Nature* 362: 855-7
- Koch, K. W. and Stryer, L. (1988) Highly cooperative feedback control of retinal rod guanylate cyclase by calcium ions. *Nature* 334: 64-6
- Korschen, H G; Illing, M; Seifert, R; Sesti, F; Williams, A; Gotzes, S; Colvilee, C; Muller, F; Dose, A; Godde, M; Molday, L; Kaupp, U B, and Molday, R S. (1995) A 240 kDa protein represents the complete β subunit of the cyclic nucleotide-gated channel from rod photoreceptors. *Neuron* 15: 627-636
- Koutalos, Y. and Yau, K. W. (1996) Regulation of sensitivity in vertebrate rod photoreceptors by calcium. *Trends Neurosci*; 19: 73-81
- Kumar, V. D. and Weber, I. T. (1992) Molecular model of the cyclic GMP-binding domain of the cyclic GMP-gated ion channel. *Biochem* 31: 4643-9
- Lagnado, L. and McNaughton, P. A. (1991) Net charge transport during sodium-dependent calcium extrusion in isolated salamander rod outer segments. *J Gen Physiol* 98: 479-95
- Lagnado, L.; Cervetto, L.; McNaughton, P. A. (1992) Calcium homeostasis in the outer segments of retinal rods from the tiger salamander. *J Physiol (Lond)* 455: 111-142
- Lagnado, L. and Baylor, D. A. (1994) Calcium controls light-triggered formation of catalytically active rhodopsin. *Nature* 367: 273-7
- Liman, E. R. and Buck, L. B. (1994) A second subunit of the olfactory cyclic nucleotide-gated channel confers high sensitivity to camp. *Neuron* 13, 611-21

- Liu, D. T.; Tibbs, G. R., and Siegelbaum, S. A. (1996) Subunit stoichiometry of cyclic nucleotide-gated channels and effects of subunit order on channel function. *Neuron* 16: 983-90
- Liu, Y.; Holmgren, M.; Jurman, M. E., and Yellen, G. (1997) Gated access to the pore of a voltage-dependent K⁺ channel. *Neuron* 19, 175-84
- Lolley, R. N. and Racz, E. (1982) Calcium modulation of cyclic GMP synthesis in rat visual cells. *Vision Res* 22: 1481-6
- Matthews, H. R.; Murphy, R. L.; Fain, G. L., and Lamb, T. D. (1988) Photoreceptor light adaptation is mediated by cytoplasmic calcium concentration. *Nature* 334: 67-9
- McCarthy, S. T.; Younger, J. P., and Owen, W. G. (1996) Dynamic, spatially nonuniform calcium regulation in frog rods exposed to light. *J Neurophysiol* 76: 1991-2004.
- Menini, A. (1995) Cyclic nucleotide-gated channels in visual and olfactory transduction. *Biophys Chem* 55: 185-96.
- Miller, J. L. and Korenbrot, J. I. (1994a) Differences in calcium homeostasis between retinal rod and cone photoreceptors revealed by the effects of voltage on the cGMP-gated conductance in intact cells. *J Gen Physiol* 104: 909-40
- Miller, J. L.; Picones, A., and Korenbrot, J. I. (1994b) Differences in transduction between rod and cone photoreceptors: an exploration of the role of calcium homeostasis. *Curr Opin Neurobiol* 4: 488-95
- Molday, R. S.; Molday, L. L.; Dose, A.; Clark-Lewis, I.; Illing, M.; Cook, N. J.; Eismann, E., and Kaupp, U. B. (1991) The cGMP-gated channel of the rod photoreceptor cell characterization and orientation of the amino terminus. *J Biol Chem* 266: 21917-22.
- Nakamura, T and Gold, G H. (1987) A cyclic nucleotide-gated conductance in olfactory receptor cilia. *Nature* 325: 442-44
- Nakatani, K. and Yau, K. W. (1988) Calcium and magnesium fluxes across the plasma membrane of the toad rod outer segment. *J Physiol* 395: 695-729
- Nakatani, K. and Yau, K. W. (1989) Sodium-dependent calcium extrusion and sensitivity regulation in retinal cones of the salamander. *J Physiol* 409: 525-48
- Nakatani, K.; Koutalos, Y., and Yau, K. W. (1995) Ca²⁺ modulation of the cGMP-gated channel of bullfrog retinal rod photoreceptors. *J Physiol* 484 (Pt 1): 69-76
- Newton, A. C. and Williams, D. S. (1993) Rhodopsin is the major in situ substrate of protein kinase C in rod outer segments of photoreceptors. *J Biol Chem* 268: 18181-6

- Nikonov, S.; Engheta, N., and Pugh, E. N. Jr. (1998) Kinetics of recovery of the dark-adapted salamander rod photoresponse. *J Gen Physiol* 111: 7-37
- Oseroff, A. R. and Callender, R. H. (1974) Resonance Raman spectroscopy of rhodopsin in retinal disk membranes. *Biochem* 13: 4243-8
- Palczewski, K.; Subbaraya, I.; Gorczyca, W. A.; Helekar, B. S.; Ruiz, C. C.; Ohguro, H.; Huang, J.; Zhao, X.; Crabb, J. W.; Johnson, R. S., and et al. (1994) Molecular cloning and characterization of retinal photoreceptor guanylyl cyclase-activating protein. *Neuron* 13: 395-404
- Perry, R. J. and McNaughton, P. A. (1991) Response properties of cones from the retina of the tiger salamander *J Physiol* 433: 561-87
- Picco, C. and Menini, A. (1993) The permeability of the cGMP-activated channel to organic cations in retinal rods of the tiger salamander. *J Physiol* 460: 741-58
- Picones, A. and Korenbrot, J. I. (1995) Permeability and interaction of Ca²⁺ with cGMP-gated ion channels differ in retinal rod and cone photoreceptors. *Biophys J* 69: 120-7.
- Ray, S.; Zozulya, S.; Niemi, G. A.; Flaherty, K. M.; Brolley, D.; Dizhoor, A. M.; McKay, D. B.; Hurley, J., and Stryer, L. (1992) Cloning, expression, and crystallization of recoverin, a calcium sensor in vision. *Proc Nat Acad Sci USA* 89: 5705-9
- Rieke, F. and Baylor, D.A. (1996) FASEB Summer Retina Meeting (Keystone, CO).
- Rebrik, T. and Korenbrot, J.I. (1997) cGMP-gated conductance in intact outer segments of cone photoreceptors with an electroporabilized inner segment. *Investig. Ophthalmol Vis Sci* 38: S722 (Abst.).
- Root, M. J. and Mackinnon, R. (1993) Identification of an external divalent cation-binding site in the pore of a cGMP-activated channel. *Neuron* 11: 459-66
- Ruiz, M. L. and Karpen, J. W. (1997) Single cyclic nucleotide-gated channels locked in different ligand-bound states. *Nature* 389: 389-92
- Stryer, L.; Hurley, J. B., and Fung, B. K. (1981) *Curr Top Membr Transp* 15: 93-108
- Sun, Z. P.; Akabas, M. H.; Goulding, E. H.; Karlin, A.; Siegelbaum, S. A.; Sun, Z. P.; Akabas, M. H.; Goulding, E. H.; Karlin, A., and Siegelbaum, S. A. (1996) Exposure of residues in the cyclic nucleotide-gated channel pore: P region structure and function in gating. Exposure of residues in the cyclic nucleotide-gated channel pore: P region structure and function in gating. *Neuron* 16: 141-9

- Tanaka, J. C.; Furman, R. E.; Cobbs, W. H., and Mueller, P. (1987) Incorporation of a retinal rod cGMP-dependent conductance into planar bilayers. *Proc Nat Acad Sci USA* 84: 724-8
- Varnum, M. D.; Black, K. D., and Zagotta, W. N. (1995) Molecular mechanism for ligand discrimination of cyclic nucleotide-gated channels. *Neuron* 15: 619-25
- Varnum, M. D. and Zagotta, W. N. (1997) Interdomain interactions underlying activation of cyclic nucleotide-gated channels. *Science* 278: 110-3
- Weber, I. T. and Steitz, T. A. (1987) Structure of a complex of catabolite gene activator protein and cyclic AMP refined at 2.5 Å resolution. *J Mol Biol* 198: 311-26
- Wells, G. B. and Tanaka, J. C. (1997) Ion selectivity predictions from a two-site permeation model for the cyclic nucleotide-gated channel of retinal rod cells. *Biophys J* 72: 127-40
- Wilden, U. and Kuhn, H. (1982) Light-dependent phosphorylation of rhodopsin: number of phosphorylation sites. *Biochem* 21: 3014-22
- Xiong, W.; Nakatani, K.; Ye, B., and Yau, K. (1997) Protein kinase C activity and light sensitivity of single amphibian rods. *J Gen Physiol* 110: 441-52
- Yau, K. W. and Baylor, D. A. (1989) Cyclic GMP-activated conductance of retinal photoreceptor cells. *Ann Rev Neurosci* 12: 289-327
- Zimmerman, A. L. and Baylor, D. A. (1986) Cyclic GMP-sensitive conductance of retinal rods consists of aqueous pores. *Nature* 321: 70-2
- Zimmerman, A. L. and Baylor, D. A. (1992) Cation interactions within the cyclic GMP-activated channel of retinal rods from the tiger salamander. *J Physiol* 449: 759-83
- Zufall, F.; Firestein, S., and Shepherd, G. M. (1994) Cyclic nucleotide-gated ion channels and sensory transduction in olfactory receptor neurons. *Ann Rev Biophys Biomolec Struct* 23: 577-607

UCSF LIBRARY

Chapter II

Calcium modulation of ligand affinity in the cGMP-gated ion channels of cone photoreceptors

Abstract

To investigate modulation of the activation of cGMP-gated ion channels in cone photoreceptors, we measured currents in membrane patches detached from the outer segments of single cones isolated from striped bass retina. The sensitivity of these channels to activation by cGMP depends on the history of exposure to divalent cations of the membrane's cytoplasmic surface. In patches maintained in 20 μM Ca^{++} and 100 μM Mg^{++} after excision, the current amplitude dependence on cGMP is well described by a Hill equation with average values of $K_{1/2}$, the concentration necessary to activate half the maximal current, of 86 μM and a cooperativity index, n of 2.57. Exposing the patch to a solution free of divalent cations irreversibly increases the cGMP sensitivity; the average value of $K_{1/2}$ shifts to 58.8 μM and n shifts to 1.8. Changes in cGMP sensitivity do not affect other functional parameters of the ion channels, such as the interaction and permeation of mono- and divalent cations. Modulation of cGMP activation depends on the action of an endogenous factor that progressively dissociates from the channel as Ca^{++} concentration is lowered below 1 μM . The activity of the endogenous modulator is not well mimicked by exogenously added calmodulin, although this protein competes with the endogenous modulator for a common binding site. Thus, the modulation of cGMP affinity in cones depends on the activity of an unidentified molecule that may not be calmodulin.

Keywords: retina, phototransduction, calmodulin, rod photoreceptor, fish

UCSF LIBRARY

Introduction

Rod and cone photoreceptors and olfactory sensory neurons respond to their appropriate stimuli with changes in membrane conductance that reflect the activity of cyclic nucleotide-gated ion channels (Fesenko et al., 1985; Haynes and Yau, 1990; Nakamura and Gold, 1987). In these cells, the stimuli activate enzymatic cascades that ultimately change the cytoplasmic concentration of either cGMP (photoreceptors) (reviews in Hurley, 1992; Pugh and Lamb, 1993; Baylor, 1996) or cAMP (olfactory neurons) (review in Reed, 1992). Because of similarities in primary structure, the cyclic nucleotide-gated channels in the sensory cells have been recognized to be members of the same gene family (reviews in Zagotta and Siegelbaum, 1996; Finn et al. 1996; Yau and Chen, 1995). Despite their general structural similarities, the chemical specificity and affinity of the ligand binding sites differ among channels of the various sensory cell types (Scott et al. 1996). For example, the channels in retinal photoreceptors have a 20- to 50-fold higher affinity for cGMP than cAMP, whereas native channels of olfactory neurons have nearly the same affinity for both nucleotides (review in Zagotta and Siegelbaum, 1996). Even in the same receptor cell type, the nucleotide affinity of the channels varies from species to species (review in Zagotta and Siegelbaum, 1996), presumably optimized to match the nucleotide cytoplasmic concentration in the cell expressing that specific channel. Furthermore, recent experiments have shown that the ligand affinity of the channels is not static, but changes as a function of Ca^{++} concentration (review in Molday, 1996). The physiological significance of this Ca^{++} dependence is not fully understood. However, it is likely to play an important role in the adaptation of the cell's response to changing background levels of stimulation (Kurahashi and Menini, 1997).

The extent to which Ca^{++} modulates the cGMP activation differs markedly between olfactory and rod photoreceptor channels. In rat olfactory neurons, for example, affinity for cAMP decreases over 100-fold when Ca^{++} is elevated to 200 μM (Chen and Yau, 1994; Liu et al., 1994; Balasubramanian et al., 1996). Affinity is measured by the value

of $K_{1/2}$, the concentration necessary to activate half the maximum ligand-gated current. In rod photoreceptors, the Ca^{++} modulation of $K_{1/2}$ has been studied in isolated membrane vesicles (Bauer, 1996), detached membrane patches (Gordon et al., 1995) and truncated outer segments (Nakatani et al., 1995; Sagoo and Lagnado, 1996). In all these preparations, the $K_{1/2}$ for cGMP activation shifts about 1.5 fold with a Ca^{++} -dependence that is half maximal at about 50 nM. Because this modulation is irreversibly lost in patches and truncated rods following exposure to solutions free of divalent cations, it has been presumed to arise from the action of a soluble, endogenous modulator (Gordon et al., 1995; Nakatani et al. 1995; Sagoo and Lagnado, 1996; Bauer, 1996). The molecular identity of this endogenous modulator in rods is not fully resolved, but the possibility that it is calmodulin has been addressed in a number of recent experiments.

Hsu and Molday (1993) first demonstrated that calmodulin can cause a Ca^{++} -dependent modulation of $K_{1/2}$ in rods. In a manner similar to the endogenous modulator, the maximum Ca^{++} /calmodulin-dependent shift in $K_{1/2}$ is about 1.5-fold (Gordon et al., 1995; Kosolapov and Bobkov, 1996; Bauer, 1996). The Ca^{++} dependence of the shift in $K_{1/2}$ in the presence of added calmodulin has a half-maximum value of about 50 nM in some studies (Hsu and Molday, 1993; Bauer 1996) and 450 nM in others (Kosolapov and Bobkov, 1996). These values, however, cannot be compared to those characteristic of the endogenous modulator because they change with the calmodulin concentration used in the experiments (Bauer, 1996). Gordon et al. (1995) and Bauer (1996) have directly investigated whether the endogenous factor and calmodulin are one and the same. In membrane vesicles there are no recognizable differences in the function of the two molecules (Bauer, 1996). However, in membrane patches the function of both molecules was found to differ in several respects, suggesting that the modulator in rods may differ from calmodulin (Gordon et al., 1995). In truncated rods, pharmacological blockers of calmodulin do not alter the Ca^{++} -dependent modulation of $K_{1/2}$ nor does added calmodulin confer modulation (Sagoo and Lagnado (1996)). Finally, Haynes and Stotz

(1997) have found that added calmodulin can modulate $K_{1/2}$ in rod membrane patches, but not in those of cones from the same species.

The cyclic nucleotide-gated channels of cone outer segments are structurally homologous to those of rods (Bonigk et al., 1993; Weyand et al., 1994), yet their functional properties differ in subtle but important ways. These functional differences may contribute to explain the differences in transduction between the two receptor types (Korenbrodt, 1995). The $K_{1/2}$ of cGMP binding is higher in cones (Haynes and Yau, 1990; Picones and Korenbrodt, 1992), than in rods (Karpen et al., 1988; Zimmerman and Baylor, 1992; Haynes and Stotz 1997); the energy of interaction of cations such as Na^+ and Li^+ with the channel is higher in cones than in rods (rods: Menini, 1990; Furman and Tanaka, 1990; Zimmerman and Baylor, 1992; cones: Picones and Korenbrodt, 1992; Haynes, 1995), and the blocking effect of 1-cis-diltiazem is also different (Haynes, 1992). Of singular functional significance is the fact that the permeability and interaction of Ca^{++} with the channels differ between the two photoreceptor types (Korenbrodt, 1995). In particular, the permeability of Ca^{++} relative to Na^+ is higher in cone than in rod channels (Picones and Korenbrodt, 1995). This difference is also observed in recombinant channels formed by cone or rod α -subunits alone (Frings et al, 1995). Whether there exists a calcium-dependent modulation of ligand binding in cone channels and what features this modulation might have has not been previously investigated. We report here that in membrane patches of cone outer segments, as in those of rods, there exists a Ca^{++} dependent modulation of cGMP activation. This modulation depends on the activity of an endogenous modulator. We further contrast the properties of rod and cone channels with respect to the modulatory effect of added calmodulin. In cones the endogenous modulator is not well mimicked by calmodulin.

Materials and Methods

Materials. We obtained striped bass (*Morone saxatilis*) from Professional Aquaculture Services (Chico, CA) and tiger salamanders (*Ambystoma tigrinum*) from Charles Sullivan (Memphis, TN). We received cGMP, 8-Br-cGMP and calmodulin (bovine brain phosphodiesterase activator) from Sigma (St. Louis, MO).

Photoreceptor isolation. Methods of cell isolation are described in detail elsewhere (Miller and Korenbrot, 1993b, 1994). Animals were dark-adapted and retinas isolated under infrared illumination. Single cones were obtained by mechanical dissociation of striped bass retinas maintained in a Ringer's solution consisting of (in mM) NaCl (143), KCl (2.5), NaHCO₃ (5), Na₂HPO₄ (1), CaCl₂ (1), MgCl₂ (1), pyruvate (5), HEPES (10), pH 7.5, osmotic pressure 309 mOsM. Rods were isolated by mechanical dissociation of tiger salamander retinas maintained in a Ringer's solution composed of (in mM) NaCl (100), KCl (2), NaHCO₃ (5), Na₂HPO₄ (1), CaCl₂ (1), MgCl₂ (1), pyruvate (5), HEPES (10), pH 7.4, osmotic pressure 227 mOsM.

Solitary photoreceptors were firmly attached to a glass coverslip derivatized with wheat germ agglutinin (Picones and Korenbrot, 1992). The coverslip formed the bottom of a recording chamber held on the stage of an upright microscope equipped with DIC optics and operated under visible light. A suspension of photoreceptors in pyruvate-Ringer's was placed on the coverslip and the cells were allowed to settle down and attach for 5 minutes. The bath solution was then exchanged with a Ringer's solution of the same composition, but in which pyruvate was isoosmotically replaced with glucose.

The recording chamber consisted of two side-by-side compartments. Cells were held in one compartment that was continuously perfused with Ringer's. The second, smaller compartment was continuous with the first one, but a movable barrier could be used to separate them (Picones and Korenbrot, 1992). We used tight-seal electrodes to obtain inside-out membrane fragments detached from the side of the outer segments of either cones or rods. After forming a giga-seal and detaching the membrane fragment, we

moved the electrode under the solution surface from the compartment containing the intact cells to the smaller compartment. The two compartments were then separated by the movable barrier and the tip of the electrode was placed within 100 μm of the opening of a 300 μm diameter glass capillary. We used this capillary and a rotary valve to deliver selected test solutions onto the cytoplasmic (outside) surface of the membrane patch.

The speed of change in membrane current in response to changes in test solutions varied from patch to patch. This variability likely reflects differences among patches in the accessibility of their cytoplasmic surface to the bath solution. In our experiments, following each solution change we monitored membrane current by repeated presentation of voltage steps and waited for the current to reach a stationary amplitude. We present and analyzed here only currents in this stationary condition (except for Figure 5).

Ionic solutions. In studies of both cone and rod membranes, we filled the tight-seal electrodes with the same solution (in mM): NaCl (157), EGTA (5), EDTA (5), Hepes (10) adjusted with NaOH to pH 7.5, osmotic pressure 305 mOsM. Free Ca^{++} concentration in this solution was $\leq 10^{-10}$ M and total Na^+ concentration was 167 mM. In all studies, the initial composition of the solution in the small compartment into which we moved the electrode was (in mM) NaCl (157), Hepes (10) adjusted with NaOH to pH 7.5, and 20 μM free Ca^{++} (total 7.637), 100 μM free Mg^{++} (total 2) with HEDTA (10). We elected to use these free divalent cation concentrations because they are sufficiently low not to block the cGMP-gated conductance (Picones and Korenbrot, 1995), yet sufficiently high to saturate the Ca^{++} -dependence of the phenomena studied here.

We used a titration method to produce solutions with free calcium concentrations between 10nM and 20 μM (Williams and Fay, 1990). This method yields accurate free calcium concentrations without the need to weigh with extreme precision chemicals of known purity. This is particularly important because 100% pure Ca^{++} buffering agents cannot be obtained commercially (Miller and Smith, 1984). Briefly, a solution containing (in mM) NaCl (157), HEPES (10), HEDTA (10) adjusted with NaOH to pH 7.5 was

divided into two parts. One part (solution A) had no added calcium. Into the other part (solution B), CaCl_2 was added to 9mM and the pH readjusted to 7.8. A small sample of this solution was then titrated with a 100mM CaCl_2 solution while monitoring its pH. The amount of CaCl_2 necessary to fully titrate HEDTA, that is to obtain pure CaHEDTA at pH 7.5, was determined from this titration. The appropriate amount of CaCl_2 was then added to the remaining solution B. Solutions A and B were mixed to obtain different free calcium concentrations (Table 1). Volumes were calculated (EqCal, BioSoft, Cambridge, UK) using published values for HEDTA binding constants (Martell and Smith, 1974). The pH was adjusted to 7.5 and solutions stored at 4 °C in plastic containers for up to one week. Solutions containing both calcium and magnesium (at concentrations of 20 μM and 100 μM free, respectively) were made by adding to solution A appropriate amounts of stocks of CaCl_2 and MgCl_2 . The concentration of divalent cations in these stocks were calibrated by measuring their osmolality.

In many of the experiments reported here we tested the electrical properties of the same membrane patch before and after removing divalent cations. Divalent cations were removed by exposing the cytoplasmic (outside) surface of the patch to a solution composed of (in mM): NaCl (157), HEPES (10), EDTA (5), EGTA (5) adjusted with NaOH to pH 7.5. We refer to this solution in the following text simply as the EDTA/EGTA solution.

Electrical Recordings. Tight-seal electrodes were made from aluminosilicate glass (Corning 1724) (1.5 x 1.0 mm od x id). We measured membrane currents under voltage clamp at room temperature (19-21 °C) with a patch-clamp amplifier (Model 8900, Dagan Instruments, Minneapolis, MN). Analog signals were low-pass filtered below 2.5 KHz with an 8 pole Bessel filter and were digitized on line at 6 KHz (FastLab, Indec, Capitola, CA). Membrane voltage was normally held at 0 mV and membrane currents were activated either by 110 msec long step changes to -40 mV or with a continuous voltage ramp that swept between -70 and +70 mV at a rate of 228 mV/s. In measurements with

Table 1

Solutions of defined free Ca⁺⁺ concentration using HEDTA

Free calcium	solution A	solution B
20 μ M	0.0586	0.9414
5 μ M	0.1993	0.8007
1 μ M	0.5545	0.4455
500 nM	0.7134	0.2866
300 nM	0.8059	0.1942
100 nM	0.9256	0.0744
50 nM	0.9614	0.0386
30 nM	0.9765	0.0235
10 nM	0.9920	0.0080

voltage ramps, the voltage was stepped from 0 to -70 mV and held at that value for 200 msec before applying the voltage ramp. This was necessary because in the presence of divalent cations there is a time dependent change in membrane current amplitude on switching from 0 to -70 mV. This time-dependent change is due to the well characterized voltage-dependent channel block by divalent cations (in rods: Zimmerman and Baylor, 1992; in cones Picones and Korenbrot, 1995). To generate I-V curves, the voltage ramp was swept in four successive trials and the currents were signal averaged. Between voltage ramp trials, membrane voltage was held at 0 mV for 1.2 sec. As usual, outward currents are positive and the extracellular membrane surface is defined as ground.

We began every experiment by determining the current amplitude before and after adding saturating cGMP concentrations. We frequently found (>50%) that membrane patches did not respond initially to the ligand. In many instances these patches became responsive after rapidly moving the electrode tip across the air-water interface. It is likely, therefore, that unresponsive patches had formed closed vesicles that opened upon crossing the air-water interface (Horn and Patlak, 1980). We only analyzed data measured in patches in which the amplitude of the current generated with saturating cGMP concentrations and the leakage current measured in the absence of cGMP did not change by more than 10% over the course of the entire experiment. Functions were fit to experimental data by least square minimization algorithms (Origin, MicroCal software, Northampton, MA). Experimental errors are presented as standard deviations.

UCST LIBRARY
JAN 17 1997

Results

The $K_{1/2}$ of the cGMP-gated currents in cones is modulated by divalent cations.

We investigated cGMP-dependent currents in inside-out patches detached from the plasma membrane of retinal cone outer segments. These patches contain only cGMP-gated ion channels (Miller and Korenbrot, 1993a). The dependence of current amplitude on cGMP concentration is well described by the Hill equation (Figure 1):

$$I = I_{max} \frac{[cGMP]^n}{[cGMP]^n + K_{1/2}^n} \quad \dots (1)$$

where I is the amplitude of the cGMP-dependent membrane current, I_{max} is its maximum value, $[cGMP]$ is the concentration of cGMP, $K_{1/2}$ is that concentration necessary to reach one half the value of I_{max} and n is a parameter that reflects the cooperative interaction of cGMP molecules in activating the membrane current.

The cGMP-dependence of the membrane current depends on the history of exposure of the membrane patch to divalent cations. In Figure 1 we present cGMP-dependent currents measured in a cone membrane patch in response to -40 mV voltage steps and in the presence of 20 μM Ca^{++} and 100 μM Mg^{++} . Currents were measured in the same patch both before and after exposure to the EDTA/EGTA solution (panels A and B). Also illustrated is the dependence of current amplitude on cGMP concentration (panel C). The data points measured both before and after exposing the patch to EDTA/EGTA were well fit by equation 1, but the values of $K_{1/2}$ and n are different. The average value of $K_{1/2}$ shifted from $86.1 \pm 18 \mu\text{M}$ to $58.8 \pm 19 \mu\text{M}$ upon exposure to EDTA/EGTA. The average value of n shifted from 2.57 ± 0.34 to 1.80 ± 0.23 (Table 2). Experimental data were included in these averages only if cGMP activation was measured in the same patch before and after exposure to the EDTA/EGTA solution. The shift in $K_{1/2}$ and n reflect a divalent cation-dependent mechanism that modulates the channel's sensitivity to the cyclic nucleotide.

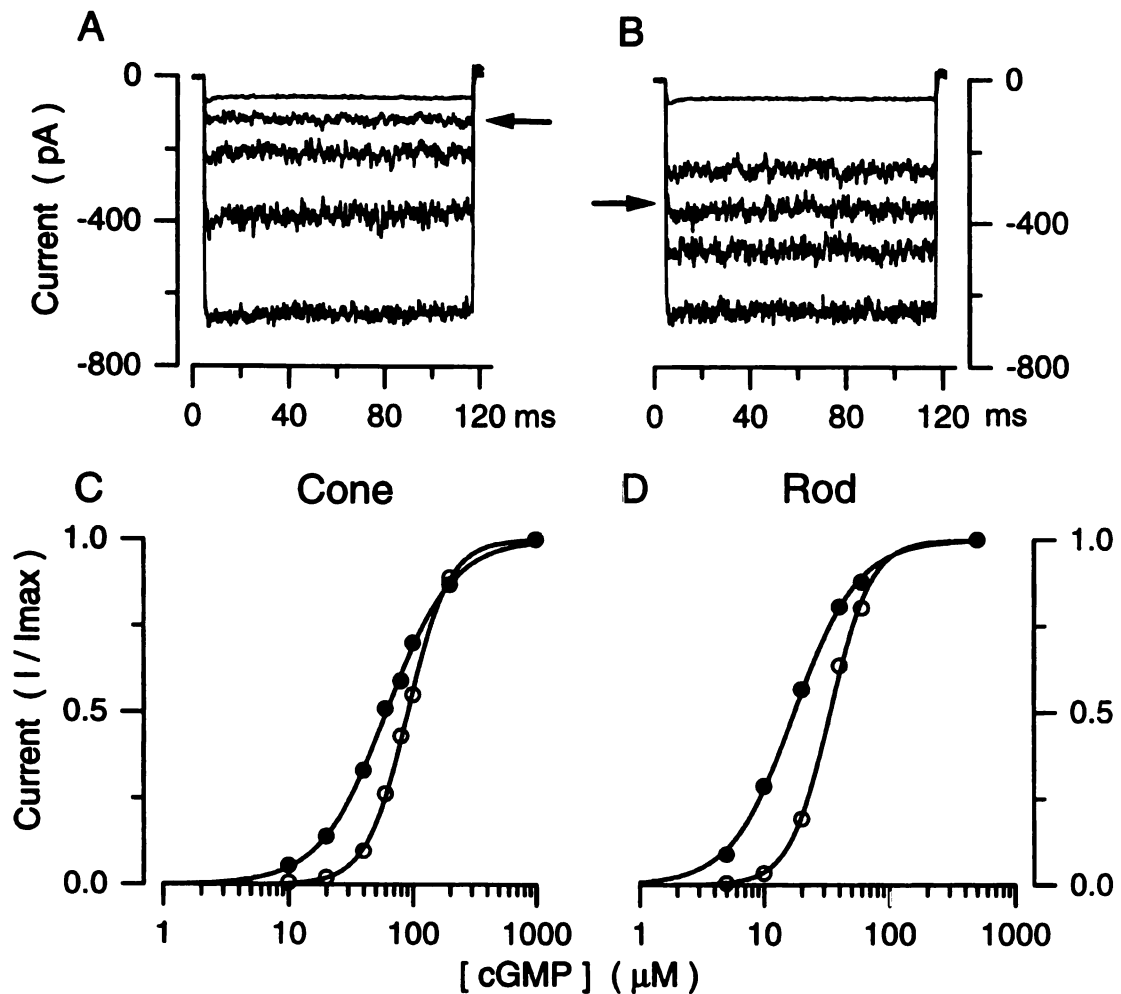


Figure 1. Modulation of cGMP-dependent currents in detached membrane patches. (A) and (B) illustrate currents measured at room temperature in a patch detached from a cone outer segment. Currents were activated with voltage steps from 0 to -40 mV in the presence of 20 μM Ca^{++} and 100 μM Mg^{++} and various cGMP concentrations (shown are currents at 0, 40, 60 (indicated by an arrow), 100 μM and 1 mM). Currents shown in (A) were measured shortly after patch excision, while those in (B) were measured in the same membrane following exposure to the EDTA/EGTA solution. The lower panels illustrate the dependence of normalized current amplitude on cGMP concentration at -40 mV before and after exposure to the EDTA/EGTA solution. Data points were normalized by dividing the amplitude at each cGMP concentration tested (I) by the maximum current (I_{max}). (C) illustrates data measured in a patch detached from a cone outer segment. The continuous curve is the best fit to the data of the Hill equation (text equation 1) with $K_{1/2} = 88.4 \mu\text{M}$ and $n = 2.73$ before exposure to EDTA/EGTA and $K_{1/2} = 61.4 \mu\text{M}$ and $n = 1.59$ afterwards. (D) illustrates data measured in rod membrane patches, where the continuous curve is the Hill equation with $K_{1/2} = 34.2 \mu\text{M}$ and $n = 2.3$ before exposure to the EDTA/EGTA solution and $K_{1/2} = 17.9 \mu\text{M}$ and $n = 1.6$ afterwards.

Table 2

Modulation of cyclic nucleotide-gated currents in
membrane patches of rods and cone*[□]

	cGMP					
	Cone			Rod		
	$K_{1/2}$ (μ M)	n	N	$K_{1/2}$ (μ M)	n	N
<u>Before</u> exposure to EDTA/EGTA solution	86.1 ± 18	2.57 ± 0.34	8	41.1 ± 7	2.58 ± 0.43	9
<u>After</u> exposure to EDTA/EGTA solution	58.85 ± 19.3	1.8 ± 0.23	8	27.5 ± 6.2	1.97 ± 0.28	9
With added calmodulin (200 nM)	70.4 ± 17.5	2.1 ± 0.25	8	37.3 ± 8.8	2.44 ± 0.48	9
	8Br-cGMP					
	Cone					
	$K_{1/2}$ (μ M)	n	N	$K_{1/2}$ (μ M)	n	N
<u>Before</u> exposure to EDTA/EGTA solution	22.1 ± 3.1	2.29 ± 0.39	6			
<u>After</u> exposure to EDTA/EGTA solution	16.4 ± 3.8	1.54 ± 0.35	6			

* Under all test conditions, currents were measured in the presence of 20 μ M Ca^{++} and 100 μ M Mg^{++}

[□] The means under all conditions tested are statistically different from each other with $p < 0.02$ as determined by a one tail Student t-test. The data for cGMP activation under the three experimental conditions specified were all measured in the same set of 8 membrane patches.

To compare the functional properties of rod and cone cGMP-gated channels, we also investigated the Ca^{++} dependent modulation in patches from the rod outer segments of tiger salamanders (Figure 1, panel D). In these membranes, in the presence of $20 \mu\text{M Ca}^{++}$ and $100 \mu\text{M Mg}^{++}$, $K_{1/2}$ for cGMP was $41.1 \pm 7 \mu\text{M}$ and n was 2.58 ± 0.43 before exposure to EDTA/EGTA and $K_{1/2}$ was $27.5 \pm 6.2 \mu\text{M}$ and n to 1.97 ± 0.28 afterwards (Table 2). Thus, in tiger salamander rods $K_{1/2}$ shifts by about 1.5-fold, similar to findings in frog rods (Gordon et al., 1995). The fractional change in $K_{1/2}$ is thus similar in rod and cone membrane patches.

Modulation of $K_{1/2}$ is not an artifact due to phosphodiesterase activity in the membrane patch

Detached outer segment patches can be structurally complex and may include not only plasma membrane but fragments of disc membranes containing phosphodiesterase (PDE) activity (Ertel, 1990). This may be a particular concern in cone outer segments, where disc and plasma membranes are continuous. The presence of PDE in the patch can lead to the artifactual appearance of variable cGMP titration curves (Ertel, 1990). We tested whether this might be a possible source of experimental artifacts in cone membrane patches by comparing cGMP-activation curves in the presence and absence of 0.5 mM IBMX , a saturating concentration of this effective cone PDE inhibitor (Gillespie and Beavo, 1989). IBMX had no effect whatsoever on the titration curves (data not shown).

We confirmed further that the modulation of $K_{1/2}$ is not an artifact due to the effect of PDE by measuring the properties of membrane currents activated by 8-Br-cGMP. This cGMP analog activates the channels, but is not efficiently hydrolyzed by the photoreceptor PDE (Zimmerman et al. 1985). Figure 2 illustrates currents activated by 8-Br-cGMP and measured in the same patch in the presence of $20 \mu\text{M Ca}^{++}$ and $100 \mu\text{M Mg}^{++}$ before and after exposure to EDTA/EGTA. As with cGMP activation, the

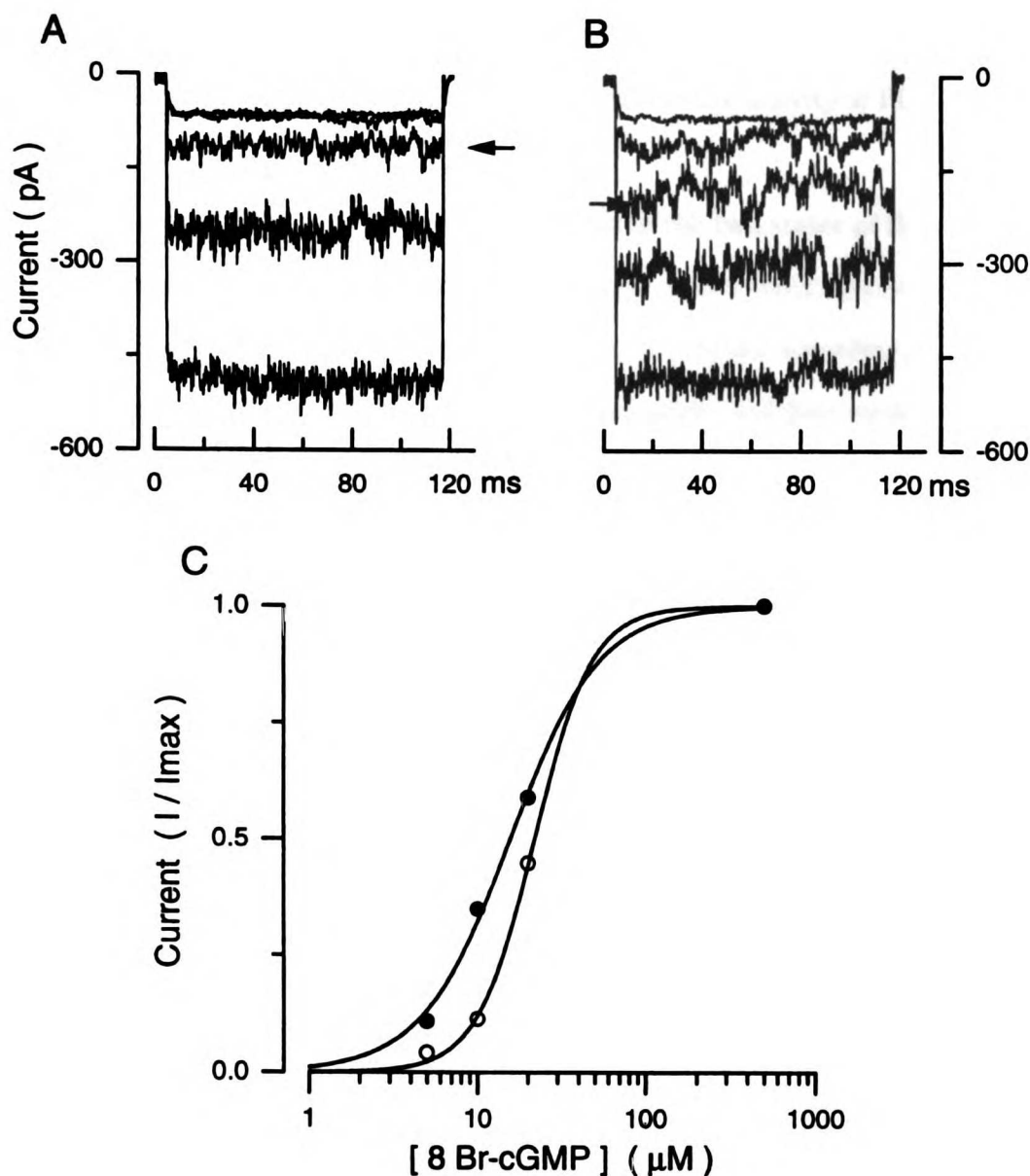


Figure 2. Modulation of 8-Br-cGMP-dependent activation of current in membrane patches detached from cone outer segments. Upper panels illustrate currents measured at room temperature in the same membrane patch before (A) and after (B) exposure to the EDTA/EGTA solution. Currents were activated with a voltage step from 0 to -40 mV in the presence of 20 μM Ca⁺⁺ and 100 μM Mg⁺⁺ and 8-Br-cGMP at 0, 5, 10 (indicated by an arrow), 20 and 500 μM. (C) illustrate the dependence of current amplitude on 8-Br-cGMP before and after exposure to the EDTA/EGTA solution. The continuous line is the best fit to the data of the Hill equation (text equation 1). $K_{1/2} = 22 \mu\text{M}$ and $n = 2.55$ before exposure to the EDTA/EGTA solution and $K_{1/2} = 15.5 \mu\text{M}$ and $n = 1.66$ afterwards.

dependence of current amplitude on 8-Br-cGMP was well described by equation 1 and removal of divalent cations shifted $K_{1/2}$ and n to lower values (Table 1). Thus, modulation of the cGMP-gated currents does not reflect the activity of PDE.

Ion permeation and selectivity are not different in the two states of ligand affinity

We investigated whether the state of modulation affects other functional properties of the cGMP-gated currents. The shape of the I-V curve reflects, according to Eyring rate theory, the energy of interaction between permeant cations and their binding sites within the channel (Alvarez et al. 1992). The success of this theoretical analysis is measured by the ability to predict the shape of the I-V curves measured under various ionic conditions. The I-V curves of the cGMP-gated channels of both cones (Picones and Korenbrot, 1992; Haynes, 1995) and rods (Zimmerman and Baylor, 1992) can be predicted using Eyring rate theory assuming the energy profile across the channels includes one binding site asymmetrically located within the membrane. If the interaction between permeant cations and the channel is affected by the state of modulation, then the shape of the I-V curve should change.

We compared in detail I-V curves measured in the same cone membrane patch before and after exposure to EDTA/EGTA. Figure 3 illustrates membrane currents measured under symmetrical NaCl solutions with 20 μM Ca^{++} and 100 μM Mg^{++} on the cytoplasmic membrane surface and no divalent cations on the extracellular surface. Currents were measured in the presence of various cGMP concentrations in the range between 40 μM and 1 mM, and activated with a continuous voltage ramp between -70 and +70 mV. The I-V curves were non-linear under all cGMP concentrations tested (Figure 3). The non-linearity is generated both by the voltage dependence of cGMP binding and the voltage dependence of divalent block (review in Yau and Baylor, 1989). To analyze the I-V curves, we determined the voltage dependence of the binding curve for cGMP by fitting equation 1 to the current measured at every voltage between -70 and

AMERICAN
LIBRARY
1997

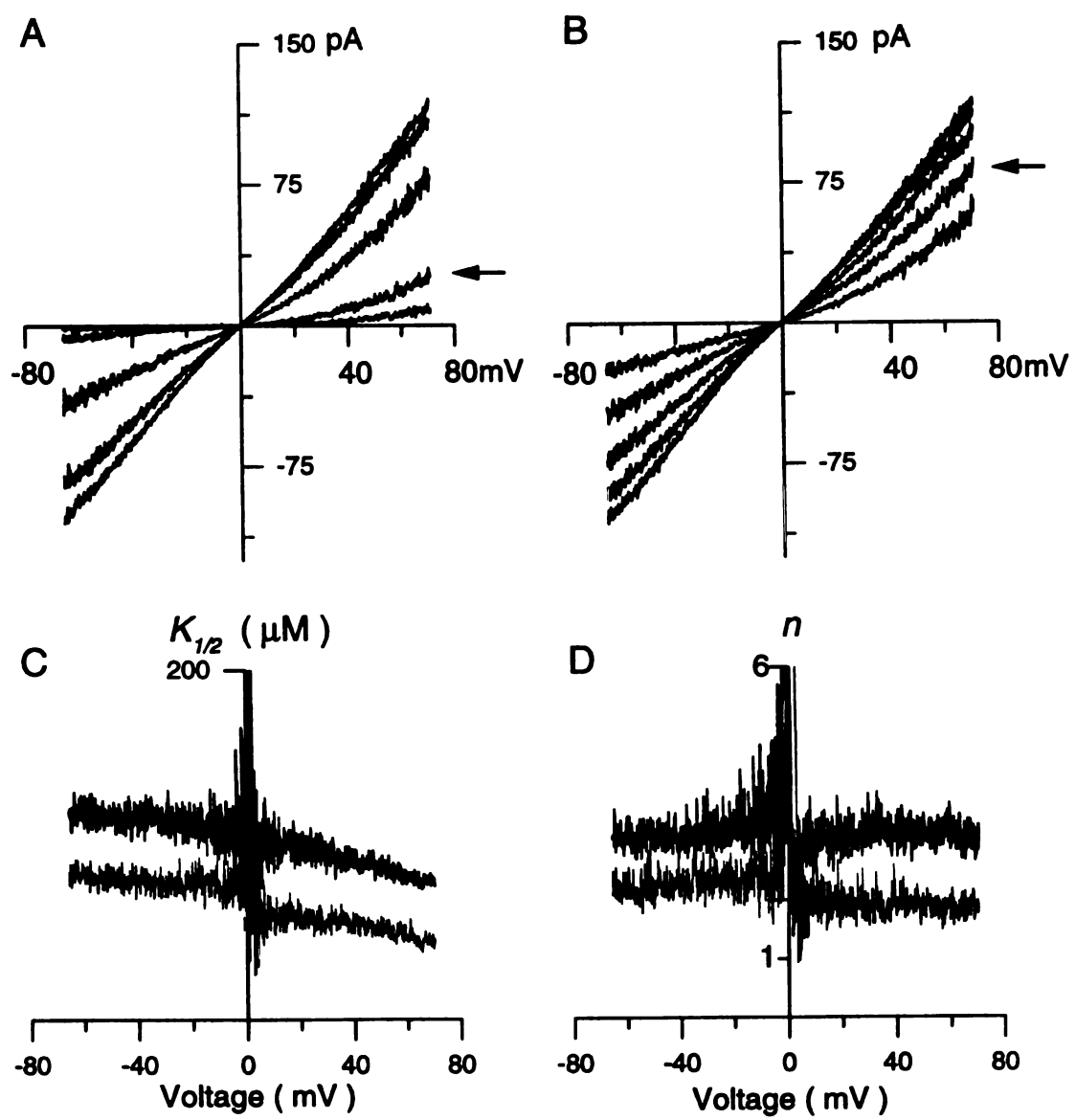


Figure 3. I-V curves measured in the same membrane patch detached from cone outer segment before (A) and after (B) exposure to the EDTA/EGTA solution. Currents were measured in the presence of 20 μM Ca^{++} , 100 μM Mg^{++} and cGMP at 0, 40, 60 (indicated by an arrow), 100, 200 μM and 1 mM on the cytoplasmic surface of the membrane. Currents were activated by a continuous voltage ramp between -70 mV and +70 mV. Each trace is the average of four current ramps from which the average ramp current measured at 0 cGMP has been subtracted. The leak conductance measured at 0 cGMP between 0 and -20 mV was 115 pS. The lower panels illustrate the voltage dependence of the $K_{1/2}$ (C) and n (D) terms in the Hill equation (text equation 1) before (thick trace) and after (thin trace) exposure to the EDTA/EGTA solution .

+70 mV. We found n not to change significantly with voltage either before or after exposure to EDTA/EGTA. $K_{1/2}$, on the other hand, was voltage-dependent, but the form of the voltage dependency was quantitatively the same before and after exposure to EDTA/EGTA (Figure 3). Thus, the I-V curves are not affected by the state of modulation. We obtained similar results in 5 other cone patches and 4 rod patches. Hence, the energy of interaction between cations and the channels, in both rods and cones, does not appear to be affected by the state of channel modulation.

We analyzed the relative Ca^{++} to Na^+ permeabilities of the channels (PCa/PNa) in the two states of ligand affinity. This is a physiologically important feature since PCa/PNa differs in channels of rods and cones (Picones and Korenbrot, 1995; Frings et al., 1995). To determine the value of PCa/PNa , we measured I-V curves (with voltage ramps) under saturating cGMP concentrations (1 mM). The concentration of NaCl was symmetric across the membrane, and we imposed CaCl_2 concentration gradients. The extracellular membrane surface was free of Ca^{++} and the cytoplasmic membrane surface was exposed to concentrations of 5 or 10 mM. The same patch was then exposed to the EDTA/EGTA solution, and the current measurement repeated. Typical results are illustrated in Figure 4. The reversal potential shifted towards negative values as the cytoplasmic Ca^{++} concentration increased, indicating that the channels are more permeable to Ca^{++} than to Na^+ . The magnitude of the shift was the same before and after exposure to EDTA/EGTA. Thus, the state of modulation does not affect the ion selectivity of the cone channels. We obtained the same results in 3 other membrane patches. The values of PCa/PNa , calculated from the shift in reversal voltage (Lewis, 1979), are similar to those we have previously reported (Picones and Korenbrot, 1995).

Effects of Ca^{++} on the endogenous modulation of cGMP affinity

The removal of both Ca^{++} and Mg^{++} results in an irreversible shift of cGMP affinity. We investigated whether this shift was specific for either cation by testing whether the

WEST LIBRARY
MAY 17 1999

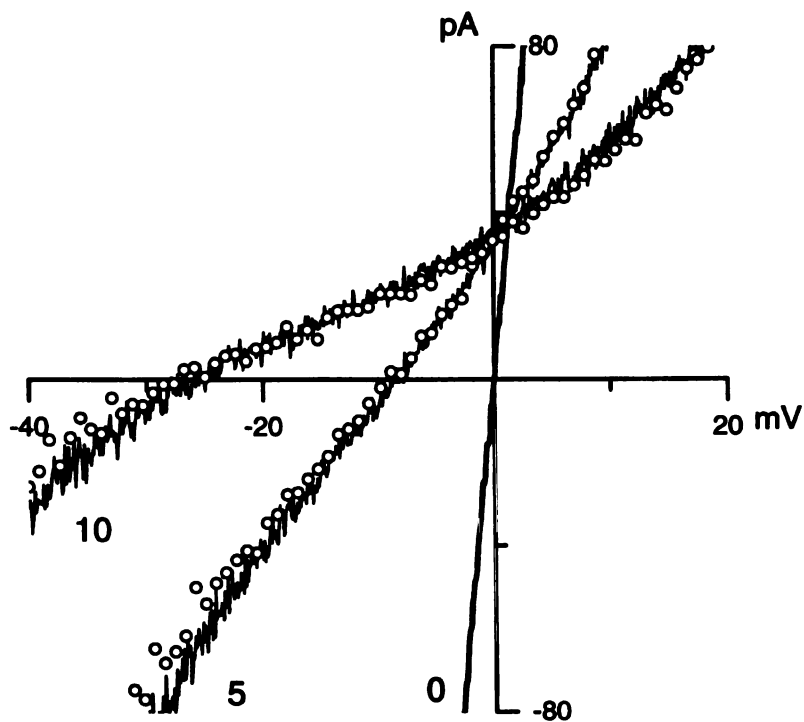


Figure 4. I-V curves measured in the same membrane patch detached from a cone outer segment before (continuous trace) and after (open circles) exposure to the EDTA/EGTA solution. Currents were measured in the presence of 1 mM cGMP and symmetric Na⁺ (167 mM) solutions. The extracellular membrane surface was free of divalent cations, while the cytoplasmic surface was bathed with solutions containing 0, 5 or 10 mM Ca⁺⁺. Currents were activated by a continuous voltage ramp between -70 mV and +70 mV. Each trace is the average of four current ramps, from which the average ramp current measured at 0 cGMP has been subtracted. The leak conductance measured at 0 cGMP between 0 and -20 mV was 70 pS. The value of membrane voltage at zero current reveals that the channels are more permeable to Ca⁺⁺ than to Na⁺, but this selectivity is unaffected by the presence or absence of the endogenous modulator. For the data shown, P_{Ca}/P_{Na}=8.6 calculated at 5 mM assuming a constant field and using ionic concentrations, not activities (Lewis, 1979).

cGMP affinity shifted when only one of the two cations was removed. Removal of Mg^{++} alone did not shift the ligand affinity. Removal of Ca^{++} alone shifted the cGMP activation curve just as when both cations were removed, but the rate of this shift was slower than that caused by the simultaneous removal of both cations.

We explored the effects of varying Ca^{++} concentration on the shift in cGMP affinity. We measured the current activated by 60 μM cGMP in the presence of 20 μM Ca^{++} and 100 μM Mg^{++} , exposed the patch for 60 sec to solutions free of cGMP with the same Mg^{++} but progressively lower Ca^{++} concentrations, and then repeated the current measurement in the 20 μM Ca^{++} , 100 μM Mg^{++} solution with cGMP. The current was unaffected at concentrations as low as 1 μM Ca^{++} . Below this concentration, current amplitude increased as Ca^{++} concentration declined (Figure 5). The increase in current amplitude at a fixed, non-saturating cGMP concentration reflects shifts in $K_{1/2}$ and n to lower values. The current continued to increase, but even at 100 nM Ca^{++} the current increase was not maximal. Addition of EDTA/EGTA achieved the maximum current enhancement and additional washes in EDTA/EGTA caused no further current enhancement (Figure 5). We made the same observations in 6 other patches. Because the shift in $K_{1/2}$ is irreversible, the experimental data do not reflect stationary conditions and, therefore, cannot be quantitatively analyzed as equilibrium dose-response data. Nonetheless, the results indicate that in detached patches, cGMP affinity is specifically modulated by Ca^{++} over a concentration range limited by about 1 μM at its upper end.

The effects of exogenous calmodulin

In rods, the Ca^{++} -dependent modulation of ligand affinity has been attributed to the action of an endogenous factor similar, and perhaps identical, to calmodulin. Calmodulin confers Ca^{++} -dependence to the cGMP activation of the channels with features that are almost indistinguishable from those of the endogenous modulator (Hsu and Molday, 1993; Gordon et al., 1995; Bauer, 1996). We explored the potential role of

AMERICAN
LIBRARY
-CSM

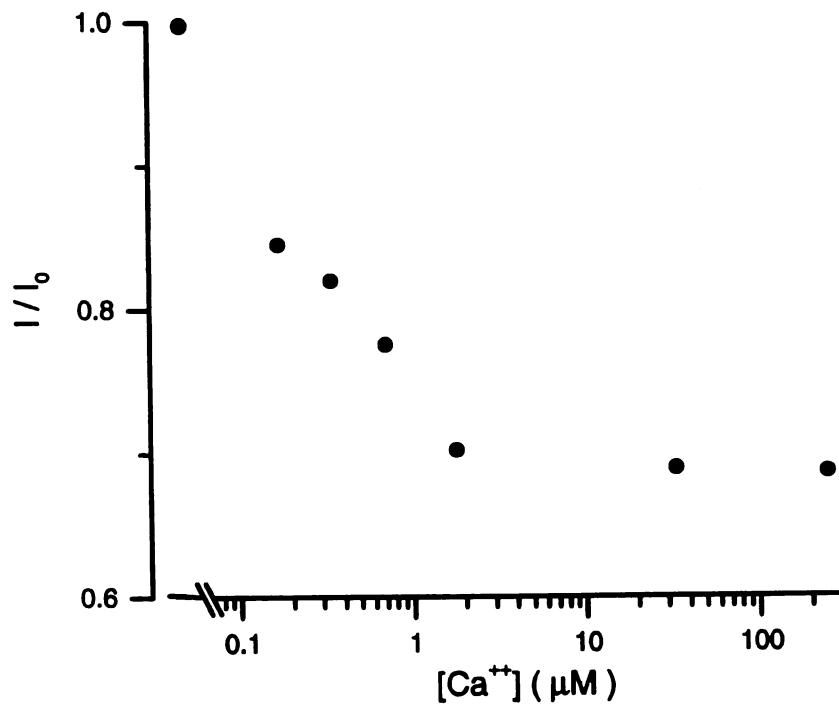


Figure 5. Ca^{++} -dependence of current amplitude in the presence of the endogenous modulator in a cone outer segment membrane patch. Currents, activated by changing membrane voltage from 0 to -40 mV, were repeatedly measured in the same patch in the presence of 60 μM cGMP, 20 μM Ca^{++} and 100 μM Mg^{++} following 60 sec exposure to solutions containing progressively lower Ca^{++} concentrations. Data points were normalized by dividing current amplitude measured after each Ca^{++} concentration tested (I) by the amplitude measured after exposure to a Ca^{++} free solution (EDTA/EGTA solution) (I_0). The data point on the far left indicates I_0 . This is the maximum possible current since repeated washes in EDTA/EGTA solution did not result in any additional current enhancement.

calmodulin in the modulation of channels in cone outer segments. In these experiments, we measured the cGMP concentration dependence of currents in the presence of 20 μM Ca^{++} and 100 μM Mg^{++} . The membrane patch was tested before and after exposure to EDTA/EGTA and then again in the continuous presence of calmodulin at a concentration of 200 nM. This concentration is effective in rod membrane patches (Gordon et al., 1995, Haynes and Stotz, 1997) and is well above the concentration that saturates modulation in rod membrane vesicles (Hsu and Molday, 1993; Bauer, 1996). In any event, the concentration of calmodulin used when testing its pharmacological action affects the Ca^{++} dependence of the phenomenon under study, but not its features at saturating Ca^{++} concentrations (see Bauer 1996 for detailed mathematical analysis).

Figure 6 illustrates typical results obtained in both rods and cones. In patches from both photoreceptor types, as expected, exposure to EDTA/EGTA lowered the values of $K_{1/2}$ and n in the cGMP titration curves. The addition of calmodulin in the presence of Ca^{++} shifted $K_{1/2}$ and n back towards their initial values. Whereas $K_{1/2}$ and n essentially reverted to their starting values in rods, the shift was never fully reversed in cones (Table 2). Thus, channels of cones and rods differ in the effectiveness with which calmodulin in high Ca^{++} shifts their sensitivity to activation by cGMP. In cones, then, the Ca^{++} -dependent regulation of cGMP activation is also likely to reflect the activity of an endogenous modulator. The modulator, however, may not be calmodulin, since this protein does not fully mimic the endogenous function.

Calmodulin competes with the endogenous modulator for binding to the channels

To test whether the endogenous modulator in cones and calmodulin share structural features, we tested whether the two compete in their binding to the channel. We investigated the effectiveness of added calmodulin to shift $K_{1/2}$ or n in the presence and absence of the endogenous modulator. If both molecules bind to the same site, then calmodulin should be without effect when added to the membrane in the presence of the

U.S. LIBRARY

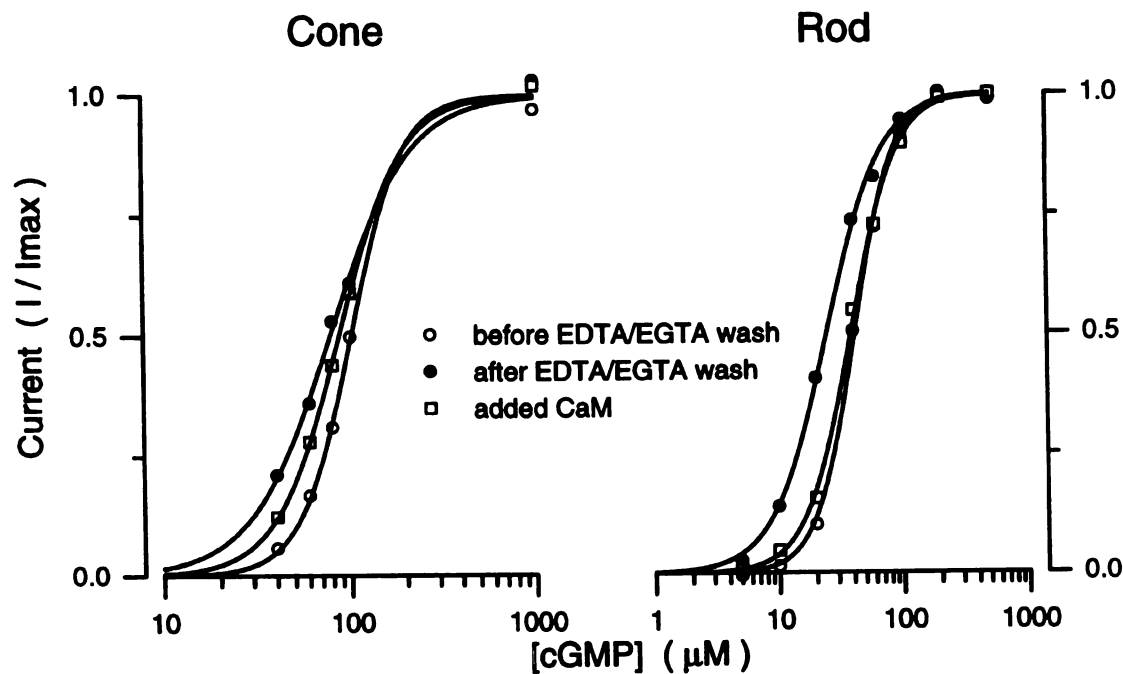


Figure 6. Effect of calmodulin on modulation of cGMP-dependent currents in detached membrane patches. In cone or rod patches, currents were activated with voltage steps from 0 to -40 mV in the presence of 20 μM Ca^{++} and 100 μM Mg^{++} and varying concentrations of cGMP. Measurements were repeated in the same patch before and after exposure to the EDTA/EGTA solution and in the continuous presence of 200 nM calmodulin. Data points were normalized by dividing current amplitude at each cGMP concentration (I) by the maximum current measured (I_{max}). The continuous line is the best fit to the data of the Hill equation (text equation 1). In cones, $K_{1/2} = 101 \mu\text{M}$ $n = 3.15$ before exposure to the EDTA/EGTA solution, $K_{1/2} = 78 \mu\text{M}$, $n = 2.0$ afterwards and $K_{1/2} = 87 \mu\text{M}$, $n = 2.55$ in the presence of calmodulin. For rods, $K_{1/2} = 41.2 \mu\text{M}$, $n = 2.78$ before exposure to the EDTA/EGTA solution, $K_{1/2} = 24.6 \mu\text{M}$, $n = 1.98$ afterwards and $K_{1/2} = 39.4 \mu\text{M}$, $n = 2.47$ in the presence of calmodulin.

endogenous modulator. That is, for calmodulin to be effective, the endogenous modulator must first be removed from its binding site.

We measured membrane currents with voltage steps between 0 and -40 mV in 20 μM Ca^{++} and 100 μM Mg^{++} in the presence of 60 μM cGMP. At this cGMP concentration, lowering $K_{1/2}$ and n will result in an increase in current amplitude despite an unchanging agonist concentration (see Figure 1). In the same patch we measured currents before and after adding 200 nM calmodulin. Calmodulin was without effect on current amplitude in membrane patches maintained in high Ca^{++} and Mg^{++} (Figure 7, panel A). As expected, removal of the endogenous modulator by brief exposure to EDTA/EGTA, shifted $K_{1/2}$ and n and therefore increased the current amplitude (Figure 7, panel B). Following exposure to EDTA/EGTA, added calmodulin was now able to shift $K_{1/2}$ towards its starting value (Figure 7, panel B). We obtained the same results in every patch tested with this protocol ($n=6$). Thus, while calmodulin and the endogenous modulator may not be the same, they appear to compete for a common site on the channels.

Ca^{++} dependence of the calmodulin-mediated modulation.

We investigated whether the channels of rods and cones differ in their interaction with Ca^{++} /calmodulin by testing the Ca^{++} -dependence of cGMP activation in the presence of 200 nM calmodulin. This Ca^{++} -dependence is itself a function of the calmodulin concentration (Bauer, 1996) and therefore it does not inform us as to what the Ca^{++} -dependence of modulation might be in the intact cell, if calmodulin were the modulator. However, it will reflect differences in the energetics of the modulator's binding site between the channels of the two cell types.

We measured the Ca^{++} -dependence of currents in membrane patches of rods and cones in the presence of fixed concentrations of calmodulin and cGMP. In each experiment, membrane patches were first exposed to the EDTA/EGTA solution to remove the endogenous modulator. In patches from single cones, we measured currents

WEST LIBRARY
MAR 27 1997

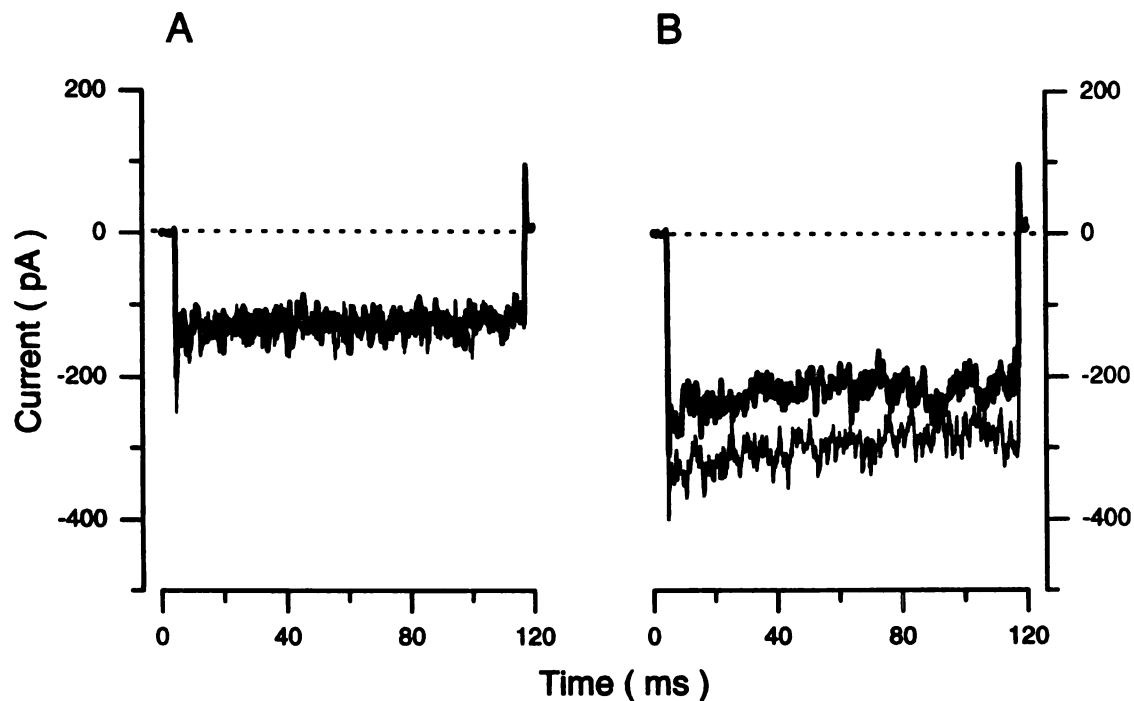


Figure 7. Competition between calmodulin and the endogenous modulator in a cone outer segment membrane patch. Currents were activated with voltage steps from 0 to -40 mV in the presence of $20 \mu\text{M Ca}^{++}$ and $100 \mu\text{M Mg}^{++}$. Shown are difference currents measured by subtracting from currents measured at $60 \mu\text{M cGMP}$ those measured in the absence of the cyclic nucleotide. The leak conductance, measured in 0 cGMP at -40 mV was 325 pS . Currents in (A) were measured shortly after excision in the absence (thick trace) or continuous presence (thin trace) of 200 nM calmodulin. Currents in (B) were measured after exposing the same membrane patch to the EDTA/EGTA solution. Again, currents were measured in the absence (thick trace) or continuous presence (thin trace) of 200 nM calmodulin. Calmodulin is completely ineffective before the endogenous modulator is removed. If the endogenous modulator is first removed by exposure to the EDTA/EGTA solution, calmodulin then causes a shift in membrane current similar in direction, but smaller in extent than that caused by the endogenous modulator.

generated by 110 ms voltage steps to -40 mV in the presence of 60 μM cGMP and varying Ca^{++} concentration between 0 and 20 μM . In the same patch we measured the effects of Ca^{++} first in the absence and then in the presence of 200 nM calmodulin (Figure 8). In cone membranes, Ca^{++} in the absence of calmodulin had a small but reproducible effect on current amplitude. The maximum change in current amplitude between 0 and 20 μM Ca^{++} in the absence of calmodulin was about 5%. In the data shown, we subtracted this effect to obtain the effect of added calmodulin alone. We studied rod channels with the same protocols except that 20 μM cGMP was used to activate the channel. Figure 8 illustrates the Ca^{++} dependence of current amplitude in the presence of calmodulin in typical patches from both rod and cone channels.

The experimental data were well fit by the function:

$$I = (I_{zero} - I_{\infty}) \frac{\frac{1}{[Ca^{++}]^n}}{\frac{1}{[Ca^{++}]^n} + \frac{1}{K_i^n}} + I_{\infty} \quad (2)$$

where I is the current, I_{zero} is the current in the absence of Ca^{++} , I_{∞} is the current in the presence of a saturating Ca^{++} concentration, $[Ca^{++}]$ is the Ca^{++} concentration, K_i is the Ca^{++} concentration at which the current is inhibited by one half and n is a parameter that reflects cooperative interaction of cation binding. This is a modified Hill equation that indicates Ca^{++} interacts cooperatively with calmodulin to block the current amplitude. For cones, $K_i = 366 \pm 131$ nM, $n = 1.6 \pm 0.47$ and $I_{\infty}/I_{zero} = 0.72 \pm 0.16$ (N=9) while for rods, $K_i = 679 \pm 187$ nM, $n = 1.81 \pm 0.44$ and $I_{\infty}/I_{zero} = 0.53 \pm 0.13$ (N=11). These values suggest that Ca^{++} /calmodulin interacts with the cGMP-gated channel of both rods and cones, but the quantitative features of this interaction differ between the two receptor types.

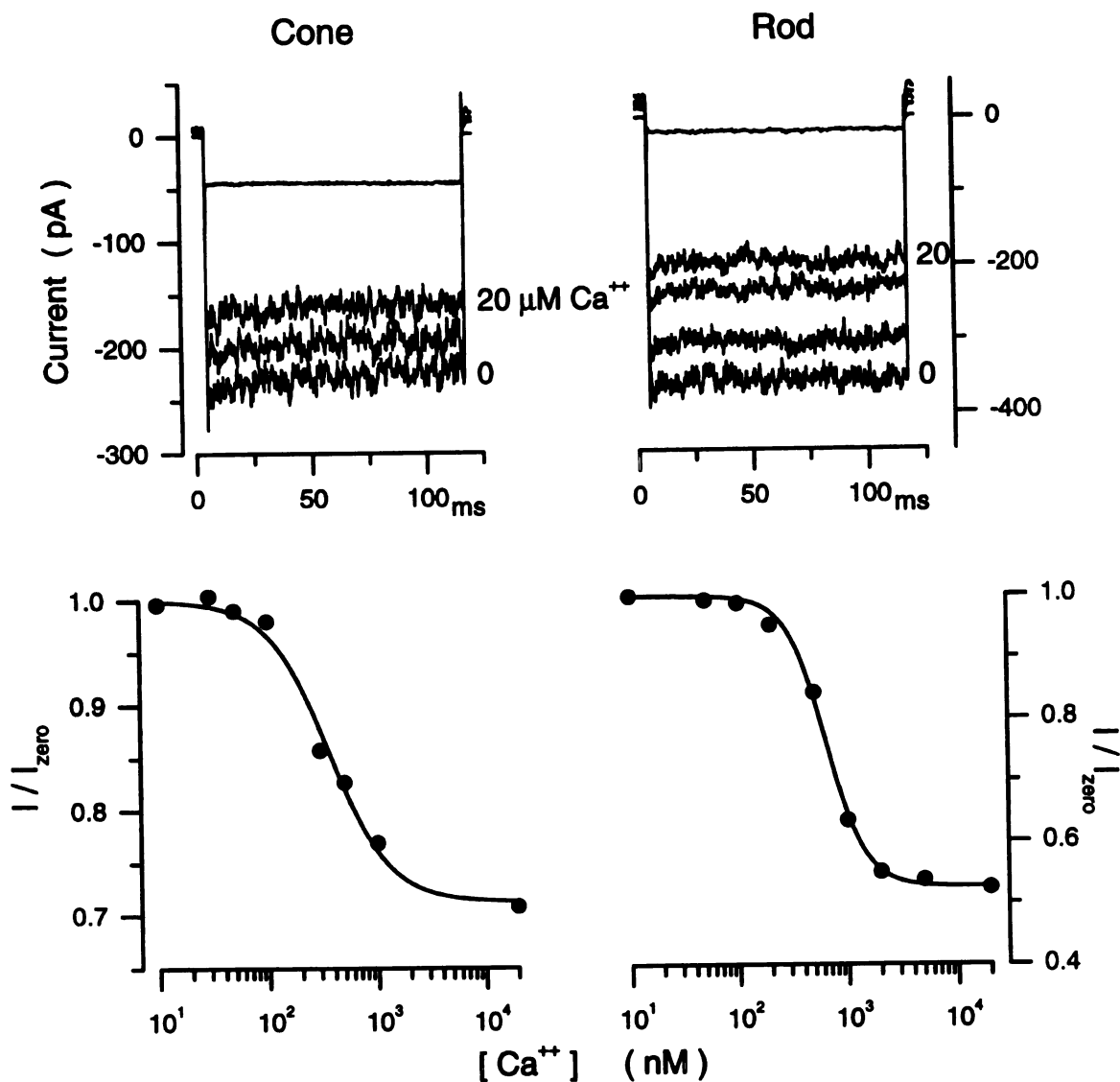


Figure 8. Ca^{++} -dependence of the effect of calmodulin on rod and cone membrane patches. Patches were first exposed to the EDTA/EGTA solution and then to one containing 200 nM calmodulin and various Ca^{++} concentrations. Currents were activated with voltage steps from 0 to -40 mV in the presence of 60 μM cGMP for cones and 20 μM cGMP for rods. For cones, shown are currents measured in the presence of cGMP and 0, 300 nM and 20 μM Ca^{++} . For rods, shown are current measured in the presence of cGMP and 0, 500 nM, 1 and 20 μM Ca^{++} . The current tracings also include the current measured in the absence of cGMP (nearly noiseless tracing). Data points are normalized cGMP-dependent current amplitudes calculated by dividing current amplitude at each Ca^{++} concentration (I) by the amplitude measured in the absence of any Ca^{++} (I_{zero}). The continuous curve is the best fit to the data of text equation 2. For cones, $K_i=357$ nM, $n=1.6$ and $I_{\infty}/I_{\text{zero}}=0.73$. For rods, $K_i=632$ nM, $n=2.4$ and $I_{\infty}/I_{\text{zero}}=0.53$.

Discussion

The cGMP-gated ion channels in detached patches from cone outer segments exhibit a Ca^{++} -dependent modulation of their affinity for the cyclic nucleotide. The dependence of current amplitude on cyclic nucleotide concentration is described by the Hill equation (equation 1) and modulation is manifested as a decrease in the apparent binding affinity ($K_{1/2}$) and cooperativity (n) as the Ca^{++} concentration is lowered. We will refer to this as the endogenous modulation of the channel. Endogenous modulation has been previously reported for the cGMP-gated channels of rods, in bovine membrane vesicles (Bauer, 1996); detached frog outer segment patches (Gordon et al., 1995) and truncated outer segments from frogs and tiger salamanders (Nakatani et al. 1995, Sagoo and Lagnado, 1996). In general, the features of channel modulation in the intact cell should not be extrapolated using data from patches alone. In the case of rods, studies in nearly intact truncated outer segments have demonstrated Ca^{++} -dependent modulation of $K_{1/2}$ that is quantitatively the same as that measured in detached membrane patches (Table 3). The caveat has been introduced, however, that the modulation in truncated rods, which is measured under stationary conditions, may underestimate the extent of modulation present in the truly intact cell (Sagoo and Lagnado, 1996). In the case of cones, modulation measured under stationary conditions in the nearly intact outer segment is larger in extent than that observed in detached membrane patches, the $K_{1/2}$ shifts about 4-fold rather than about 1.5-fold (Rebrik and Korenbrot, 1997).

The endogenous modulation is Ca^{++} dependent, but the quantitative features of this dependence cannot be fully studied in membrane patches because modulation is irreversibly lost as Ca^{++} concentration is reduced and, therefore, equilibrium dose-response curves cannot be determined. In cone patches the shift in $K_{1/2}$ is observed at concentrations starting at and below $1 \mu\text{M}$ Ca^{++} in the presence of $100 \mu\text{M}$ Mg^{++} . This differs from data reported for modulation of channels in rods. In rod membrane patches, under experimental conditions similar to those we have reported for cones, modulation

Table 3

Modulation of cGMP-activated current
in rod outer segments

	Membrane Patches			Truncated outer segments		
	$K_{1/2}$ (μM)	n		$K_{1/2}$ (μM)	n	
Endogenous modulator	41.1 ± 7	2.58 ± 0.43	(1)	40	2.4	(2)
				37 ± 8	2.3 ± 0.6	(3)
Free of modulator	27.5 ± 6.2	1.97 ± 0.28	(1)	27	2	(2)
				28 ± 6	2.2 ± 0.6	(3)

(1) Tiger salamander, this report

(2) Bullfrog, Nakatani et al., 1995

(3) Tiger salamander, Sagoo and Lagnado, 1996

occurs starting at and below 22 nM (Gordon et al., 1995). This difference is significant and may suggest that in cones channel modulation may play a role in dim light, when only small changes in Ca^{++} concentration are expected, whereas in rods it may play a relevant role only in signals generated by relatively bright light (see Bauer, 1996). It is important to recognize that the Ca^{++} dependence of modulation reported for other rod preparations, for example, washed bovine membrane vesicles (Bauer, 1996) or amphibian truncated rods (Nakatani et al., 1995, Sago and Lagnado, 1996) may differ from data in detached patches because in each preparation the conditions of equilibrium between the modulator and the channel may be different. In the detached membrane patch the effective concentration of unbound modulator is essentially zero. Therefore, the initial condition (high Ca^{++}) is not at equilibrium and the modulator is kinetically “locked” onto the channel. The only information that can be reliably established is the Ca^{++} concentration at which the modulator becomes “unlocked” over a reasonably short time course (60 secs).

The features of the interaction between the modulator and the channel in the intact cone photoreceptor and its functional role in transduction and/or adaptation are yet to be specified in detail. Although the magnitude of the modulation, a shift of about 1.5-fold in $K_{1/2}$ may appear modest, the effect of this modulation on current amplitude can be expected to be large, particularly at low cGMP concentrations. From our experimental results, the change in current expected when Ca^{++} changes from 1 μM to 10 nM is given by:

$$\frac{I_{lo}}{I_{hi}} = [\text{cGMP}]^{n_{lo}-n_{hi}} \left(\frac{[\text{cGMP}]^{n_{hi}} + K_{hi}^{n_{hi}}}{[\text{cGMP}]^{n_{lo}} + K_{lo}^{n_{lo}}} \right) \quad (3)$$

where I_{lo} and I_{hi} are the currents at 10 nM and 20 μM Ca^{++} , respectively, $[\text{cGMP}]$ is the ligand concentration, K_{lo} and K_{hi} are the values for $K_{1/2}$ and n_{lo} and n_{hi} are the values for n at 10 nM and 20 μM Ca^{++} , respectively. Figure 9 plots equation 3 with $[\text{cGMP}]$ in units

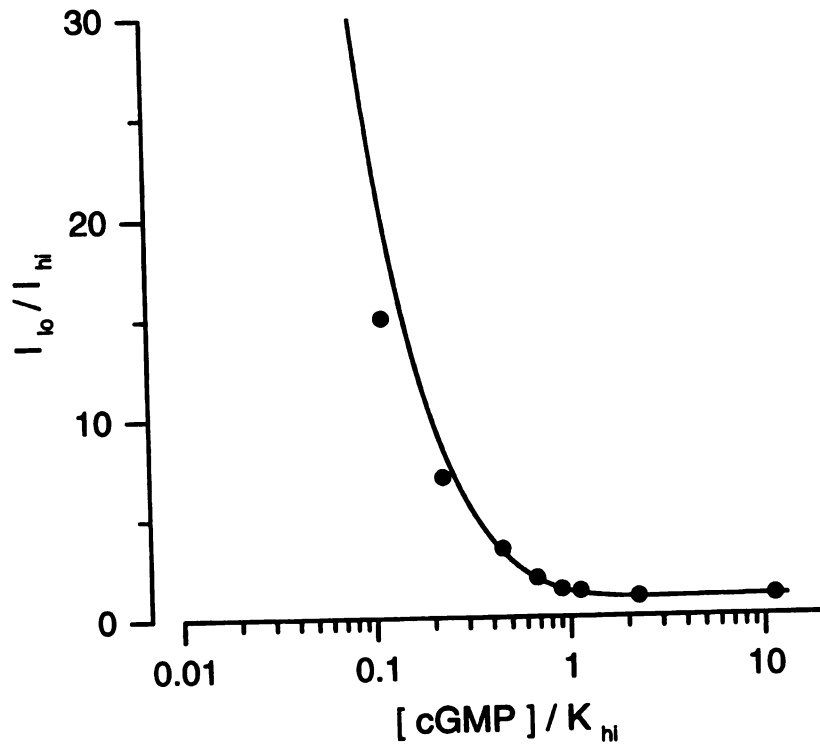


Figure 9. The effect of Ca^{++} modulation of ligand affinity on current amplitude as a function of cGMP concentration. Data points are the ratio of current amplitudes activated by cGMP at -40 mV in the same cone membrane patch before (I_{hi}) and after (I_{lo}) exposure to the EDTA/EGTA solution. cGMP concentration is expressed in units of K_{hi} , the value of $K_{1/2}$ measured before exposure to the EDTA/EGTA solution. The continuous curve is the function presented in the text as equation 3. The data shown are a single set selected because their values are similar to the statistical mean of our experimental sample. For the data shown $K_M=88.4 \mu\text{M}$, $n_M=2.73$ and $K_{lo}=61.4 \mu\text{M}$, $n_{lo}=1.59$.

of K_{hi} . Also shown are data points for currents activated by various cGMP concentrations and measured in a single cone patch before and after exposure to the EDTA/EGTA solution. The concentration of cGMP in the dark can be expected to be between $0.16x$ and $0.31xK_{hi}$ since only 1 to 5% of the channels are open in darkness (Cobbs et al., 1985). Thus, if the modulation of the channel in the intact cell is similar to that in the patch, the amplitude of the light sensitive current could change by as much as 5- to 10-fold in response to changes in cytoplasmic Ca^{++} concentration. As equation 3 indicates, and Figure 9 illustrates, the effectiveness of Ca^{++} as a modulator increases dramatically as the cGMP concentration is lowered. Under steady illumination, when cGMP concentration is expected to be lower than in the dark, the physiological role of Ca^{++} modulation is likely to be especially significant.

The endogenous modulation of $K_{1/2}$ in photoreceptor membrane patches is irreversibly lost upon removal of divalent cations, but can be restored, even if to a limited extent, by calmodulin. These results suggest that endogenous modulation arises from the activity of a "calmodulin-like" protein, since calmodulin not only restores modulation but also competes with the endogenous modulator for the same binding site. As has been argued in reports of similar phenomena in rod patches, it is unlikely that Ca^{++} modulation arises from phosphorylation, since test solutions lacked nucleotides, or from phosphatase activity, because these enzymes are inhibited by lowering Ca^{++} (Gordon et al., 1995). Thus, modulation of both rod and cone channels likely arises from the activity of an endogenous factor that, like calmodulin, interacts with the channel in a Ca^{++} -dependent manner: it is bound to the channels at high Ca^{++} , dissociates from them in the absence of Ca^{++} and is then lost to the solution.

The molecular identity of the endogenous modulator is under investigation. Calmodulin exists at high concentration in the rod outer segment (Kohnken et al., 1981; Bauer, 1996). Hsu and Molday (1993) first reported that calmodulin causes a Ca^{++} -dependent shift in $K_{1/2}$ in rod channels of thoroughly washed bovine outer segment

membrane vesicles (see also Hsu and Molday, 1994, Bauer, 1996). Similarly, Ca^{++} /calmodulin shifts the $K_{1/2}$ of channels in rod outer segment membrane patches (Gordon et al., 1995; Kosolapov and Bobkov, 1996; Haynes and Stotz 1997). Gordon et al. (1995) compared the functional properties of the interaction of the endogenous modulator and calmodulin with the channels in frog rod outer segment membrane patches. Several features of this interaction were quantitatively different between calmodulin and the endogenous modulator, and the authors were not convinced the two molecules were the same. In contrast, Bauer (1996), in studies of bovine rod membrane vesicles, did not find quantitative differences between the endogenous modulator and added calmodulin. Thus, the endogenous modulator in rods is “calmodulin-like”, but it is not possible to confirm that it is calmodulin itself.

In contrast to the relative similarity between calmodulin and the endogenous modulator in studies of isolated rod membranes, added calmodulin was found ineffective in inducing a Ca^{++} -dependent shift of $K_{1/2}$ in truncated rods of tiger salamander from which the endogenous modulator was first removed (Sagoo and Lagnado, 1996). This finding is surprising because calmodulin, independently of whether it is the endogenous modulator, should have had an effect on the truncated outer segment current since it modulates the channel in membrane patches detached from the same cells (our Figure 6), as well as in patches from frog rods (Gordon et al., 1995; Kosolopov and Bobkov, 1996). We do not have a simple explanation for this experimental puzzle, but it is possible that calmodulin cannot efficiently gain access to the channels within the truncated outer segment.

Data are not available on the concentration of calmodulin in cone outer segments nor its association with their cGMP-gated channels. In our direct comparison, we found that calmodulin did not quantitatively mimic the activity of the endogenous factor: Calmodulin shifted $K_{1/2}$ and n to a lesser extent than did the endogenous factor. Indeed, Haynes and Stotz (1997) have reported that in patches of catfish cone outer segments,

calmodulin entirely failed to modulate $K_{1/2}$. They, however, did not explore the properties of a possible endogenous modulator: in their experiments the initial condition was to hold the membrane patch in a solution containing EDTA and EGTA to remove any endogenous modulator. Thus, while calmodulin does not appear to modulate $K_{1/2}$ in catfish cones, whether any modulation occurs at all is unclear. While it might be surprising that cones in striped bass exhibit modulation while those in catfish do not, it is possible. This issue should be addressed experimentally.

The failure of bovine calmodulin to fully mimic the action of the endogenous modulator in striped bass cones could be due to sequence differences between bovine and fish calmodulin, rather than the non identity between calmodulin and the endogenous modulator. This is not likely, however, since the amino acid sequence of calmodulin is nearly 100% identical among vertebrates (Friedberg, 1990). While the endogenous modulator may not be calmodulin in cones, the two molecules are likely to have structural features in common. Calmodulin is a member of a large family of proteins that contain EF hands, a Ca^{++} -binding structural motif consisting of a select sequence of about 30 amino acids that fold into a helix-loop-helix pattern (Kretsinger, 1979; Klee and Vanaman, 1982). Since the endogenous modulator binds Ca^{++} and competes with calmodulin for binding to the channels, it is probably also a member of this family of Ca^{++} binding proteins. We have found, however, that other EF hand-containing proteins expressed in photoreceptors, such as GCAP1 and GCAP 2 (review in Polans et al., 1996) do not restore modulation to the channels. Furthermore, these proteins do not compete with calmodulin for binding to the channels (Hackos, Palcweski, Baher and Korenbrot, unpublished observation). Knowledge of the specificity of interaction with the channel of different members of the EF hand protein family will be important for the eventual identification of the endogenous modulator.

The state of channel modulation does not affect other functional properties of the channel. In both rods and cones the interaction and permeation of mono- and divalent

WOLF LIBRARY

cations with the channel are unaffected by the state of modulation, as is the voltage-dependence of cGMP binding. Since these functional properties likely reflect the structure of the "pore" region of the channel, the interaction between the endogenous modulator and the channel probably occurs in a structural domain distant from the "pore".

The interaction between calmodulin, Ca^{++} and the target protein is complex. The binding affinity of the three elements for each other changes depending on the identity of the target protein. For example, calmodulin in solution binds four Ca^{++} ions with affinities in the micromolar range, but in the presence of a target protein the affinity for Ca^{++} can be elevated by several orders of magnitude (review in Klee, 1988; Gnegy, 1995). Moreover, the Ca^{++} -dependence of a calmodulin-mediated effect on a given target protein changes with the mole ratio of calmodulin to target protein (Bauer, 1996). Therefore, the Ca^{++} -sensitivity of the modulation by calmodulin observed in membrane patches of rods or cones cannot be assumed to be the same as in the intact cell unless the mole ratio of channel to calmodulin were the same. The differences in Ca^{++} -dependence of $K_{1/2}$ modulation in rod and cone channels in the presence of calmodulin must reflect differences in the molecular details of the interaction of calmodulin with the channels.

Reference List

- Alvarez, O, Villaroel, A, and Eisenman, G. 1992. Calculation of ion currents from energy profiles and energy profiles from ion currents in a multibarrier, multisite, multioccupancy channel model. *Meth. Enzymol.* 207:816-854.
- Balasubramanian, S., J.W. Lynch, and P.H. Barry. 1996. Calcium-dependent modulation of the agonist affinity of the mammalian olfactory cyclic nucleotide-gated channel by calmodulin and a novel endogenous factor. *J Membr Biol* 152:13-23.
- Bauer, P.J. 1996. Cyclic GMP-gated channels of bovine rod photoreceptors: affinity, density and stoichiometry of Ca(2+)-calmodulin binding sites. *J Physiol* 494:675-685.
- Baylor, D. 1996. How photons start vision. *Proc Natl Acad Sci U S A* 93:560-565.
- Bonigk, W., W. Altenhofen, F. Muller, A. Dose, M. Illing, R.S. Molday, and U.B. Kaupp. 1993. Rod and cone photoreceptor cells express distinct genes for cGMP-gated channels. *Neuron* 10:865-877.
- Chen, T.Y. and K.W. Yau. 1994. Direct modulation by Ca(2+)-calmodulin of cyclic nucleotide-activated channel of rat olfactory receptor neurons. *Nature* 368:545-548.
- Cobbs, W. H., A. E. Barkdoll III and E. N. Pugh Jr. 1985. Cyclic GMP increases photocurrent and light sensitivity of retinal cones. *Nature.* 317:64-66.
- Ertel, E.A. 1990. Excised patches of plasma membrane from vertebrate rod outer segments retain a functional phototransduction enzymatic cascade. *Proc Natl Acad Sci U S A* 87:4226-4230.
- Fesenko, E.E., S.S. Kolesnikov, and A.L. Lyubarski. 1985. Induction by cyclic GMP of cationic conductance in plasma membrane of retinal rod outer segments. *Nature* 313:310-313.
- Finn, J.T., M.E. Grunwald, and K.W. Yau. 1996. Cyclic nucleotide-gated ion channels: an extended family with diverse functions. *Ann Rev Physiol* 58:395-426.
- Friedberg, F. 1990. Species comparison of calmodulin sequence. *Protein Sequence Data Analysis* 3:335-337.
- Frings, S., R. Seifert, M. Godde, and U.B. Kaupp. 1995. Profoundly different calcium permeation and blockage determine the specific function of distinct cyclic nucleotide-gated channels. *Neuron* 15:169-179.
- Furman, R.E. and J.C. Tanaka. 1990. Monovalent selectivity of the cyclic guanosine monophosphate-activated ion channel. *J Gen Physiol* 96:57-82.

- Gillespie, P.G. and J.A. Beavo. 1989. Inhibition and stimulation of photoreceptors phosphodiesterase by dipyridamole and M&B 22,948. *Mol Pharmacol* 36:773-781.
- Gnegy, M.E. 1995. Calmodulin: Effects of cell stimuli and drugs on cellular activation. *Prog Drug Res* 45:33-65.
- Gordon, S.E., J. Downing-Park, and A.L. Zimmerman. 1995. Modulation of the cGMP-gated ion channel in frog rods by calmodulin and an endogenous inhibitory factor. *J Physiol* 486 :533-546.
- Haynes, L.W. 1992. Block of the cyclic GMP-gated channel of vertebrate rod and cone photoreceptors by l-cis-diltiazem. *J Gen Physiol* 100:783-801.
- Haynes, L.W. 1995. Permeation of internal and external monovalent cations through the catfish cone photoreceptor cGMP-gated channel. *J Gen Physiol* 106:485-505.
- Haynes, L.W. and S.C. Stotz. 1997. Modulation of rod, but not cone, cGMP-gated photoreceptor channel by calcium-calmodulin. *Vis Neurosci* 14:233-239.
- Haynes, L.W. and K.-W. Yau. 1990. Single channel measurement from the cGMP-activated conductance of catfish retinal cones. *J Physiol* 429:451-481.
- Horn, R. and J. Patlak. 1980. Single channel currents from excised patches of muscle membrane. *Proc Natl Acad Sci U S A* 77:6930-6934.
- Hsu, Y.T. and R.S. Molday. 1993. Modulation of the cGMP-gated channel of rod photoreceptor cells by calmodulin *Nature* 361:76-79.
- Hsu, Y.T. and R.S. Molday. 1994 . Interaction of calmodulin with the cyclic GMP-gated channel of rod photoreceptor cells. Modulation of activity, affinity purification, and localization. *J Biol Chem* 269:29765-29770.
- Hurley, J.B. 1992. Signal transduction enzymes of vertebrate photoreceptors. *J Bioenerg Biomembr* 24:219-226.
- Karpen, J.W., A. Zimmerman, L. Stryer, and D.A. Baylor. 1988. Molecular mechanics of the cGMP-activated channel of retinal rods. *Cold Spring Harbor Symposium on Quantitative Biology* 53:325-332.
- Klee, C B. 1988. Calmodulin. *In* Molecular aspects of cellular regulation. Cohen, P. and C. B. Klee, eds. Elsevier, Amsterdam. 35.
- Klee, C.B. and T.C. Vanaman. 1982. Calmodulin. *Adv Protein Chem* 35:213-321.

- Kohnken, R.E., J.G. Chafouleas, D.M. Eadie, A.R. Means, and D.G. McConnell. 1981. Calmodulin in bovine rod outer segments. *J Biol Chem* 256:12517-12522.
- Korenbrod, J.I. 1995. Ca²⁺ flux in retinal rod and cone outer segments: differences in Ca²⁺ selectivity of the cGMP-gated ion channels and Ca²⁺ clearance rates. *Cell Calcium* 18:285-300.
- Kosolapov, A.A. and Y. Bobkov. 1996. Modulation of the cGMP-activated conductance of the plasma membrane of photoreceptor cells by calmodulin. *Biochem Mol Biol Int* 38:871-877.
- Kretsinger, R.H. 1979. The informational role of calcium in the cytosol. *Adv Cyclic Nucleotide Res* 11:1-26.
- Kurahashi, T. and A. Menini. 1997. Mechanism of odorant adaptation in the olfactory receptor cell. *Nature* 385:725-729.
- Lewis, C.A. 1979. Ion-concentration dependence of the reversal potential and the single channel conductance of ion channels at the frog neuromuscular junction. *J Physiol* 286:417-445.
- Liu, M., T.Y. Chen, B. Ahamed, J. Li, and K.W. Yau. 1994. Calcium-calmodulin modulation of the olfactory cyclic nucleotide-gated cation channel. *Science* 266:1348-1354.
- Martell, A E and Smith, R M 1974. Critical Stability Constants, Vol. 1. Plenum Press. New York.
- Menini, A. 1990. Currents carried by monovalent cations through cyclic GMP-activated channels in excised patches from salamander rods. *J Physiol* 424:167-185.
- Miller, D.J. and G.L. Smith. 1984. EGTA purity and the buffering of calcium ions in physiological solutions. *Am J Physiol* 246:C160-C166.
- Miller, J.L. and J.I. Korenbrot. 1994. Differences in calcium homeostasis between retinal rod and cone photoreceptors revealed by the effects of voltage on the cGMP-gated conductance in intact cells. *J Gen Physiol* 104:909-940.
- Miller, J.L. and J.I. Korenbrot. 1993a. In retinal cones, membrane depolarization in darkness activates the cGMP-dependent conductance. A model of Ca homeostasis and the regulation of guanylate cyclase. *J Gen Physiol* 101:933-960.

- Miller, J.L. and J.I. Korenbrot. 1993b. Phototransduction and adaptation in rods, single cones, and twin cones of the striped bass retina: a comparative study. *Vis Neurosci* 10:653-667.
- Molday R S. 1996. Calmodulin regulation of cyclic-nucleotide-gated channels. *Curr Opin Neurobiol* 6:445-452.
- Nakamura, T. and G.H. Gold. 1987. A cyclic nucleotide-gated conductance in olfactory receptor cilia. *Nature* 325:442-444.
- Nakatani, K., Y. Koutalos, and K.-W. Yau. 1995. Ca²⁺ modulation of the cGMP-gated channel of bullfrog retinal rod photoreceptor. *J Physiol* 484:69-76.
- Picones, A. and J.I. Korenbrot. 1995. Permeability and interaction of Ca²⁺ with cGMP-gated ion channels differ in retinal rod and cone photoreceptors. *Biophys J* 69:120-127.
- Picones, A. and J.I. Korenbrot. 1992. Permeation and interaction of monovalent cations with the cGMP-gated channel of cone photoreceptors. *J Gen Physiol* 100:647-673.
- Polans, A., W. Baehr, and K. Palczewski. 1996. Turned on by Ca²⁺! The physiology and pathology of Ca(2+)-binding proteins in the retina. *Trends Neurosci* 19:547-554.
- Pugh, E.N. Jr and T.D. Lamb. 1993. Amplification and kinetics of the activation steps in phototransduction. *Biochim Biophys Acta* 1141:111-149.
- Rebrik, T. and J.I. Korenbrot. 1997. cGMP-gated conductance in intact outer segments of cone photoreceptors with an electroporabilized inner segment. *Inv Ophthal Vis Sci* 38:S722 (Abstract)
- Reed, R.R. 1992. Signaling pathways in odorant detection. *Neuron* 8:205-209.
- Sagoo, M.S. and L. Lagnado. 1996. The action of cytoplasmic calcium on the cGMP-activated channel in salamander rod photoreceptors. *J Physiol* 497:309-319.
- Scott, S.P., R.W. Harrison, I.T. Weber, and J.C. Tanaka. 1996. Predicted ligand interactions of 3'5'-cyclic nucleotide-gated channel binding sites: comparison of retina and olfactory binding site models. *Protein Eng* 9:333-344.
- Weyand, I., M. Godde, S. Frings, J. Weiner, F. Muller, W. Altenhofen, H. Hatt, and U.B. Kaupp. 1994. Cloning and functional expression of a cyclic-nucleotide-gated channel from mammalian sperm. *Nature* 368:859-863.

- Williams D A and F.S. Fay. 1990. Intracellular calibration of the fluorescent calcium indicator Fura-2. *Cell Calcium* 11:75-83.
- Yau, K.W. and D.A. Baylor. 1989. Cyclic GMP-activated conductance of retinal photoreceptor cells. *Annu Rev Neurosci* 12:289-327.
- Yau, K-W and Chen, T-Y. 1995. Cyclic nucleotide-gated channels. *In* Ligand- and voltage-gated channels. R. Alan North, Editor. CRC Press, Boca Raton. 307-337.
- Zagotta, W.N. and S.A. Siegelbaum. 1996. Structure and function of cyclic nucleotide-gated channels. *Annu Rev Neurosci* 19:235-263.
- Zimmerman, A.L. and D.A. Baylor. 1992. Cation interactions within the cyclic GMP-activated channel of retinal rods from the tiger salamander. *J Physiol* 449:759-783.
- Zimmerman, A.L., G. Yamanaka, F. Eckstein, D.A. Baylor, and L. Stryer. 1985. Interaction of hydrolysis-resistant analogs of cyclic GMP with the phosphodiesterase and light-sensitive channel of retinal rod outer segments. *Proc Natl Acad Sci U S A* 82:8813-8817.

Chapter III

Divalent Cation Permeability is a Function of Gating in Native and Recombinant Photoreceptor Cyclic Nucleotide Gated Channels

UWST LIBRARY

Abstract

Cyclic nucleotide-gated ion channels in photoreceptors select Ca^{++} over Na^+ and are blocked by Ca^{++} in a voltage-dependent manner. Previous studies have investigated these features in the presence of cGMP concentrations sufficient to open all available channels. In intact cells, however, at most only a few percent of the channels are open since the physiological cGMP concentration is low. We investigated ion selectivity and channel block as a function of cGMP concentration in membrane patches detached from the outer segments of either tiger salamander rod or striped bass cone photoreceptors. Recombinant bovine rod channels expressed in *Xenopus* oocytes were also examined. We measured I-V curves and reversal potentials in the presence of bi-ionic solutions of differing monovalent cations or in the presence of symmetric solutions of Na^+ with divalent cations added to the cytoplasmic membrane surface. The relative selectivity between Na^+ and either NH_4^+ , Cs^+ , methylammonium or dimethylammonium is the same at all cGMP concentrations tested (from 0 to 1 mM) for the rod, cone channels, and recombinant channels. In contrast, the relative selectivity between Na^+ and either Ca^{++} or Sr^{++} changes by a factor of about 3.42 and 4.25 respectively in rod channels and 1.55 (for Ca^{++}) in cone channels as a function of the cGMP concentration. When both the α and β subunits of the bovine rod channel are expressed, a similar cGMP-dependent shift (2.14-fold) in Ca^{++} selectivity is observed. In contrast, the divalent cation selectivity of channels made from the α subunit alone is independent of cGMP. The dependence of $P_{\text{divalent}}/P_{\text{Na}}$ on cGMP in all channels tested (except those made from α subunits alone) is well described by a Hill function with the same parameters that describes the cGMP dependence of current amplitude (open probability). Thus, surprisingly, the divalent cation selectivity of photoreceptor cyclic nucleotide channels is correlated with gating. These results suggest that the pore can exist in at least one intermediate gating state present at low cGMP concentrations which has divalent cation selectivity properties distinct from those of the fully open state.

Keywords: retina, phototransduction, rod photoreceptor, fish, beta subunit, selectivity

UWST LIBRARY

Introduction

Ion channels gated by cGMP are present at high concentrations in the outer segment membranes of both rod and cone photoreceptors. These channels generate electric signals in response to light-induced changes in the cGMP concentration. In the dark, only a small fraction (1-5%) of the total number of channels are open at any one time (Cobbs et al., 1985). Light activates a cGMP phosphodiesterase (PDE) which lowers the cGMP concentration, causing channels to close, resulting in an electrical response. Therefore, under physiological conditions, the fraction of open channels is always between zero and 1-5%, which implies that the cGMP concentration is significantly lower than the channel's $K_{1/2}$ for cGMP binding.

The pore of the cGMP-gated channel is relatively nonselective, allowing sodium, potassium, calcium and magnesium to permeate the channel under physiological conditions. Calcium permeation is a particularly important property of the pore since calcium acts as a second messenger communicating information about the number of open channels to the cell's internal biochemical machinery (Korenbrod and Miller, 1986; Torre, et al., 1986). In particular, calcium plays a critical role in the process of light adaptation, which does not occur if calcium concentration changes are prevented by manipulation of the solution bathing the cells (Nakatani and Yau, 1988b; Fain et al., 1989; Matthews et al., 1990). Phototransduction in cones is qualitatively similar to that in rods and it is thought that the basic transduction mechanisms are the same (Hestrin and Korenbrot, 1990). However, cones are roughly 10-100 fold less sensitive to light than rods, they have much faster time courses, and are able to adapt over a much greater range of background light illumination than rods. The mechanisms underlying these differences are not known, but may be due in large part to differences in calcium homeostasis between the two cell types (Miller and Korenbrot, 1994a; Miller et al., 1994b) - in particular, differences in the rate of calcium efflux through the Na-Ca,K exchanger and differences in the calcium permeability of the cGMP-gated channels.

WOLF LIBRARY

Exactly how much calcium permeates the channel has been studied in the intact cell by measuring the decay properties of the electrogenic Na-Ca,K exchange pump following a bright light flash, or by measuring the reversal potential when the channel is placed in calcium and sodium gradients. The first technique allows an indirect estimation of the fractional calcium current under physiological conditions, which has been found to be 10-15% in rods and 20-25% in cones (Perry and McNaughton, 1991; Lagnado et al., 1992; Nakatani and Yau, 1988a; Cobbs and Pugh, 1987). Reversal potential measurements have revealed calcium to sodium permeability ratios of 8.3 in rods and 20.3 in cones (Picones and Korenbrot, 1995), indicating that cone channels are about 2.4-fold more permeable to calcium than rod channels. However, all permeability measurements to date have been made with channels opened by saturating and therefore non-physiological concentrations of cGMP. While attempts to calculate fractional calcium current from relative permeability measurements have been made (Wells and Tanaka, 1997; Haynes, 1995a), it has remained an assumption that calcium permeability and other pore properties do not vary as a function of [cGMP].

The classical model of an ion channel pictures the selectivity filter and gate as separate and independent structures (Hille, 1992). Thus, while the gating machinery controls access to the pore, it does not affect pore properties such as ion selectivity. Therefore, classically, calcium permeability would not be expected to vary as a function of [cGMP]. However, two recent sets of experiments indicate that cGMP-gated channels may not function in this classical way: 1) It has been demonstrated (Sun et al., 1996) that the gate and the selectivity filter are confined to the narrow region of the pore. In the closed state of the channel, the pore acts as a gate, preventing all ions from permeating, while in the open state the pore behaves as a selectivity filter, preventing only certain ions from permeating. Thus, the pore changes structure as the channel is gated. 2) Several intermediate gating states (subconductance states) have been identified and the probability of the channel existing in any one substate has been shown to be a function of

the cGMP concentration (Ruiz and Karpen, 1997). Thus, the channel can exist in states with altered pore structure at low cGMP concentrations.

Using excised patches from the outer segment membrane of both rod and cone photoreceptors, we show that the permeability for divalent cations increases as a function of cGMP concentration. This indicates that the channel's gating machinery is coupled to the selectivity filter. We further show that this increase is much greater for rod channels than for cone channels, which reveals that under physiological cGMP concentrations, cone channels are about 7.5-fold more permeable to calcium relative to sodium than rod channels, significantly larger than has been previously measured at saturating concentrations of cGMP. Experiments with recombinant bovine rod channels reveals that cGMP-dependent shifts in divalent cation permeability are a property of heteromeric $\alpha\beta$ channels and not channels made from the α subunit alone. The permeabilities of several monovalent cations relative to sodium were found not to change as a function of [cGMP], including bulky organic cations, implying that the physical size of the pore does not change when the channel is gated, only the relative selectivity for divalent cations. These data indicate that at low cGMP concentrations, the channel can exist in a substate with a different pore structure and therefore different pore properties than the channel state that exists at saturating [cGMP]. This "intermediate" state has lower divalent cation selectivity and possibly increased sensitivity to divalent cation block, but identical pore size and monovalent ion selectivity when compared with the fully open state.

WOLF IDIOT JCMN

Materials and Methods

Materials. We obtained striped bass (*Morone saxatilis*) from Professional Aquaculture Services (Chico, CA) and tiger salamanders (*Ambystoma tigrinum*) from Charles Sullivan (Memphis, TN). We received cGMP and 8-Br-cGMP from Sigma Chemical Co. (St. Louis, MO). 1-cis-diltiazem was a generous gift of Tanabe Seiyako Co., LTD. (Osaka, Japan).

Photoreceptor Isolation. Methods of cell isolation are described in detail elsewhere (Miller and Korenbrot, 1993b; Miller and Korenbrot, 1994a). Animals were dark adapted and retinas were isolated under infrared illumination. Single cones were obtained by mechanical dissociation of Striped Bass retinas maintained in a Ringer's solution consisting of (mM): 143 NaCl, 2.5 KCl, 5 NaHCO₃, 1 Na₂HPO₄, 1 CaCl₂, 1MgCl₂, 5 pyruvate, 10 HEPES, pH 7.5, osmotic pressure 309 mOsM. Rod outer segments were isolated by mechanical dissociation of tiger salamander retinas maintained in a Ringer's solution composed of (mM): 100 NaCl, 2 KCl, 5 NaHCO₃, 1 Na₂HPO₄, 1 CaCl₂, 1 MgCl₂, 5 pyruvate, 10 HEPES, pH 7.5, osmotic pressure 227 mOsM.

Solitary photoreceptors were firmly attached to a glass coverslip derivitized with either wheat germ agglutinin or concanavalin A (Picones and Korenbrot, 1992). The coverslip was placed into the chamber and held firmly down with a glass clamp. Cells were visualized with an upright microscope equipped with DIC optics and operated under visible light. A suspension of photoreceptors in pyruvate Ringer's was placed on the coverslip and the cells were allowed to settle down and attach for 5 min. The bath solution was then exchanged with a Ringer's solution of the same composition, but in which pyruvate was isosmotically replaced with glucose.

The recording chamber consisted of two side-by-side compartments. Cells were held in one compartment that was continuously perfused with Ringer's. The second, smaller compartment was continuous with the first one, but a movable teflon barrier

10071000

could be used to separate them (Picones and Korenbrot, 1992). We used tight-seal electrodes to obtain inside-out membrane patches detached from the side of the outer segments of either cones or rods. After forming a giga-seal and detaching the patch, we moved the electrode under the solution surface to the second compartment and then separated the two compartments using the movable barrier. The tip of the electrode was then placed within 100 μm of the opening of a 30- μm diameter glass capillary. We used this capillary and a rotary valve to deliver selected solutions onto the cytoplasmic surface (outside) of the membrane patch.

Expression of Channels in *Xenopus* oocytes. Plasmids containing either the α or β subunits of the bovine rod channel flanked by the beta-globin 5' and 3' untranslated regions (Liman et al., 1992) were kindly provided by the laboratory of William Zagotta (Univ. of Washington, Seattle, WA). We used this vector linearized with Pst I (α subunit) or Nhe I (β subunit) as a template for *in vitro* runoff transcription. Transcription reactions were conducted using 7 μg of template DNA, 0.33 mM NTPs, 1.33 mM $\text{m}^7\text{G}(5')\text{ppp}(5')\text{G}$ cap analog (GibcoBRL), 10 mM DTT, 150 units of Rnasin (Promega) and 80 units of T7 RNA polymerase (Promega) in an optimized transcription buffer (Promega) with a total volume of 150 μl . This reaction was allowed to proceed for 2.5 hours at 37°C. The Template DNA was then removed by adding 5 units of RQ1 DNase (Promega) and incubating at 37°C for an additional 30 min. We then purified the resulting RNA by extractions with phenol/chloroform (1:1, vol/vol) and chloroform followed by ethanol precipitation. Using this procedure, we generally obtained about 200 μg of RNA, which was resuspended in 100 μl of diethyl pyrocarbonate-treated water at a concentration of about 2 $\mu\text{g}/\mu\text{l}$. Ready-to-inject *Xenopus laevis* oocytes were obtained from the laboratory of L.Y. Jan (Univ. of California, San Francisco, CA). Each oocyte was injected with 45 nl of RNA (90 ng). When both a and b subunits were injected together, we mixed the RNA at a mole ratio of 4:1 (β : α) before injection. The oocytes

were then maintained in ND96 media supplemented with 2.5 mM sodium pyruvate, as well as 100 units/ml penicillin and 100 µg/ml streptomycin at 18°C with continuous gentle agitation. Oocytes were suitable for patch clamp experiments 2-5 days after injection. Immediately before patch clamping, oocytes were incubated for 5 min. in a hypertonic solution composed of (mM): 200 NaCl, 10 HEPES, 1CaCl₂, 1MgCl₂, pH 7.5. The vitelline membrane could then be mechanically removed with fine forceps.

Ionic Solutions. In studies of both rod and cone photoreceptor membranes, we filled the electrodes with the same solution (mM): 150 NaCl, 5 BAPTA, 10 HEPES, adjusted with TMA-OH to pH 7.5, osmotic pressure 300 mOsm. BAPTA was used as a calcium chelator so that any calcium entering the internal solution from the outside was rapidly removed without changing the internal pH, which effects the calcium permeability of cGMP-gated channels (Tanaka, 1993). Free Ca⁺⁺ concentration in this solution was < 10⁻¹⁰ M. In all studies, the patch was initially exposed to a solution composed of (mM): 150 NaCl, 1 EDTA, 1 EGTA, 10 HEPES, adjusted with NaOH to pH 7.5 for at least 2 min. in order to completely remove the endogenous modulator of the channel (Hackos and Korenbrot, 1997).

All solutions (including the solutions described above) were made by mixing calibrated stock solutions. Stock solutions of permeant cations were made by weighing out enough solid to make a 900 mM solution. The osmotic pressures of this solution as well as several serial dilutions were then measured and compared to numbers in the Handbook of Chemistry and Physics (CRC). Any differences were corrected for by either adding more solid or diluting the solution until the numbers matched. This was necessary for obtaining accurate solutions since we found that even new bottles of monovalent or divalent cation chloride salts had absorbed enough water to cause significant errors in cation concentration. TMA-OH was used to titrate the pH in all solutions since it did not add any additional permeant cations.

Solutions used in *Xenopus* oocyte recordings identical to the photoreceptor cell solutions except that Cl^- ions were replaced with methansulfonate in order to eliminate the very large divalent-activated Cl^- conductance in these membranes (Miledi and Parker, 1984). These solutions were made by titrating 150mM methansulfonic acid the appropriate monovalent hydroxide salt. In order to use a AgCl electrode in the absence of Cl^- ions, we designed a pipette holder that included a AgCl plug imbedded in a 1.5% agar solution containing 1M KCl which was immediately adjacent to the methansulfonate internal solution.

Electrical Recordings. Tight-seal electrodes were made from aluminosilicate glass (1724; Corning Glass Works, Corning, NY) (1.5 x 1.0 mm, o.d. x i.d). We measured membrane currents under voltage clamp at room temperature with a patch clamp amplifier (#8900; Dagan Instruments, Minneapolis, MN). Analog signals were low pass filtered below 1.0 kHz with an eight pole Bessel filter and were digitized on line at 3 kHz (FastLab; Indec, Capitola, CA). Membrane voltage was normally held at 0 mV and membrane currents were activated with continuous voltage ramps from either -70 to +70 mV or -30 to +30mV lasting either 1.0 or 0.5 sec. in duration respectively. Before applying the voltage ramp, the voltage was stepped from 0 to -70 mV or from 0 to -30 mV and held at that value for 200 ms. This was necessary because in the presence of divalent cations, there is a time-dependent change in the membrane current amplitude on switching from 0 to -70 mV. This time-dependent change is due to the well characterized voltage-dependent channel block by divalent cations (in rods, Zimmerman and Baylor, 1992; in cones, Picones and Korenbrot, 1995). Between voltage ramps, membrane voltage was held at 0 mV for 2-5 sec. As usual, outward currents are positive and the extracellular membrane surface is defined as ground.

We found that when working with high-current patches in the presence of bi-ionic solutions of monovalent cations, holding the voltage at 0 mV between ramps resulted in a

sustained current (as a result of the non-zero reversal potential) that after a few seconds caused enough cation mixing to alter the measured reversal potential in a cGMP-dependent manner. This problem was completely eliminated by simply setting the holding potential to the reversal potential between ramps. We began each experiment by measuring I-V curves under symmetric NaCl solutions, first in the absence and then in the presence of 1 mM cGMP. The point at which these two curves meet was used to define the zero-voltage point for all the I-V curves measured during the experiment. After the experiments, these curves were again measured. We only analyzed data measured in patches in which this zero-voltage point did not change and in which the leak and saturated conductance did not change by > 10%. Functions were fit to experimental data using least square minimization algorithms (Origin; MicroCal Software, Northampton, MA). Experimental errors are presented as standard deviations.

Permeability Calculations. We calculated permeability ratios using the Goldman-Hodgkin-Katz constant field current equation. Under conditions of bi-ionic monovalent cation solutions, we used the equation:

$$\frac{PX}{PNa} = \frac{[Na]_o}{[X]_i} e^{-\frac{F\Delta V_{rev}}{RT}} \quad (1)$$

where PX/PNa is the permeability ratio of the cation X relative to Na⁺, ΔV_{rev} is the measured reversal potential, [Na]_o is the extracellular Na⁺ activity, and [X]_i is the intracellular activity of cation X. F, R, and T have their usual thermodynamic meanings.

In conditions of symmetric Na⁺ with Ca⁺⁺ (or other divalent cation) added to the intracellular side of the membrane, we used the following equation derived from a more general equation given by (Lewis, 1979)

$$\frac{PCa}{PNa} = \frac{[Na]}{4[Ca]_i} \left(e^{-\frac{2F\Delta V_{rev}}{RT}} - 1 \right) \quad (2)$$

where [Na] is the Na⁺ activity on both sides of the membrane and [Ca]_i is the intracellular Ca⁺⁺ activity.

11/11/11 10:11 AM

Ionic activities for the monovalent cations used in this study were calculated using activity coefficient tables (Robinson and Stokes, 1959). Activity coefficients for Ca^{++} in the presence of monovalent cations were taken from Butler (1968) and then squared in accordance with the Guggenheim convention. Coefficients for Sr^{++} were assumed to be the same as for Ca^{++} .

Results

The ratio between Ca^{++} and Na^+ permeability depends on cGMP concentration

We investigated cGMP-gated channels in inside-out patches detached from the plasma membrane of tiger salamander rod outer segments. These patches contain only cGMP-gated ion channels (Miller and Korenbrot, 1993a). Fig. 1 illustrates I-V curves recorded under conditions of saturating cGMP (500 μM) and in either symmetrical solutions of 150 mM Na^+ , or symmetrical 150mM Na^+ with 10mM Ca^{++} added to the cytoplasmic side of the patch. In the absence of Ca^{++} , the I-V curves exhibited a reversal potential of zero (as is expected under symmetrical solutions), and a slight outward rectification characteristic of rod cGMP-gated channels, as has been noted before (Menini, 1990; Furman and Tanaka, 1990; Zimmerman and Baylor, 1992). The addition of Ca^{++} causes two characteristic changes in the I-V; the reversal potential shifts toward more negative values and the current is blocked by Ca^{++} in a voltage-dependent manner. The negative reversal potential shift indicates that Ca^{++} is more permeable than Na^+ .

We found for the rod channel an average reversal potential shift in 10mM Ca^{++} of -6.3 ± 0.27 mV, which results in an average value for PCa/PNa of 6.48 ± 0.35 (using eqn. 2). This is similar to previously published values measured under conditions of saturating cGMP (Picones and Korenbrot, 1995). However, under physiological conditions, only 1-5% of the total number of channels in the rod outer segment are open in the dark (Cobbs et al., 1985), indicating that the physiological cGMP concentration is very low. To test whether the pore has the same Ca^{++} selectivity at lower and more physiological cGMP concentrations, we measured I-V curves at several subsaturating concentrations of cGMP (5, 10, 20, 40 μM) with symmetric 150mM Na^+ and 10mM Ca^{++} on the cytoplasmic side of the patch (Fig 2a). Since even small changes in the leak current can result in large changes in the apparent reversal potential, we analyzed recordings only when there was no significant change in the leak conductance during a measurement of a collection of I-V

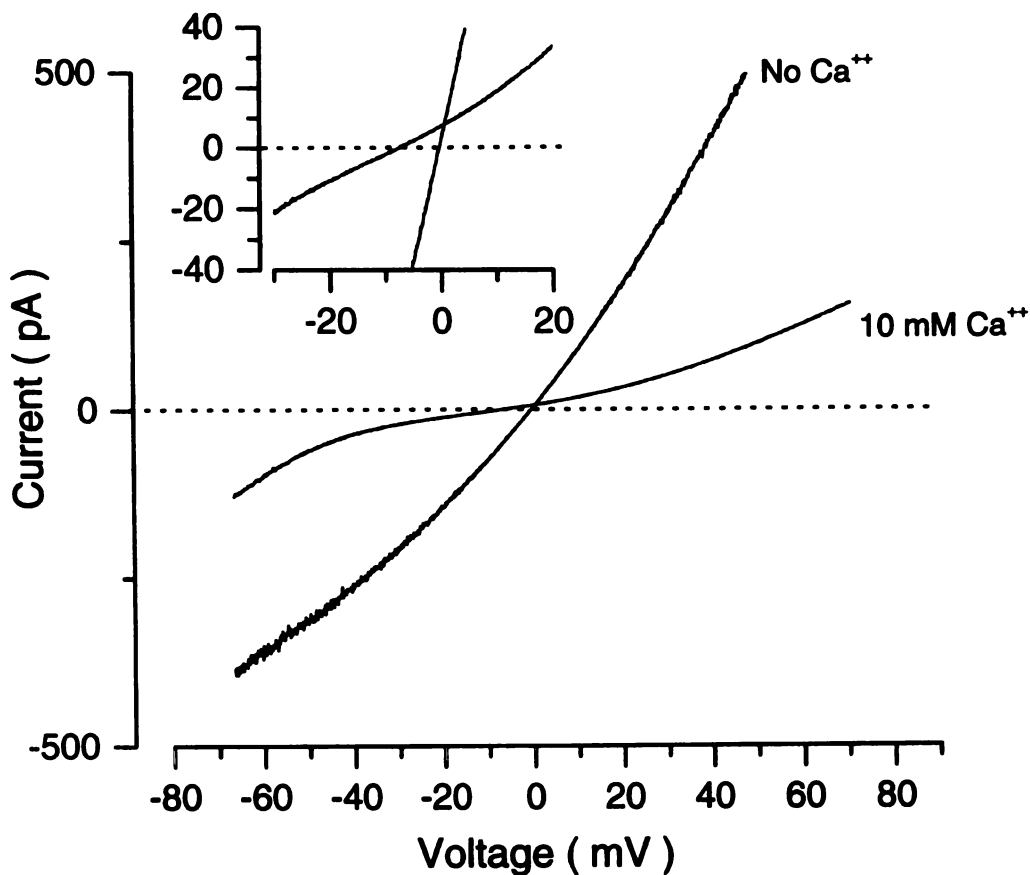


Figure Legends

Figure 1. Effect of 10mM Ca^{++} on the I-V curve recorded from the retinal rod channel. Recordings were made from inside-out patches detached from tiger salamander outer segment membranes. Currents were activated with a voltage ramp from -70mV to $+70\text{mV}$ with a 1 sec timecourse. In conditions of symmetric 150mM NaCl and in the absence of divalent cations, $300\mu\text{M}$ cGMP elicited a large current with a slightly outwardly rectified I-V curve, as shown. With 10mM Ca^{++} added to the cytoplasmic side of the patch, the current it blocked in a voltage-dependent manner and the reversal potential is shifted to the left (inset). This indicates that these channels are permeable to Ca^{++} . The extent of the reversal potential shift in this patch is -7.3 mV , which with eqn. 2 implies $P_{\text{Ca}}/P_{\text{Na}} = 7.8$. The currents shown have been altered by the subtraction of the leak current recorded under the same conditions in the absence of cGMP.

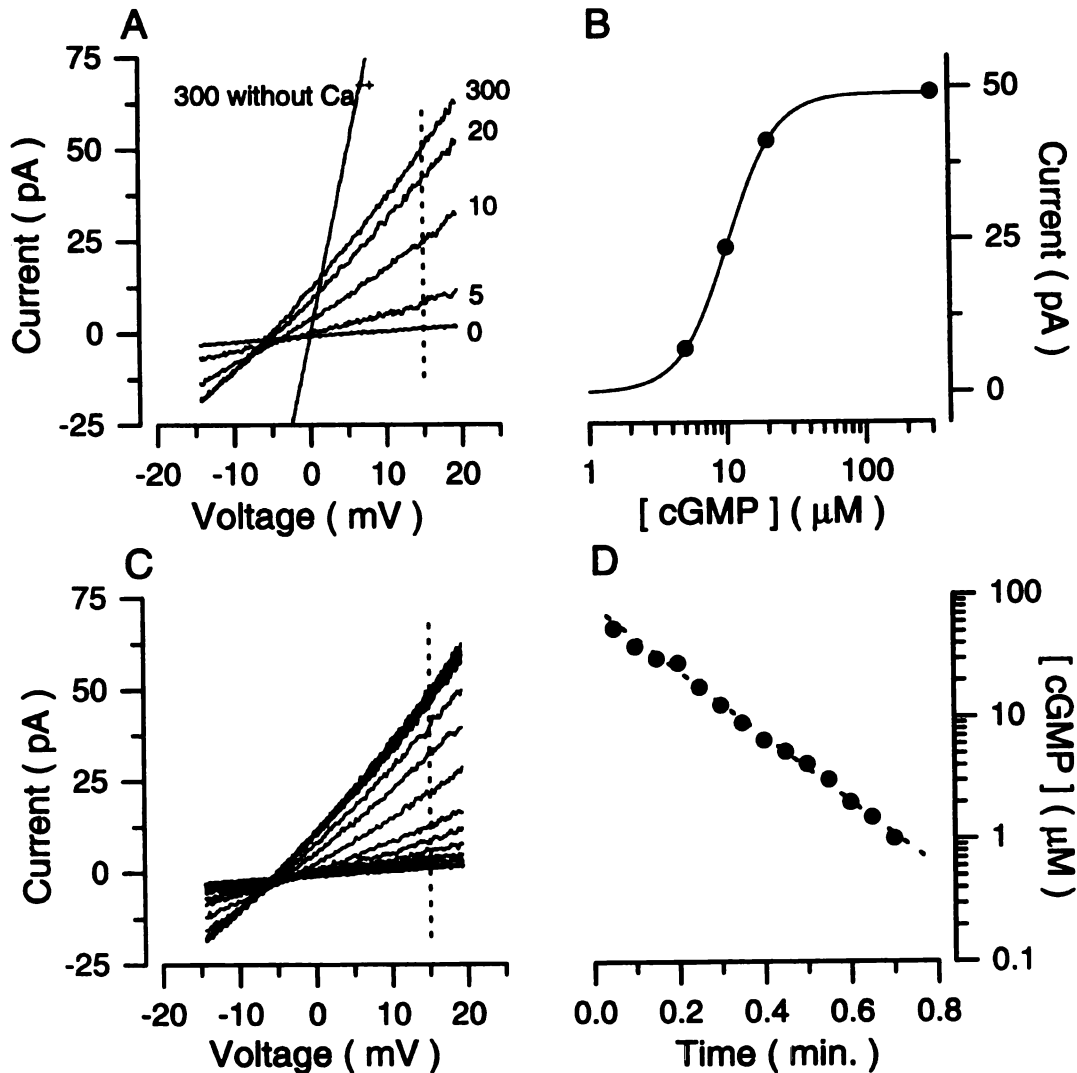


Figure 2. Method for rapidly obtaining large numbers of I-V curves at different cGMP concentrations. Initially, the patch was exposed to a solution 150mM NaCl and I-V curves were recorded in both the absence and presence of 300 μM cGMP (A). The point where these two curves meet is defined as 0 mV for the rest of the experiment. The patch was then exposed to a solution containing both 150mM NaCl and 10mM Ca^{++} . I-V curves under these conditions were then obtained for 0, 5, 10, 20, and 300 μM cGMP (A) using at voltage ramp protocol from -30mV to $+30\text{mV}$. (B) Measurement of the current at $+15\text{mV}$ (indicated by the dashed line) yielded a set a points that could be well fit by a Hill equation with the following parameters: $K_{1/2} = 10.3\mu\text{M}$, $n = 2.48$. This Hill function was then be used to determine the cGMP concentrations for each of the I-V curves shown in panel C. These were recorded by first exposing the patch to 300mM cGMP, and then allowing the cGMP to slowly diffuse out of the patch (which took about 1 min.). The resulting cGMP concentrations were then plotted as a function of time (D). A line could be fit well to these data when graphed on a lin-log plot, indicating that cGMP diffused out of the patch exponentially with a time course of 6 sec.

curves. This however was very difficult to achieve when attempting to measure I-V curves at many different cGMP concentrations. Therefore, we used an alternative method to rapidly record a large number of additional I-V curves at differing cGMP concentrations by first exposing the patch to a pulse of 500 μ M cGMP, and then allowing the cGMP to slowly diffuse out of the patch while repeatedly measuring I-V curves. The rate of cGMP diffusion was highly variable from patch to patch, but in many cases, this timecourse was slow enough (> 1 min) that individual I-V curves (each measured in 1/2 sec) could be assumed to have been measured at constant [cGMP]. To determine the actual values of [cGMP] for each ramp, we measured the $K_{1/2}$ and hill coefficient for the patch. Briefly, a point was chosen from each ramp (usually +15mV) and compared to the following Hill function fitted to the I-V curves measured at known [cGMP] (Fig 2b).

$$I = I_{\max} \frac{[cGMP]^n}{[cGMP]^n + K_{1/2}^n} \quad (3)$$

where I is the amplitude of the cGMP-dependent membrane current, I_{\max} is its maximum value, [cGMP] is the concentration of cGMP, $K_{1/2}$ is that concentration necessary to reach one half the value of I_{\max} and n is a parameter that reflects the cooperative interaction of cGMP molecules in activating the membrane current. The resulting cGMP concentrations were then graphed as a function of time (Fig 2c). A line could be well fit to the points graphed on a log-lin scale, indicating exponential diffusion of cGMP out of the patch as expected for a simple first-order diffusion process.

Fig. 3a shows a blown-up view of the center of several I-V curves measured at different cGMP concentrations. The reversal potential shifts toward less negative voltages as the cGMP concentration decreases. This reveals that the channel becomes more permeable to Ca^{++} as it is gated. Fig. 3b shows the reversal potential plotted as a function of [cGMP] and fig. 3c shows PCa/PNa as calculated by Eqn. 2 plotted as a

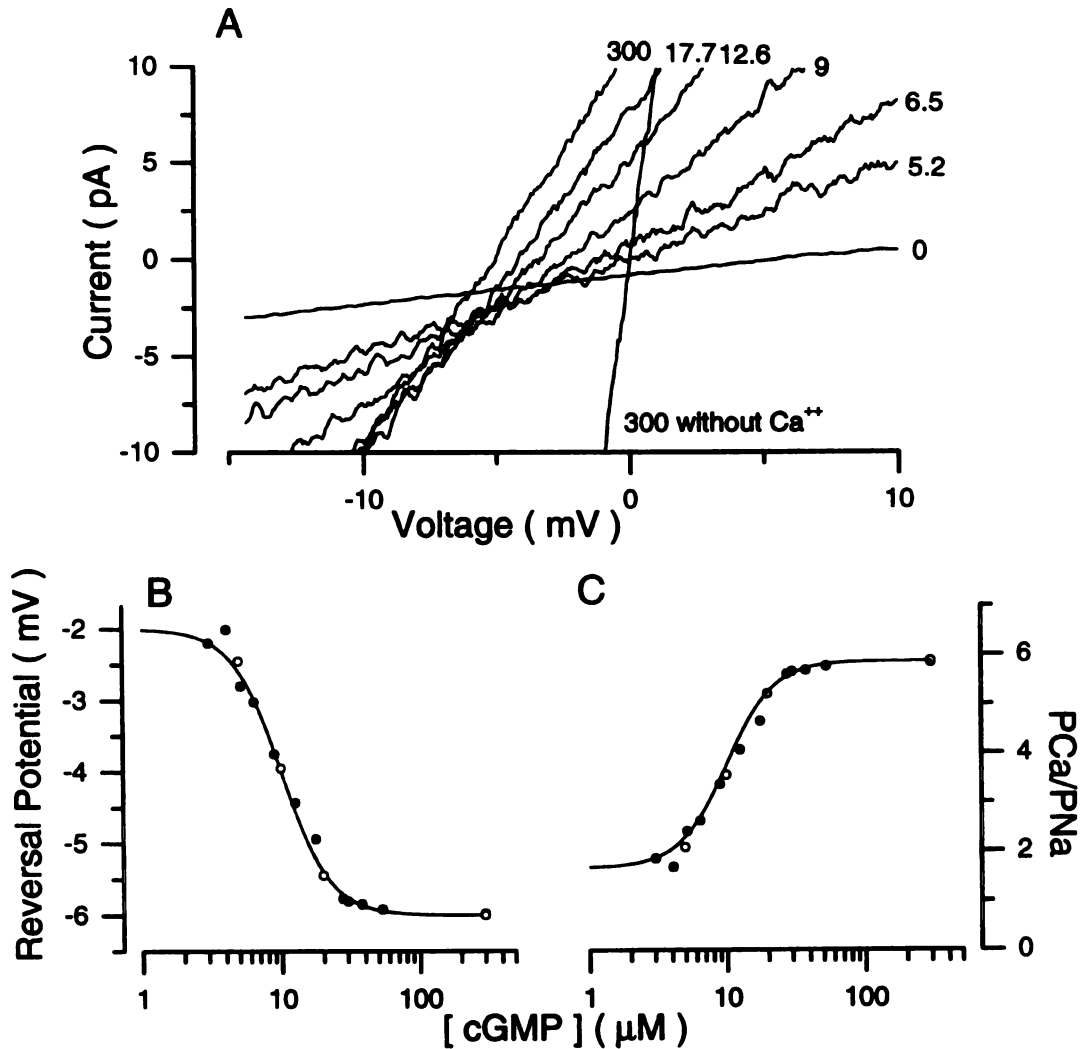


Figure 3. Relative Ca^{++} permeability as a function of cGMP concentration. Panel A shows a blown-up view of the I-V curves shown in fig. 2. The concentration of cGMP calculated for each of the I-V curves is indicated to the right of each curve (in μM). The reversal potentials were measured by fitting a line to the I-V curves from -15 to $+10$ mV. The point with which this line intersected the leak current (recorded in 10mM Ca^{++}) was taken as the reversal potential. These reversal potentials were then plotted with respect to cGMP concentration (B). Open circles indicate reversal potentials measured from I-V curves at experimentally defined cGMP concentrations ($5, 10, 20, 300 \mu\text{M}$). Closed circles are reversal potentials determined from I-V curves measured while allowing cGMP to diffuse slowly out of the patch, where the cGMP concentrations have been determined from the Hill equation (see fig. 2). The curve through the data is the same Hill function ($K_{1/2} = 10.3\mu\text{M}, n = 2.48$) defined for this patch were we have adjusted the minimum and maximum values to fit the data. For this patch, $\text{min} = -2.0$ mV, $\text{max} = -6.1\text{mV}$. Panel C shows the same data after application of eqn. 2 to determine PCa/PNa for each measured reversal potential. Open and closed circles have the same meaning as before. The same Hill function as before was graphed onto the data with $\text{min} = 1.7$ and $\text{max} = 5.93$.

function of [cGMP]. Both reversal potential and PCa/PNa can be well fit to the following Hill function

$$\frac{PX}{PNa} = \min + (\max - \min) \frac{[cGMP]^n}{[cGMP]^n + K_{1/2}^n} \quad (4)$$

by allowing the minimum and maximum values to vary while using the same $K_{1/2}$ and n that describes the cGMP-dependent current as a function of [cGMP]. The minimum value of the Hill function is uncertain due to the difficulty of determining the reversal potential from such a small signal. We found the average parameters to be $\min = 1.89 \pm 0.52$, $\max = 6.48 \pm 0.35$, $K_{1/2} = 17.2 \pm 8.6 \mu\text{M}$, $n = 2.43 \pm 0.37$ ($n=14$). The extent of the decrease in relative Ca^{++} permeability between saturating cGMP and zero cGMP (\max/\min) was found to be on average 3.42 ± 0.95 ($n=14$).

Shifts in the reversal potential are not present in symmetrical Na^+ solutions

Patches excised from the rod outer segment often have so many channels that a -70 mV voltage pulse produces currents as high as 1-2 nA. These high current voltage pulses show an slow exponential decline even in symmetrical Na^+ solutions. This is caused by an accumulation of excess Na^+ ions on one side of the patch, resulting in a Na^+ gradient and thus a shift in the reversal potential (Zimmerman and Baylor, 1992). To verify that the reversal potential shifts observed in the presence of 10mM Ca^{++} while allowing cGMP to slowly diffuse out of the patch are not an artifact caused by this mechanism, we looked for the presence of reversal potential shifts as a function of [cGMP] in symmetrical Na^+ solutions, where no such shifts should occur. Fig. 4a shows I-V curves measured under these conditions at a large number of different cGMP concentrations generated with the cGMP washout technique in a similar way as shown in figs. 2 and 3. Fig. 4b plots the reversal potential as a function of [cGMP], and reveals that the reversal potential is completely independent of [cGMP], as expected. This shows that the shifts

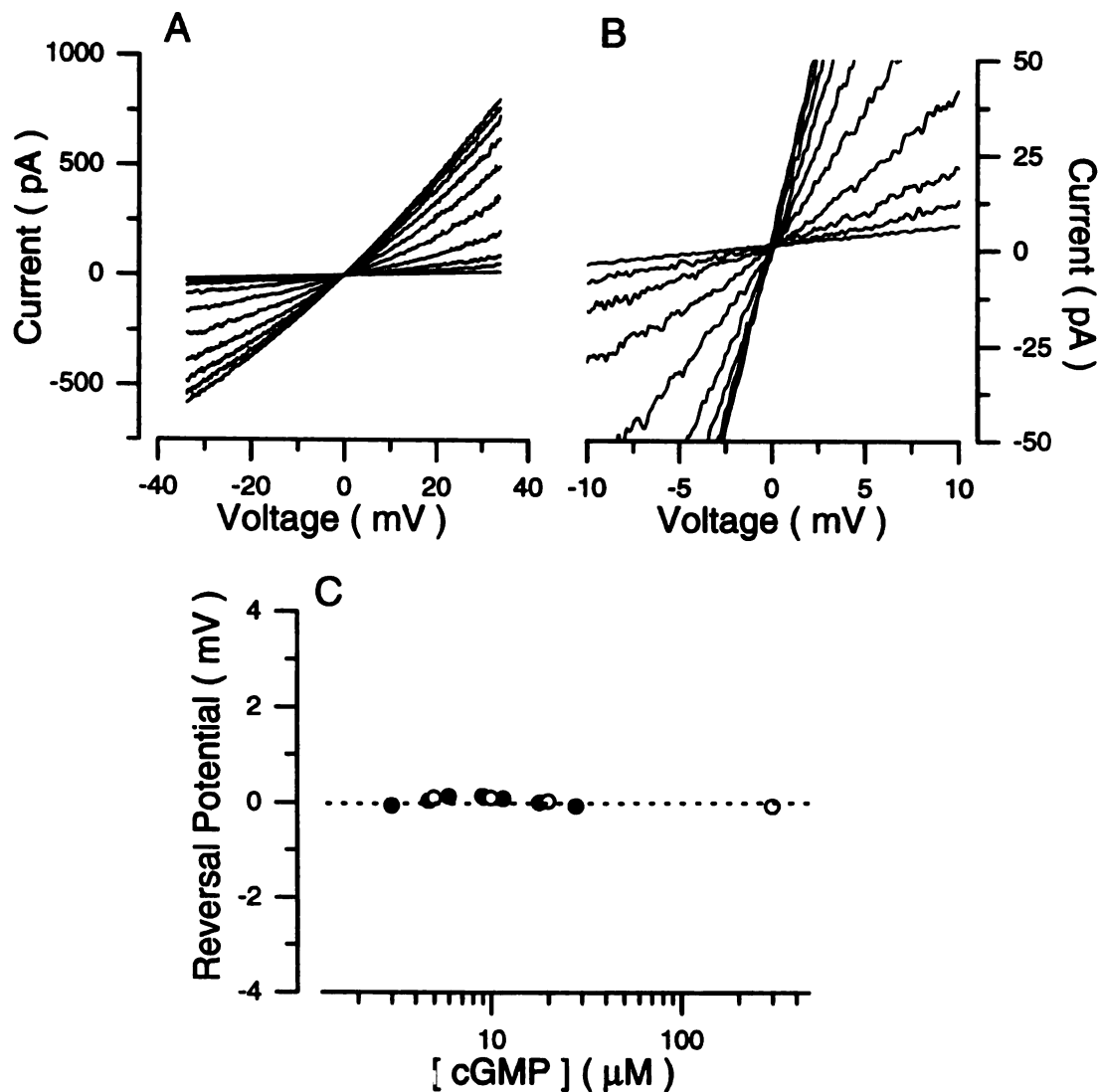


Figure 4. Reversal potential as a function of cGMP in symmetric 150mM NaCl conditions. We activated tiger salamander patches with voltage ramps from -30mV to $+30\text{mV}$ to determine the I-V curves under conditions of symmetric 150mM NaCl solutions. After fitting a Hill function to the current at $+15\text{mV}$ at defined cGMP concentrations ($K_{1/2} = 10.1\ \mu\text{M}$, $n = 2.43$), we exposed the patch to $300\ \mu\text{M}$ cGMP and allowed the cGMP to diffuse out of the patch while recording I-V curves (panel A). A blown-up view near the origin is shown in panel B. The reversal potentials were measured by fitting a line to the data between -10mV and $+10\text{mV}$ and plotted as a function of cGMP concentration (panel C). The reversal potential was zero for all cGMP concentration tested (dashed line).

observed as a function of [cGMP] in the presence of 10mM Ca⁺⁺ are real, and not the result of an artifact due to changes in the Na⁺ gradient. Changes in the Ca⁺⁺ gradient might also occur under these conditions, but this would result in reversal potential shifts in the opposite direction to those observed.

The ratio of Sr⁺⁺ to Na⁺ permeability is also a function of [cGMP]

With the observation that the ratio of the Ca⁺⁺ to Na⁺ permeability changes as a function of [cGMP], it was of interest to determine whether this [cGMP] dependency was true for other divalent cations besides Ca⁺⁺. Mg⁺⁺ was found too difficult to work with since its permeability at saturating [cGMP] is smaller than that of Ca⁺⁺, and it is a more potent blocker of the rod cGMP-gated channel. This makes the reversal potential shifts caused by Mg⁺⁺ difficult to measure, especially at low [cGMP]. While Sr⁺⁺ is also less permeable than Ca⁺⁺, it is a weak blocker, and thus the reversal potential is easy to measure accurately. We recorded I-V curves in the presence of 20mM Sr⁺⁺ applied to the cytoplasmic side of the channel (fig. 5a). In the presence of saturating cGMP (500μM), the reversal potential was found to be -5.3 ± 0.21 mV (n=8). Using eqn. 2, this indicates that $PSr/PNa = 2.71 \pm 0.13$. Fig. 5a shows I-V curves measured under the same ionic conditions with differing [cGMP]. The reversal potential was found to shift to less negative values as [cGMP] was decreased. Fig. 5b plots the reversal potential as a function of [cGMP]. As was found in the case of Ca⁺⁺, the reversal potential shifts due to Sr⁺⁺ could be well fit to a Hill function with $K_{1/2} = 14.8 \pm 6.2$ μM and $n = 2.6 \pm 0.32$ (n=8), identical parameters as the Hill function that describes current as a function of [cGMP] in the presence of 20mM Sr⁺⁺. This was also true for fig. 5c, where PSr/PNa is plotted as a function of [cGMP]. The average parameters obtained (by fitting with eqn. 4) were $\min = 0.64 \pm 0.27$, $\max = 2.71 \pm 0.13$, $K_{1/2} = 14.8 \pm 6.2$, $n = 2.6 \pm 0.32$ (n=8). The extent of Sr⁺⁺ permeability decrease was on average 4.25 ± 2.75 (n=8).

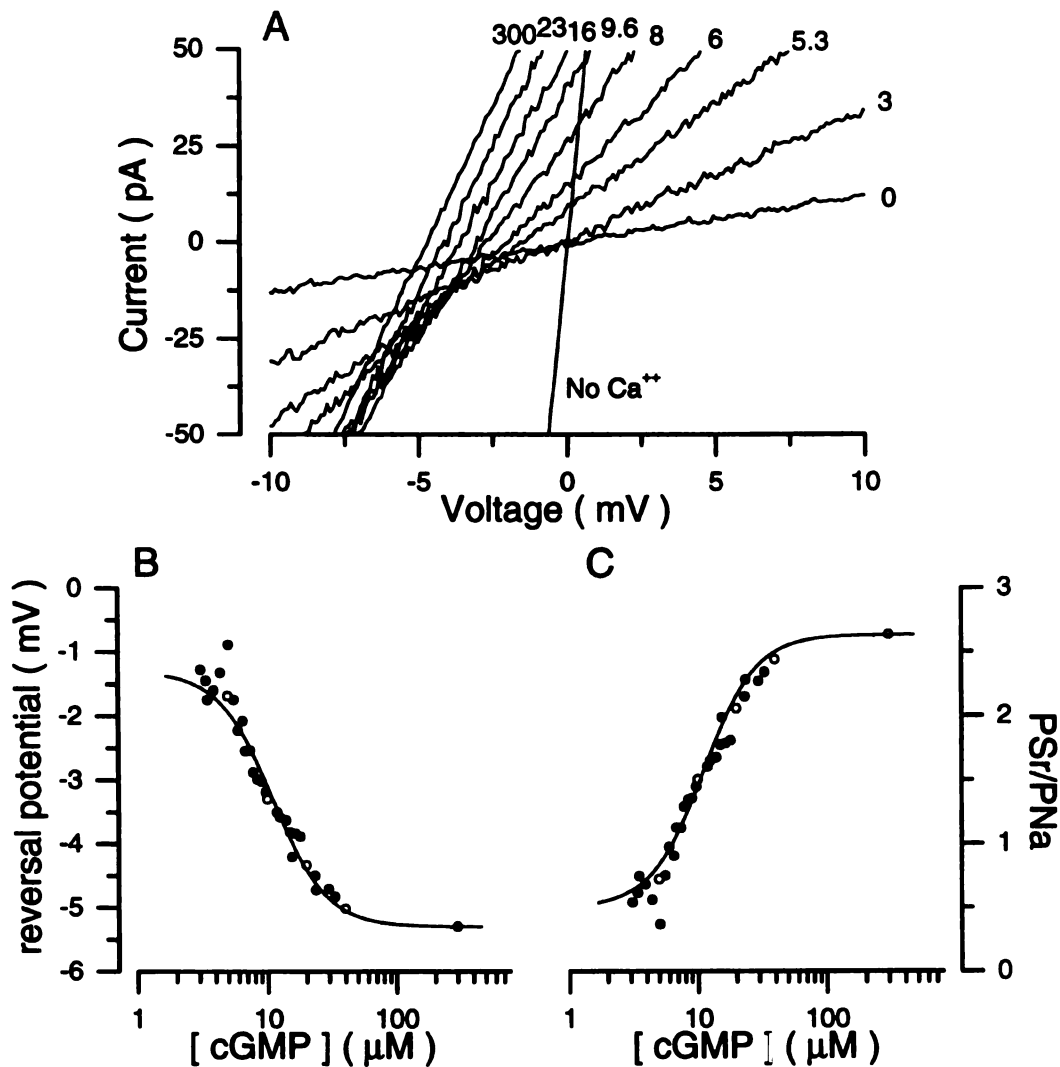


Figure 5. Relative permeability for Sr^{++} as a function of cGMP concentration. (A) I-V curves of the current activated by 0, 5, 10, 20, 40, or 300 μM cGMP were obtained from -30mV to $+30\text{mV}$ under conditions of symmetric 150mM NaCl and in the presence and absence of 20mM Sr^{++} applied to the cytoplasmic side of the patch. Additional curves were obtained by the cGMP washout method (fig. 2). As before, a Hill function ($K_{1/2} = 11.0\text{mM}$, $n = 2.1$ for this figure) was fit to the currents measured at $+15\text{mV}$ from the I-V curves measured at defined cGMP concentrations from which we calculated the cGMP concentrations of all the other I-V curves. (B) Reversal potentials measured from the I-V curves plotted as a function of cGMP concentration. Open circles represent reversal potentials measured at defined cGMP concentrations and closed circles are data from cGMP washout experiments. The Hill function plotted onto the data is the same Hill function determined above adjusted so that $\text{min} = -1.38\text{mV}$ and $\text{max} = -5.33\text{mV}$. (C) PSr/PNa calculated from eqn. 2 for each measured reversal potential (C). The same Hill function was fit to the data with $\text{min} = 0.47$ and $\text{max} = 2.71$.

The selectivity between different monovalent cations does not change as a function of [cGMP]

We tested whether cGMP-dependent shifts in permeability ratios was specific to divalent cations by determining whether the reversal potential in the presence of bi-ionic solutions of Cs^+ and Na^+ or NH_4^+ and Na^+ changes as a function of [cGMP]. Cs^+ and NH_4^+ were chosen since they both are significantly different in permeability compared with Na^+ , Cs^+ being less permeable and NH_4^+ being more permeable. Under bi-ionic conditions of either 150mM Cs^+ or 150mM NH_4^+ at 500 μM cGMP, the reversal potential was found to be 18.1 ± 1.6 mV (n=8) for Cs^+ and -22.2 ± 2.2 mV for NH_4^+ (n=6) (Fig. 6). From Eqn. 1, we find that $P_{\text{Cs}}/P_{\text{Na}} = 0.50 \pm 0.03$ (n=8) and $P_{\text{NH}_4}/P_{\text{Na}} = 2.44 \pm 0.21$ (n=6). Ramps at different [cGMP] were measured using either defined cGMP solutions or by allowing cGMP to slowly diffuse out of the patch. In both cases, the reversal potentials for bi-ionic solutions of Cs^+ and NH_4^+ remained the same at all cGMP concentrations tested. Thus, the selectivity of the channel for monovalent cations does not change as a function of [cGMP].

We also tested bi-ionic solutions of methylammonium and Na^+ or dimethylammonium and Na^+ . These organic monovalent cations are significantly less permeable than their parent molecule NH_4^+ since they are bulky enough to not fit very well through the cGMP-gated channel pore. Since these organic monovalent cations are therefore sensitive to the dimensions of the pore, the permeability of methylammonium and dimethylammonium and many other organic cations of various sizes and shapes have been used to show that the rod cGMP-gated channel pore has dimensions of approximately 0.38 x 0.5 nm (Picco and Menini, 1993). At 500 μM cGMP, we found the reversal potentials to be 16.5 ± 1.5 mV (n=4) for methylammonium and 52.0 ± 2.2 mV (n=5) for dimethylammonium (fig. 7). Eqn. 1 gives relative permeabilities of 0.53 ± 0.03 for methylammonium and 0.13 ± 0.011 for dimethylammonium, in agreement with previous measurements (Picco and Menini, 1993). We then varied cGMP concentration

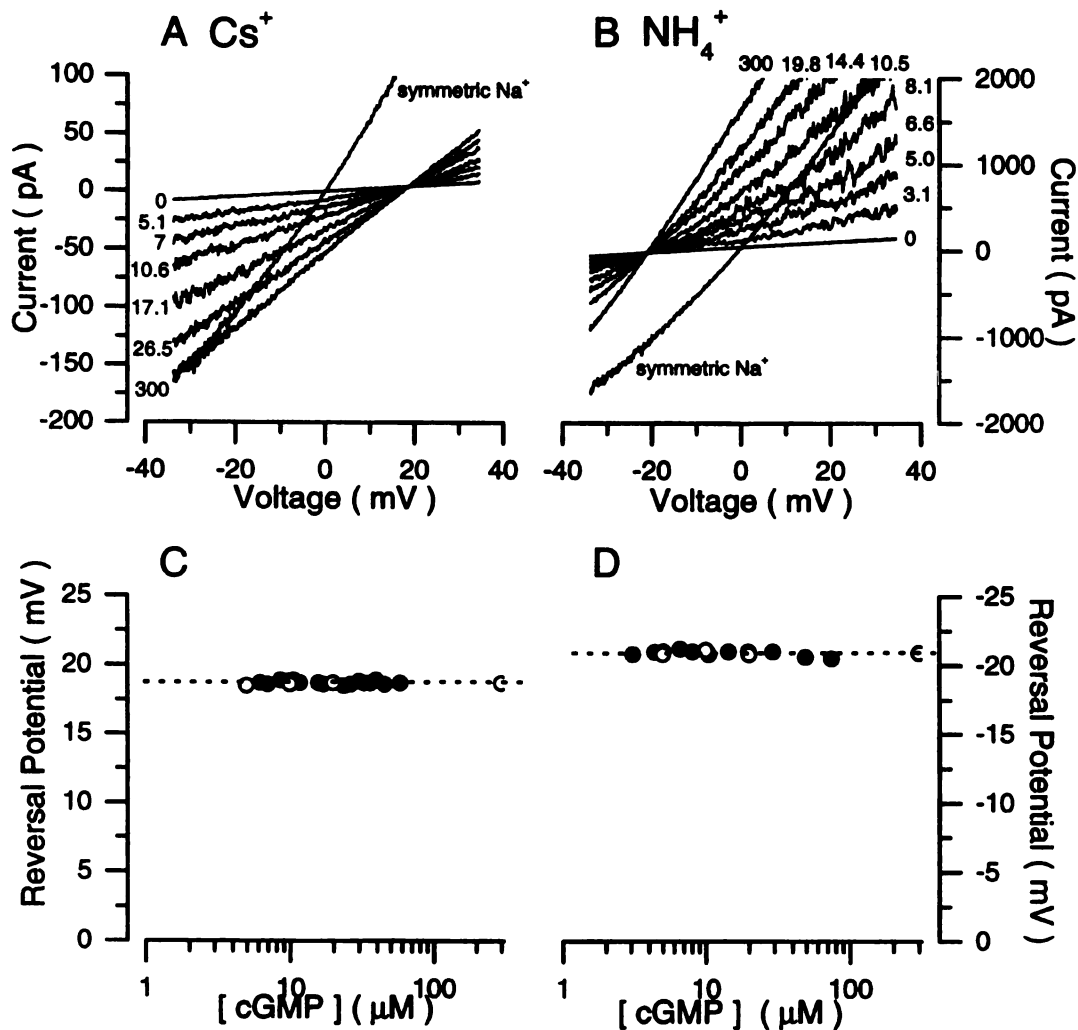


Figure 6. Selectivities of Cs^+ and NH_4^+ relative to Na^+ as a function of cGMP concentration. We measured a series of I-V curves from -70mV to $+70\text{mV}$ in either bi-ionic solutions of 150mM CsCl and NaCl (A) or 150mM NH_4Cl and NaCl (B). The cGMP concentrations were calculated using a method similar to that shown in fig. 2. Also plotted in A and B is the I-V curve at $500\ \mu\text{M}$ cGMP in symmetric 150mM NaCl solutions, which defined 0mV . Reversal potentials determined from the I-V curves were plotted as a function of cGMP for both measurements in Cs^+ (C) and NH_4^+ solutions (D). The dashed line represents the mean value of these reversal potentials, which were $18.6\ \text{mV}$ for Cs^+ and $-20.8\ \text{mV}$ for NH_4^+ , yielding (after application of eqn. 1) $\text{PCs}/\text{PNa} = 0.49$ and $\text{PNH}_4/\text{PNa} = 2.31$. Open circles indicate data recorded at defined cGMP concentrations, as before.

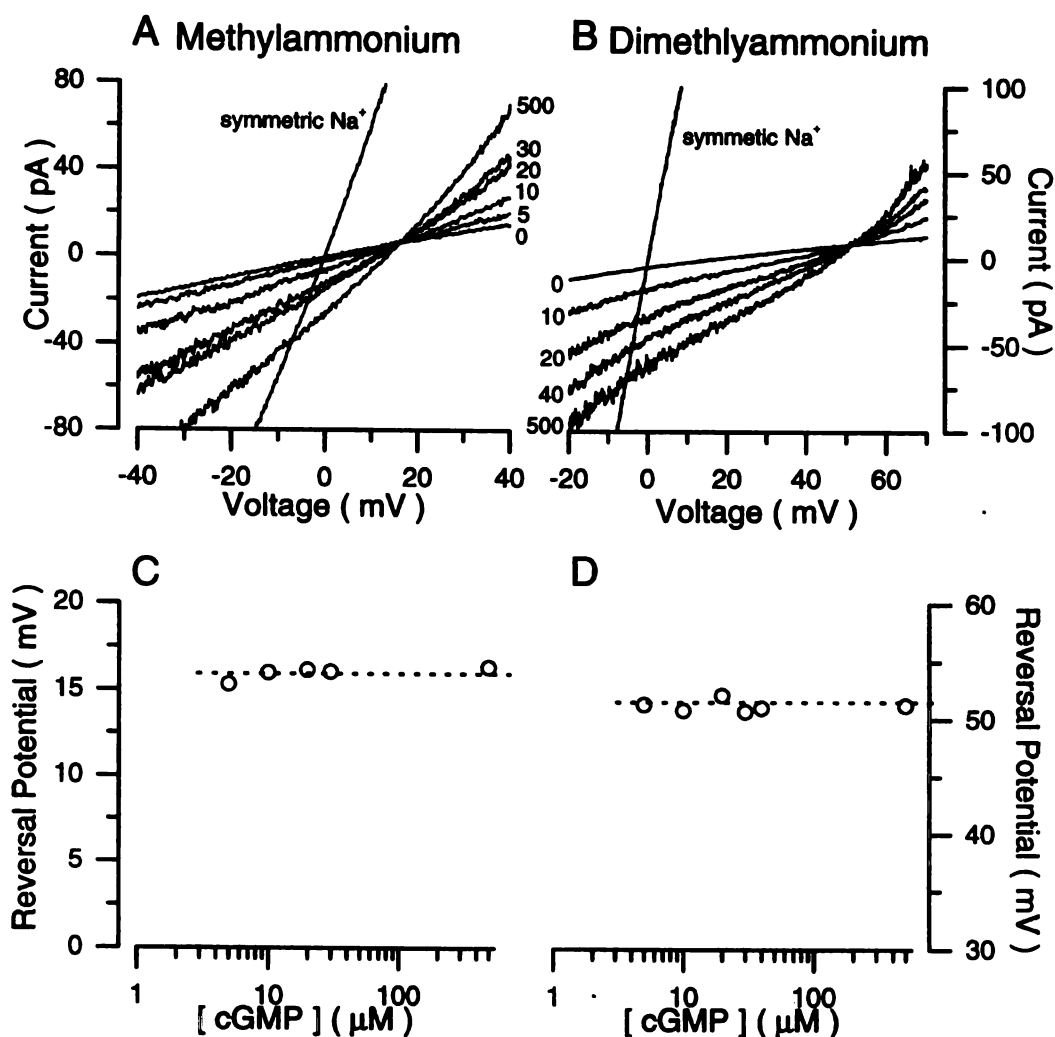


Figure 7. Selectivities for methylammonium and dimethylammonium relative to Na⁺ as a function of cGMP concentration. We measured a series of I-V curves from -70mV to +70mV in either bi-ionic solutions of 150mM methylammonium-Cl and 150mM NaCl (panel A) or 150mM dimethylammonium-Cl and 150mM NaCl (B). Either 0, 5, 10, 20, 30, 40 or 500μM cGMP was used to activate the cGMP-dependent current. Also shown in A and B are I-V curves measured in symmetric NaCl for use in defining the 0 mV point. Reversal potentials were determined from the I-V curves and plotted as a function of cGMP for methylammonium (C) and dimethylammonium (D) solutions. The dashed line represents the mean value for the reversal potentials, which was found to be 16.0 mV for methylammonium and 51.5 mV for dimethylammonium.

to obtain a series of I-V curves, the reversal potentials of which were measured (fig. 7). As in the cases of Cs⁺ and NH₄⁺, we found no changes in reversal potential and therefore permeability of these organic monovalent cations as a function of [cGMP]. Therefore, the selectivity for organic monovalent cations, and thus the effective pore diameter, does not change as a function of [cGMP].

Sensitivity to divalent cation block increases with decreasing [cGMP]

cGMP-dependent changes in divalent cation permeability likely reflect state-dependent changes in the detailed interaction of the pore with divalent cations. These differences in pore structure might lead to differences in other divalent cation dependent phenomena such as voltage-dependent pore block. To examine this possibility, we determined the sensitivity to block by Ca⁺⁺ in the presence of different cGMP concentrations. I-V curves were measured in the presence of 150mM symmetric NaCl solutions with and without 5mM Ca⁺⁺ added to the cytoplasmic side of the patch at several defined cGMP concentrations. To reduce noise, 5-10 I-V curves were recorded and averaged for each condition tested. Plotted in fig. 8a are g/g_{max} curves obtained by dividing the I-V curve recorded in the presence of 5mM Ca⁺⁺ by I-V curve recorded in the absence of Ca⁺⁺ for each cGMP concentration tested. This indicates the extent of block by 5mM Ca⁺⁺ as a function of voltage. Thus, as cGMP is decreased, the extent of block and therefore the sensitivity to block by Ca⁺⁺ increases. Fig. 8b shows the sensitivity to block as a function of [cGMP] at -40 mV. The same Hill function used to describe the cGMP-dependence of either channel current or divalent cation permeability is plotted with the data, showing that Ca⁺⁺ block has the same dependence of [cGMP]. Fig. 8c shows the effect of cGMP-dependent Ca⁺⁺ block on the $K_{1/2}$ of the channel (shown as a function of voltage at zero and 5mM Ca⁺⁺). Ca⁺⁺ block dependent on [cGMP], by definition, must cause an apparent shift in channel's sensitivity to cGMP. This increase in $K_{1/2}$ is shown at -40mV as a function of cGMP in fig. 8d. Thus, whether Ca⁺⁺ is altering gating or blocking the pore

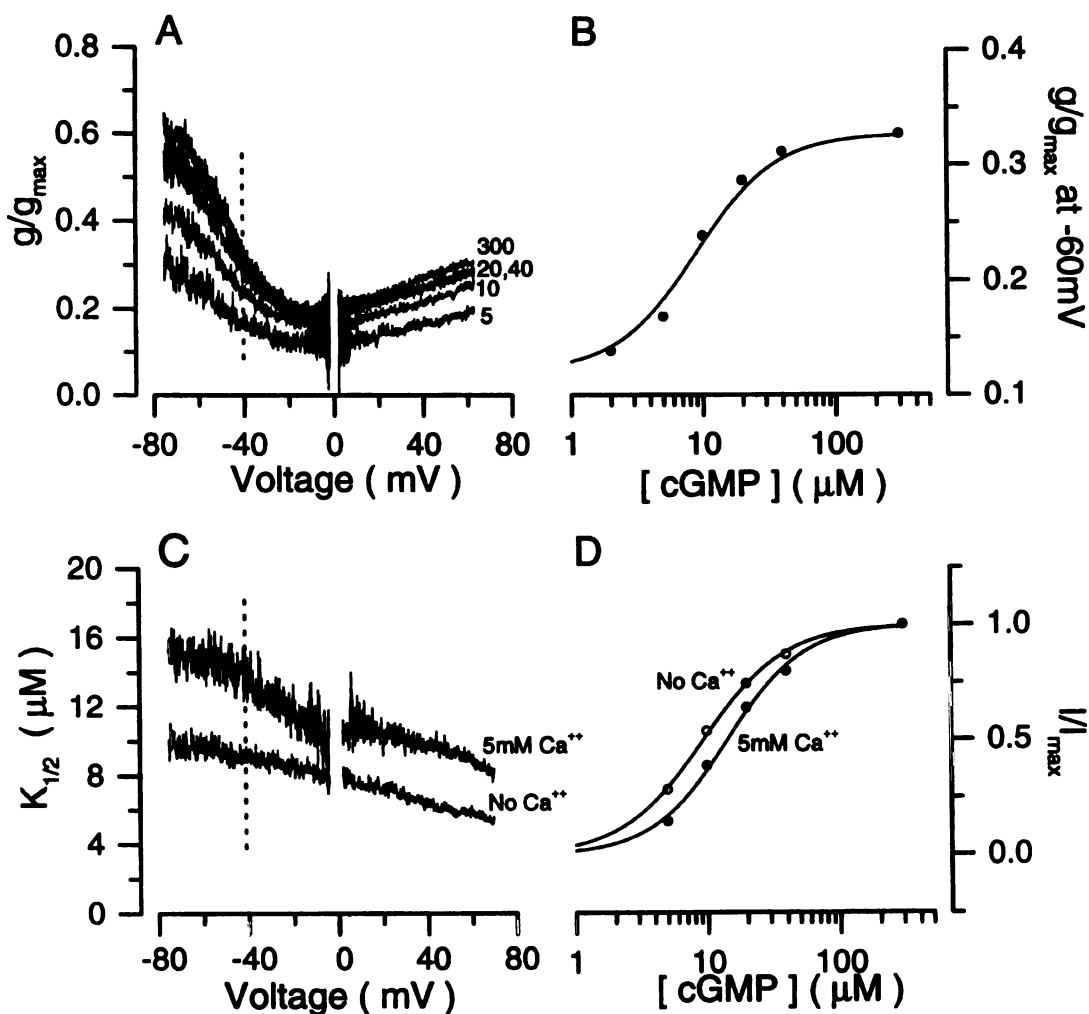


Figure 8. Calcium block as a function of cGMP concentration. (A) Blocking functions (g/g_{\max}) graphed as a function of voltage and obtained by dividing leak subtracted I-V curves obtained in symmetric 150mM NaCl solutions with 5mM Ca^{++} added to the cytoplasmic side of the patch by leak subtracted I-V curves obtained in the absence of Ca^{++} . CGMP-dependent currents were activated by 5, 10, 20, 40, or 300 mM cGMP as indicated to the right of each curve. (B) Fractional calcium block at -40 mV (dashed line in panel A at -40 mV shows origin of this data) graphed as a function of cGMP concentration. The same Hill function ($K_{1/2} = 9.43 \mu\text{M}$, $n = 1.4$) that describes the current at -40 mV in the presence of 5mM Ca^{++} (see panel D) is shown plotted with the data. The min and max values for this function were adjusted to fit the data (min = 0.095, max = 0.33). (C) Effect of cGMP-dependent Ca^{++} block on the effective $K_{1/2}$ for cGMP binding. These curves were calculated by fitting point-by-point the I-V curves at either zero or 5mM Ca^{++} to a Hill equation (eqn. 3). (D) Fractional current (I/I_{\max}) measured at -40 mV plotted as a function of cGMP in either the absence (open circles) or presence (closed circles) of 5mM Ca^{++} . Hill functions were fit to these data, which represent a single point in C (dashed line), with parameters $K_{1/2} = 9.43 \mu\text{M}$, $n = 1.4$ (zero Ca^{++}) and $K_{1/2} = 14.2 \mu\text{M}$, $n = 1.5$ (5mM Ca^{++}).

in a cGMP-dependent way cannot be distinguished using the data presented here (see discussion).

Relative Ca^{++} permeability also depends of [cGMP] in cone channels

Cone cGMP-gated channels are significantly more permeable to Ca^{++} than channels from rods (Picones and Korenbrot, 1995; Haynes, 1995a; Frings et al., 1995). However, these measurements were made under conditions of saturating and therefore nonphysiological cGMP concentrations. It is therefore necessary to examine the difference in Ca^{++} permeability between the rod and cone channels at physiological cGMP concentrations. Fig. 9a shows I-V curves recorded from inside-out patches excised from Striped Bass cone outer segments under either symmetrical 150mM NaCl solutions or symmetrical NaCl with 5mM Ca^{++} added to the cytoplasmic side of the patch. At saturating cGMP, we find a reversal potential shift of -9.4 ± 0.5 mV, which implies that in cones, $\text{P}_{\text{Ca}}/\text{P}_{\text{Na}} = 21.7 \pm 1.65$ (n=12), consistent with earlier measurements (Picones and Korenbrot, 1995). Several I-V curves were measured in the presence of Ca^{++} at several different defined concentrations of cGMP and also at many different cGMP concentrations generated by allowing cGMP to diffuse out of the patch. Similarly to the rod channel, the reversal potential was found to shift to less negative values as [cGMP] was decreased. This indicates that the cone channel also becomes less permeable to Ca^{++} at low [cGMP]. Fig. 9b shows reversal potential measurements graphed as a function of [cGMP], and fig. 9c shows $\text{P}_{\text{Ca}}/\text{P}_{\text{Na}}$ as calculated using eqn. 2 as a function of [cGMP]. The dependence of $\text{P}_{\text{Ca}}/\text{P}_{\text{Na}}$ could be well described by the same Hill function (eqn. 4) that describes the apparent cGMP binding affinity as recorded in the same patch at +15mV. On average, we found that $K_{1/2} = 43 \pm 14$ μM , $n = 2.8 \pm 0.4$, $\text{min} = 14.0 \pm 1.6$, $\text{max} = 21.7 \pm 1.7$ (n=12). The extent of decrease in Ca^{++} permeability between saturating and zero cGMP (max/min) was 1.55 ± 0.21 (n=12). This indicates

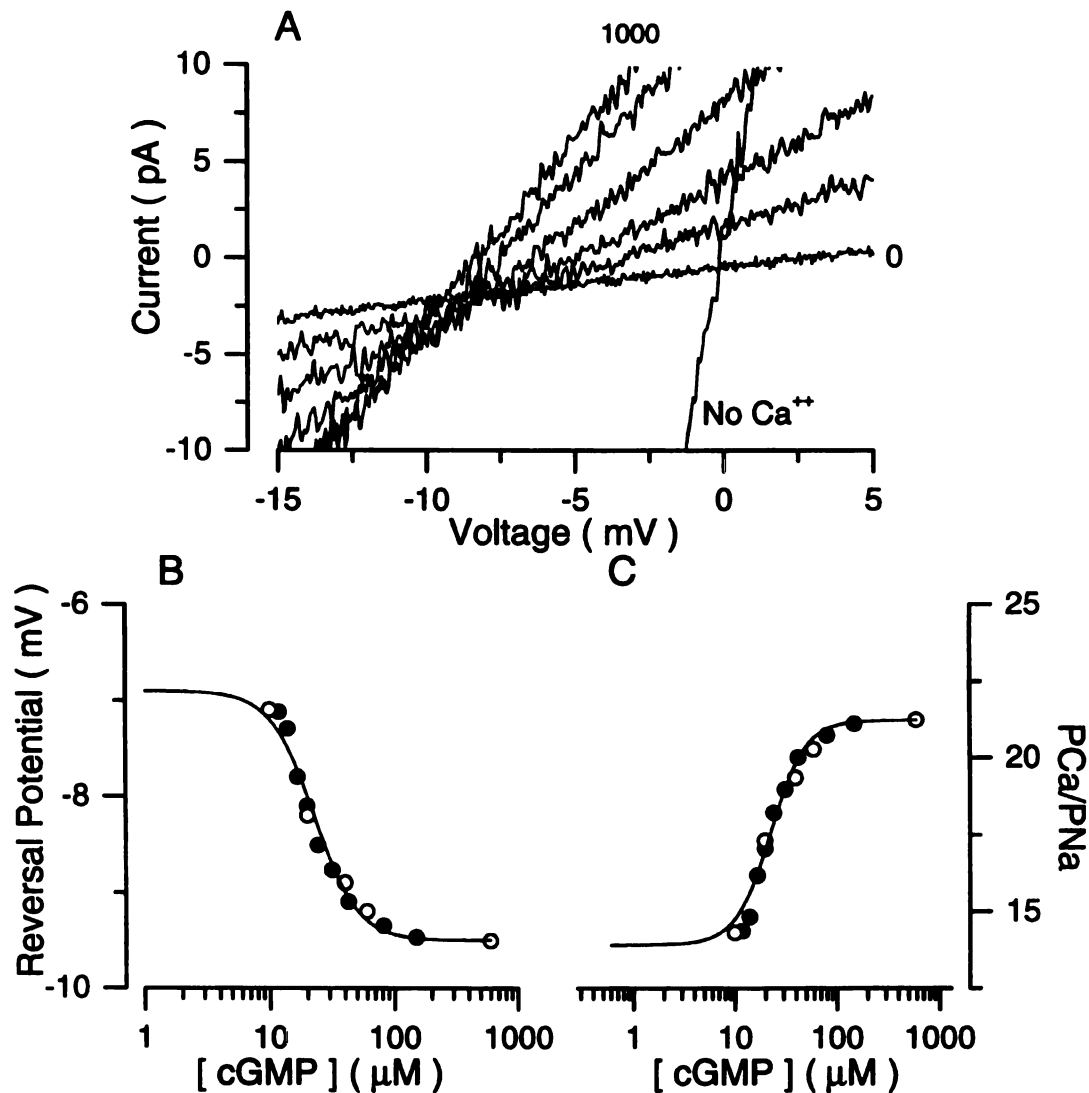


Figure 9. Permeability for Ca^{++} relative to Na^+ as a function of cGMP concentration in cone channels. (A) I-V curves generated using voltage ramps from -30mV to $+30\text{mV}$ on patches excised from the striped bass cone outer segment membrane under conditions of symmetric 150mM NaCl with 5mM Ca^{++} added to the cytoplasmic side of the patch. The cGMP concentration of each curve was calculated from the Hill equation (as shown in fig. 2) and is indicated at the right of each curve. Also shown is the I-V curve measured in the absence of Ca^{++} . (B) Reversal potential measurements plotted as a function of cGMP concentration. Open circles are data obtained at defined cGMP concentrations ($10, 20, 40, 60, 600\text{mM}$) and closed circles indicate data obtained by allowing cGMP to slow diffuse out of the patch. The Hill function plotted with the data is the same as that which describes the cGMP-dependence of the current at $+15\text{mV}$ in the presence of 5mM Ca^{++} ($K_{1/2} = 22.5\mu\text{M}$, $n = 2.5$) which has been adjusted (see eqn. 4) with $\text{min} = -6.91\text{mV}$ and $\text{max} = -9.5\text{mV}$. (C) PCa/PNa calculated using eqn. 2 and plotted as a function of cGMP. The same Hill function was plotted and adjusted with $\text{min} = 13.9$ and $\text{max} = 21.2$.

that the ratio of relative Ca^{++} permeability between cone and rod channels is 7.41 ± 0.85 at physiological cGMP concentrations.

Selectivity between different monovalent cations is independent of [cGMP] in cone channels

With the observation that divalent permeability is a function of [cGMP] in the cone channel, we tested whether the selectivity for different monovalent cations was independent of cGMP, as it is for the rod channel. As before, we studied Cs^+ and NH_4^+ permeability using bi-ionic solutions of 150mM Cs^+ and Na^+ or 150mM NH_4^+ and Na^+ . Fig. 10 shows I-V curves recorded at different [cGMP] by allowing cGMP to diffuse out of the patch for both Cs^+ (fig. 10a) and NH_4^+ (fig. 11b). The resulting reversal potentials are shown for Cs^+ and NH_4^+ in figs. 10c and 10d respectively. On average, the reversal potential shifted to 4.2 ± 0.53 (n=5) for Cs^+ and -16.4 ± 1.4 mV (n=6) for NH_4^+ , which with eqn. 1 gives $P_{\text{Cs}}/P_{\text{Na}} = 0.87 \pm 0.02$ and $P_{\text{NH}_4}/P_{\text{Na}} = 1.94 \pm 0.11$, similar to previous measurements of monovalent cation selectivity in cones (Picones and Korenbrot, 1992; Haynes, 1995b). We found no changes in the reversal potentials at different cGMP concentrations.

Relative cation selectivity of recombinant bovine rod cGMP-gated channels

Cyclic nucleotide channels (at least those from rods and olfactory neurons) are made up of two subunits, α and β (Chen et al., 1993; Bradley, J., et al., 1994; Liman and Buck, 1994; Korschen et al., 1995). Functional channels are formed with either the α subunit alone or with both α and β subunits together as a heteromeric channel (which we will refer to as the α channel and the $\alpha\beta$ channel respectively). We investigated whether expressed channels containing only the α subunit exhibit cGMP-dependent divalent cation permeability in a similar way to native cGMP-gated channels, or whether both α and β subunits are required. Fig. 11 shows I-V curves obtained from *Xenopus* oocyte

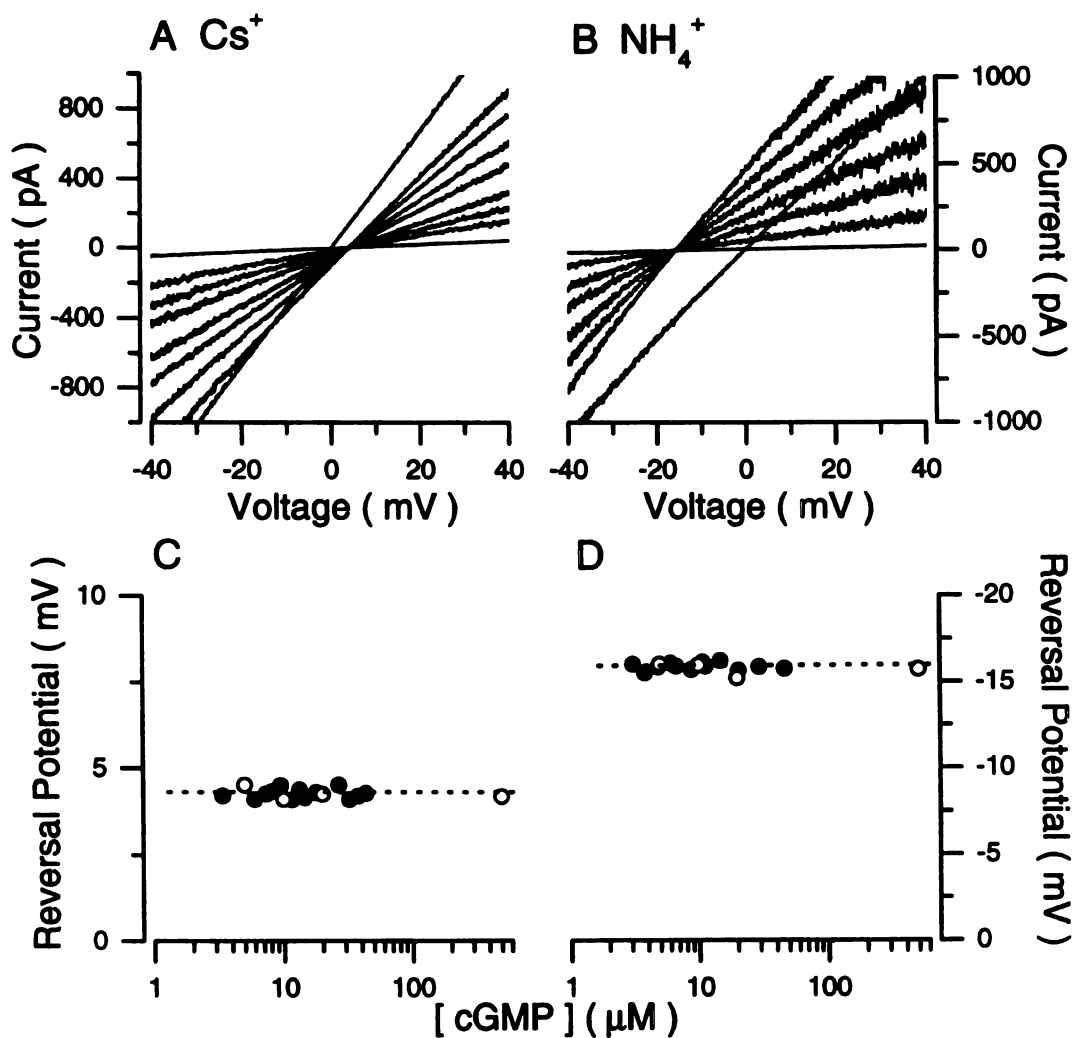


Figure 10. Relative permeabilities for Cs^+ and NH_4^+ with respect to Na^+ as a function of cGMP concentration in cone channels. I-V curves were measured using voltage ramps from -70mV to $+70\text{mV}$ while exposing a membrane patch to bi-ionic solutions of either 150mM CsCl and 150mM NaCl (A) or 150mM NH_4^+ and 150mM NaCl (B). The cGMP concentrations indicated to the right of each I-V were calculated from the Hill equation (fig. 2). Also shown are I-V curves recorded in symmetric 150mM NaCl solutions. Reversal potentials were determined as before (see methods) and plotted as a function of cGMP for bi-ionic Cs^+ solutions (C) and bi-ionic NH_4^+ solutions (D). As before, open circles indicate data recorded at defined cGMP concentrations. The dashed lines represent the mean values of the reversal potentials, which were 4.3 mV and -15.8 mV for Cs^+ and NH_4^+ respectively.

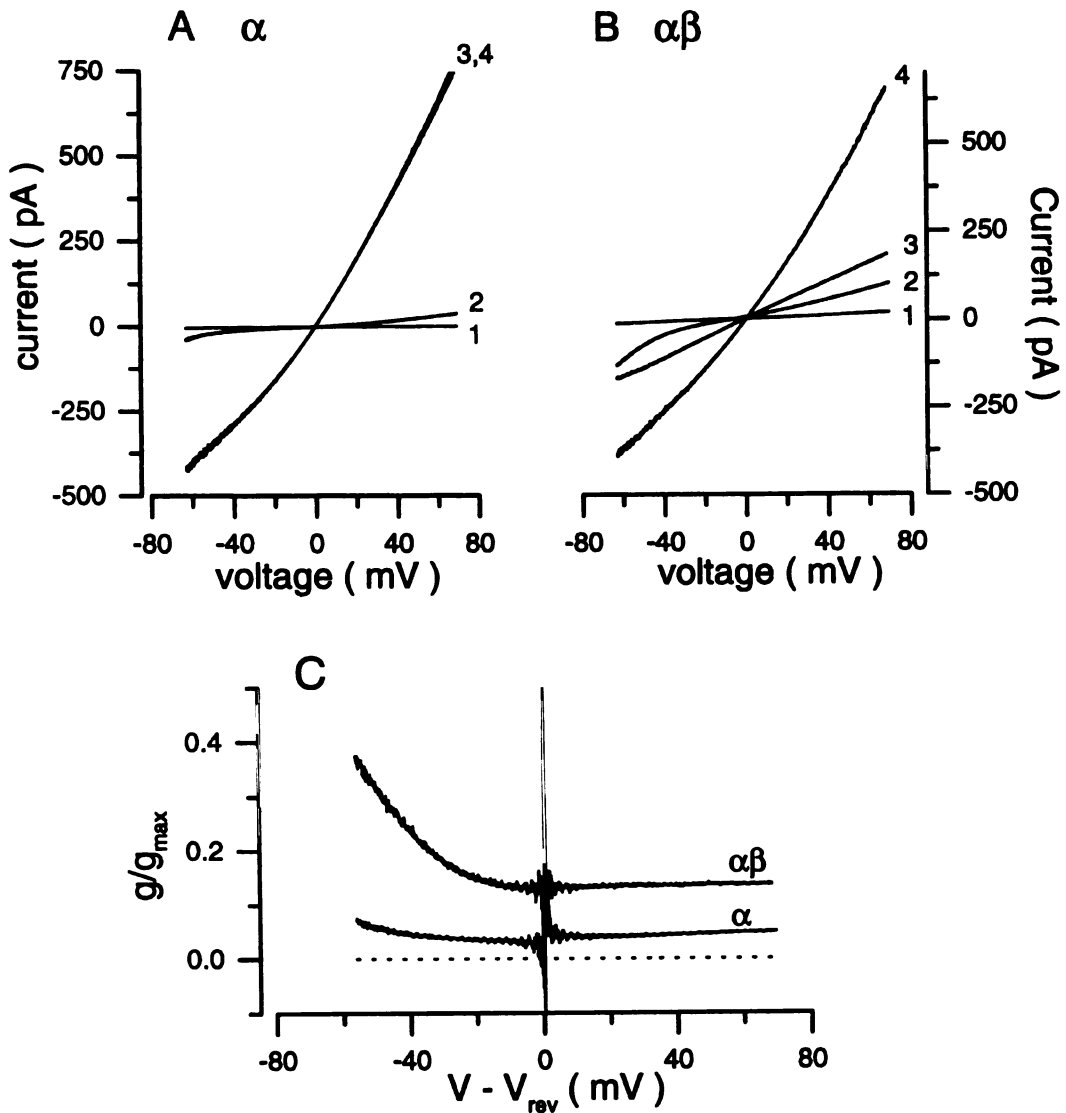


Figure 11. Calcium block of recombinantly expressed rod α and $\alpha\beta$ channels. I-V curves were generated using voltage ramps from -70mV to $+70\text{mV}$ on inside-out patch from *Xenopus* oocytes expressing either α (A) or $\alpha\beta$ (B) bovine rod cGMP-gated channels. Recordings were made under conditions of 150mM symmetric NaCl in either the absence (1) or presence (4) of $600\mu\text{M}$ cGMP, and also with $10\mu\text{M}$ l-cis-diltiazem (3) or 10mM Ca^{++} (2) added to the cytoplasmic side of the membrane. (C) Calcium blocking curves (g/g_{\max}) obtained by dividing the I-V curve recorded in the presence of 10mM Ca^{++} by the I-V curve in the absence of Ca^{++} (both at 600mM cGMP) and plotted as a function of $V - V_{\text{rev}}$. The extent of block between -10mV and $+10\text{mV}$ was found to be 86.7% for the $\alpha\beta$ channel and 95.9% for the α channel, indicating that the $\alpha\beta$ channel has 3.25-fold higher current than the α channel at voltages near the reversal potential in the presence of 10mM Ca^{++} .

patches containing either the bovine rod α subunit (fig. 11a) or $\alpha\beta$ heteromeric channels (fig. 11b) under conditions of either symmetrical 150mM Na^+ solutions or symmetrical Na^+ with 10mM Ca^{++} added to the cytoplasmic side of the patch. To verify that we have indeed correctly assembled $\alpha\beta$ heteromeric channels, we also determined the I-V curves in the presence of 10 μM l-cis-diltiazem, which only blocks $\alpha\beta$ channels (Chen et al., 1993; Korschen et al., 1995). As expected, l-cis-diltiazem did not block the channels when the α subunit is expressed alone (fig. 11a), but it does partially block channels formed from both subunits (fig. 11b), indicating that most of the channels in the patch contained β subunits. Fig. 11c shows that homomeric α channels are much more sensitive to block by Ca^{++} than $\alpha\beta$ channels, as has been noted before (Korschen et al., 1995).

In order to look for shifts in PCa/PNa as a function of cGMP, we measured I-V curves in the presence of symmetric 150mM Na^+ with 10mM Ca^{++} added to the cytoplasmic side of the membrane at 0, 40, 60, 80, and 600 μM cGMP (α channel, fig. 12a; $\alpha\beta$ channel, fig. 12b). We also measured a large number of I-V curves by allowing cGMP to diffuse out of the patch as before (not shown). In patches containing only the α subunit, the measured reversal potential is the same at all cGMP concentrations tested, while in patches containing $\alpha\beta$ channels, the reversal potential increases with cGMP concentration in a similar way as that of the native rod channel (fig. 3). Fig. 12c shows the reversal potentials plotted as a function of [cGMP] and fig. 12d shows the PCa/PNa as calculated by Eqn. 2 plotted in the same way. On average, we found for channels made from only the α subunit a reversal potential shift of -4.8 ± 1.2 mV (n=7), which implies that $\text{Pca/PNa} = 4.6 \pm 0.79$. As in the case of the native channel, both the reversal potential and Pca/PNa for the $\alpha\beta$ channel could be well fit by a Hill function (eqn. 4) with the same parameters as describes the current as a function of cGMP. On average, we found these parameters to be $\Delta V_{\text{rev,max}} = -8.4 \pm 1.1$ mV, $\Delta V_{\text{rev,min}} = -4.6 \pm 2.2$ mV,

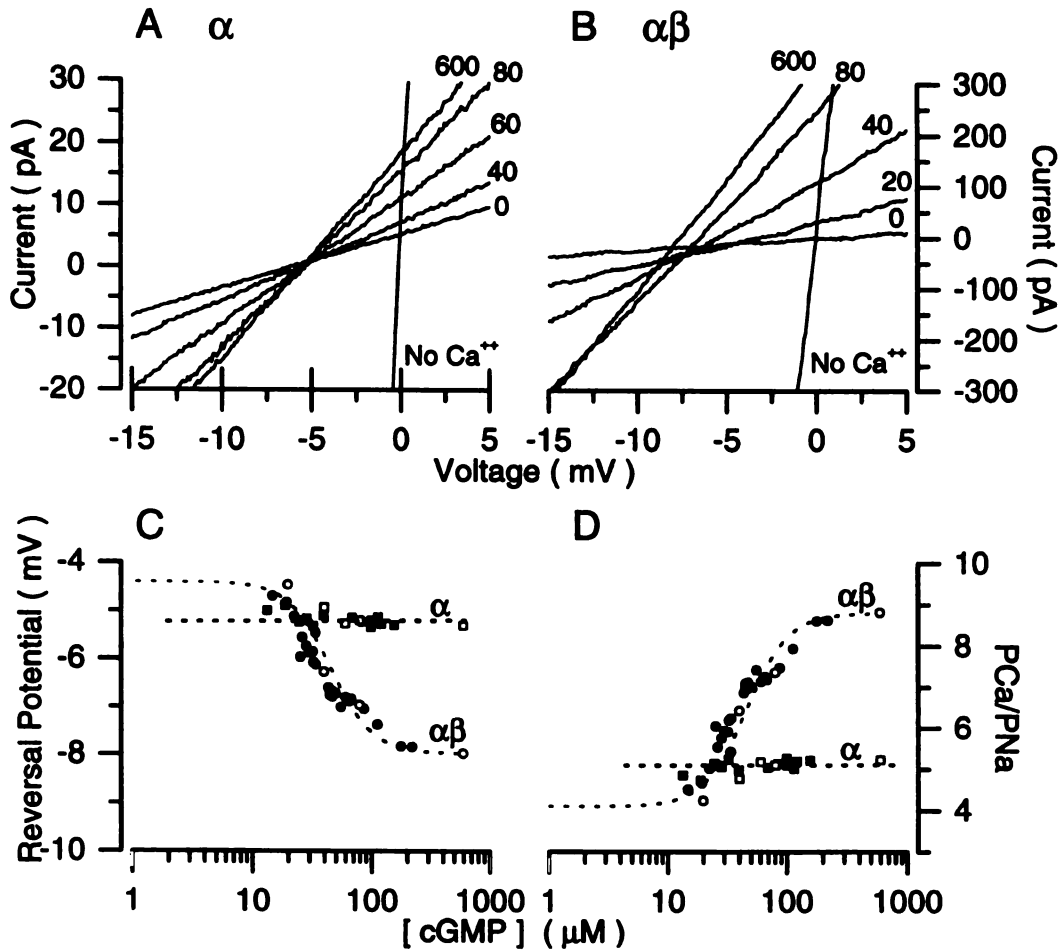


Figure 12. Relative Ca^{++} permeability as a function of cGMP in expressed rod α and $\alpha\beta$ channels. We recorded I-V curves from membranes containing either α (A) or $\alpha\beta$ (B) channels using voltage ramps from -30mV to $+30\text{mV}$ at several different cGMP concentrations ($0, 20, 40, 80, 600\mu\text{M}$) under conditions of symmetric 150mM NaCl with 10mM Ca^{++} added to the cytoplasmic side of membrane. To reduce noise, each I-V curve shown is the average of 10 curves measured at each cGMP concentration. Additional curves were recorded without averaging using the washout technique described in fig. 2 (not shown). Also shown are I-V curves measured in the absence of Ca^{++} to define the 0mV position. Reversal potential values were determined by fitting a line to each I-V curve from -10mV to $+10\text{mV}$ and calculating the voltage at which each line crossed the I-V curve measured in the absence of Ca^{++} . (B) Reversal potentials for both α and $\alpha\beta$ channels plotted as a function of cGMP concentration. Squares represent measurements from patches with only a channels and circles are from $\alpha\beta$ channel recordings. Open symbols are data measured at defined cGMP concentrations. The mean value for the a channel reversal potential (dashed line) is -5.2mV . The same Hill function that describes the current-cGMP relationship for this patch ($K_{1/2} = 45.4\mu\text{M}$, $n = 2.45$) is also plotted and modified to fit the $\alpha\beta$ channel data with parameters $\text{min} = -4.38\text{mV}$ and $\text{max} = -8.0\text{mV}$. (D) PCa/PNa calculated from eqn. 2 and plotted as a function of cGMP concentration. Symbols are the same as in C. The mean PCa/PNa for the a channel (dashed line) is 5.1 and the Hill function adjustment parameters are $\text{min} = 4.1$ and $\text{max} = 8.8$.

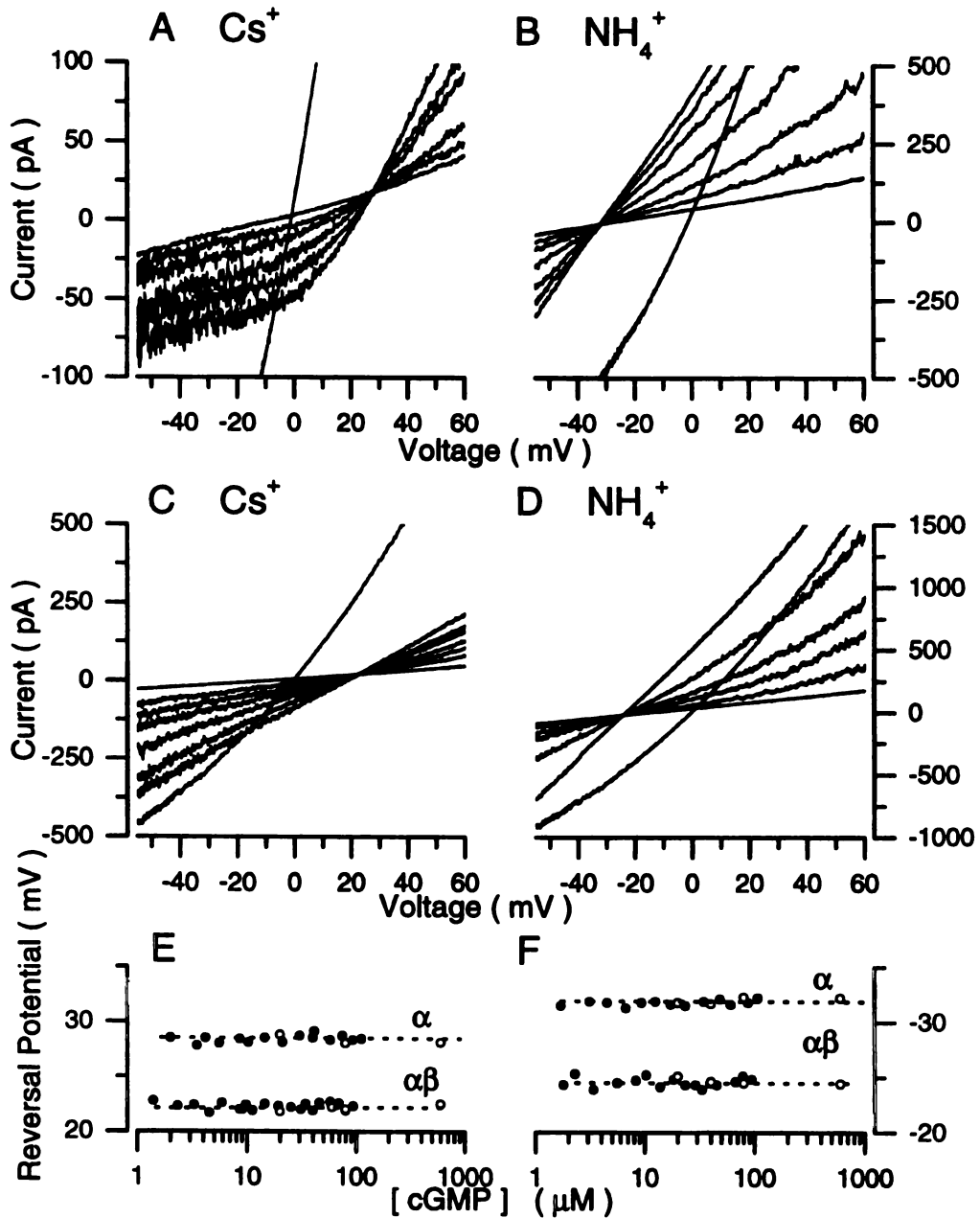


Figure 13. Relative permeabilities for Cs^+ and NH_4^+ with respect to Na^+ as a function of cGMP concentration in recombinant α and $\alpha\beta$ channels. No cGMP-dependent reversal potential shifts are observed in the presence of bi-ionic solutions of NH_4^+ and Na^+ (B, D) or Cs^+ and Na^+ (A, C) for either channels made from the α subunit alone (A, B) or channels made from both α and β subunits (C, D). Measured reversal potentials for Cs^+ (E) or NH_4^+ (F) are shown plotted as a function of [cGMP]. For these recordings, the average reversal potentials are: α , Cs^+ , 28.3 mV; $\alpha\beta$, Cs^+ , 22.5 mV; α , NH_4^+ , -31.8 mV; $\alpha\beta$, NH_4^+ , -24.5 mV.

$PCa/PNa_{max} = 9.4 \pm 1.1$, $PCa/PNa_{min} = 4.4 \pm 1.4$, $K_{1/2} = 45.2 \pm 15.6 \mu M$, $n = 2.6 \pm 0.24$ (n=12), with a total extent of permeability difference (max/min) of 2.14 ± 0.63 (n=12). To determine whether the permeability shifts we observed for the $\alpha\beta$ channel were specific for divalent cations, we tested whether the permeabilities for the monovalent cations Cs^+ and NH_4^+ changed as a function of cGMP concentration. Fig. 12 shows I-V curves recorded from channels made from either α subunits alone or both α and β subunits in the presence of bi-ionic solutions of Na^+ and either Cs^+ and NH_4^+ . In all cases, Cs^+ was significantly less permeable than Na^+ and NH_4^+ was significantly more permeable. All I-V curves were qualitatively similar to equivalent recordings of native rod channels (fig. 6) except in the case of the homomeric α channel in the presence of bi-ionic solutions of Na^+ and Cs^+ , which displays a saturation-like nonlinearity at membrane potentials more negative than the reversal potential (fig. 12a). We found no evidence of cGMP-dependent shifts in recordings of either channel in the reversal potentials and therefore permeabilities of either Cs^+ and NH_4^+ . The α channel was in general more selective among monovalent cations than the $\alpha\beta$ channel. Mean values of V_{rev} for the α channel were Cs^+ , 28.6 ± 2.5 mV (n=8); NH_4^+ , -31.2 ± 1.8 mV (n=8) and for the $\alpha\beta$ channel were Cs^+ , 21.9 ± 1.9 mV (n=6); NH_4^+ , -24.5 ± 2.2 mV (n=6). Using eqn. 1, this implies for the α channels $PCs/PNa = 0.33 \pm 0.03$ and $PNH4/PNa = 3.49 \pm 0.25$, and for the $\alpha\beta$ channels $PCs/PNa = 0.43 \pm 0.32$ and $PNH4/PNa = 2.67 \pm 0.23$.

Discussion

In this study we show that photoreceptor cyclic nucleotide-gated channels exhibit calcium permeability that is dependent on the concentration of cGMP (fig. 2). Under conditions of high cGMP, calcium permeability is relatively high. However, when the channels are presented with more physiologically relevant concentrations of cGMP, calcium permeability is significantly smaller. The dependence of calcium permeability on [cGMP] can be very well described by the same Hill function used to describe the open probability of the channel as a function of [cGMP]. Shifts in permeability were not seen for any of the monovalent cations tested. Other divalent cations such as Sr^{++} show the same dependence of permeability with [cGMP] as does Ca^{++} . This effect is seen in CNG channels from both rods and cones and in recombinant rod channels made from both α and β subunits, but is absent in recombinant channels containing only α subunits.

In the traditional model of an ion channel, the ion permeation pathway (pore) and gating mechanism are viewed as two separate and independent protein structures (Hille, 1992). In this simple model, the gate should affect access of ions to the pore, not the structure of the pore itself. Since the pore is defined as the part of the channel that directly interacts with the permeating ions, any gating-induced alteration in ion selectivity must be viewed as an alteration in the structure of the pore. Thus, our observation that the relative selectivity of divalent over monovalent cations changes as a function of gating must be viewed as evidence for gating-induced alterations in the pore structure.

One possible alternative explanation that could give rise to the gating-dependent selectivity changes we have observed here is that there are actually two or more distinct species of cGMP-gated ion channels present in our patches. One of the channel types would have relatively high sensitivity to cGMP but a rather low divalent cation permeability. The other type of channel would have a lower sensitivity to cGMP and a high divalent cation permeability. Thus, at saturating cGMP concentrations, both of the channel types would be open and therefore the observed relative permeability for divalent

cations would be the weighted sum of the permeabilities of the two channel types. As the cGMP concentration is lowered, the low sensitivity channel would start to close, causing the observed divalent cation permeability to decrease since a larger fraction the total open channels would be of the high sensitivity, low divalent cation permeable type.

In photoreceptor membranes, there is evidence that there may be two distinct species of cGMP-gated channels present (Koch et al, 1987; Torre et al., 1992). Experiments on bovine outer segment vesicles reveal the presence of two cGMP-dependent components that show different Ca^{++} efflux kinetics. However, since the kinetically fast (high permeability) component has higher affinity for cGMP, this observation cannot explain the results presented here (Koch et al., 1987). There is in fact evidence that these two kinetic components may reflect vesicles with and without Na-Ca,K exchanger pumps and not two different types of cGMP-gated channels (Schnetkamp, P.M., 1987). Single channel recordings from the rod inner segment membrane occasionally show cGMP-gated channels with slower kinetics than the much more common rapid flickering channel (Torre et al., 1992). These slow channels may represent channels composed of only α subunits. However, no difference in cGMP binding affinity was observed between the two channel types.

In *Xenopus* oocytes expressing $\alpha\beta$ channels, we expect that some percentage of the observed channels contain only α subunits. However, we find that α channels are in general slightly less sensitive to cGMP ($K_{1/2} = 52.3 \pm 10.8 \mu\text{M}$ (n=7) for α channels and $K_{1/2} = 45.2 \pm 15.6 \mu\text{M}$ (n=12) for $\alpha\beta$ channels in the presence of 10mM cytoplasmic Ca^{++}) and are less permeable to divalent cations. Therefore, mixtures of α and $\alpha\beta$ channels cannot explain the shifts in divalent cation permeability that we observe. The effect of a small amount of contaminating α channels should in fact be a small decrease in the total extent of the measured cGMP-dependent reversal potential shift. It is possible, however, that some form of modulation specific to $\alpha\beta$ channels alters the properties of a fraction of the expressed channels, creating in effect two types of channels.

While the only known form of modulation specific to $\alpha\beta$ channels is calmodulin binding, which is known not to affect Ca^{++} permeability (Hackos and Korenbrot, 1997), it is possible, though unlikely, that some other form of modulation, for example phosphorylation, is playing a role in our observations.

We believe that cGMP-dependent shifts in divalent cation permeability are reflective of real structural changes in the pore. Gating dependent structural changes in the CNG channel pore have been observed previously in several experiments. Fodor et al. (1997) observed that the pore region has an altered structure in the closed state of the channel. They found that the local anesthetic tetracaine blocks the bovine rod α channel in both a voltage dependent and state dependent manner, suggestive of a molecule that binds within the pore but is sensitive to the gating state of the channel. Furthermore, they found that the mutation E363G within the pore substantially decreased tetracaine block. This suggests that a salt bridge between the positive charge of tetracaine and the negative charge of E363 is important for tetracaine binding. The fact that tetracaine does not bind to the open channel may indicate that a conformational change within the pore alters either the position of E363 or its accessibility to tetracaine. Sun et al. (1996) have shown when certain residues known to be within the pore are altered to cysteines, they are accessible to cysteine-modifying reagents when applied to either the internal or external side of the channel in either the open or closed state. This argues against the flap-door mechanism for gating that has been proposed for K^+ channels and suggests that the pore itself gates CNG channels. This also implies that the CNG channel pore undergoes structural changes during gating.

While pore structural changes are necessary to explain cGMP-dependent selectivity changes, they are not sufficient. Since the closed state of the channel does not conduct, its presence does not alter the selectivity of the pore, even if its structure is different from that of the open state. At least one conducting intermediate gating state is required. To explain the cGMP-dependent divalent cation permeability shifts observed here, this

intermediate state should be preferentially present at low cGMP concentrations and should have a significantly smaller divalent cation permeability than the fully open state (fig. 13). An excellent candidate for such an intermediate state or states are the well known subconductance states of CNG channels.

The CNG channel subconductance states have been well described previously (Haynes et al., 1986; Zimmerman and Baylor, 1986; Tanaka et al., 1987; Hanke et al., 1988; Bennett et al., 1991). Generally, 2-3 subconductance states have been observed at low cGMP concentrations, and since CNG channels are tetrameric with four cyclic nucleotide binding sites (Liu et al., 1996), these subconductance states have been interpreted as representing the distinct states of one, two, or three bound cGMP molecules. Ruiz and Karpen (1997) have recently shown that this interpretation is incorrect. Using the photocrosslinkable cGMP analogue APT-cGMP, they were able to isolate single CNG channels locked in a specific ligand-bound state. The results indicate that the number of bound cGMP molecules alters the probability of occupying particular gating states, but does not define which state is occupied. In addition, the channels do not have a significant open probability until at least three ligands are bound. Triply liganded channels display two strong subconductance states in addition to the fully open state, while the fully liganded channel mainly occupies only the fully open conductance state.

Can our results be explained if the proposed intermediate state suggested by this study is identified as the subconductance state or states of the triply liganded channel? Ruiz and Karpen (1997) only examined α channels which, as we have shown, has divalent cation permeability that is not cGMP-dependent. Therefore, we would predict that these subconductance states do not have different selectivities for divalent cations. The native channel certainly has gating-dependent subconductance states, but there is no information yet available as to which gating states these represent. Therefore, we would suggest that at least one of the subconductance states of the native channel must have reduced divalent cation permeability. To directly test this idea, it would be necessary to

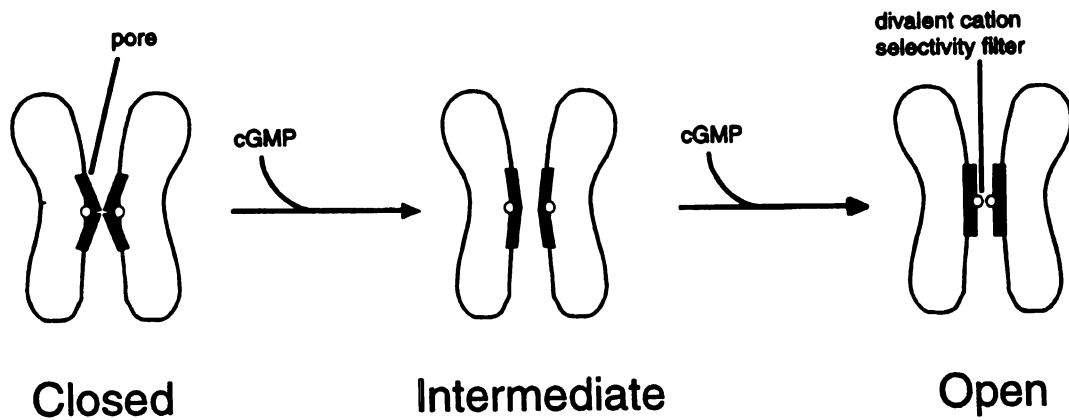


Figure 14. Intermediate state model. The observed shifts in divalent cation permeability as a function of gating can be explained by the presence of an intermediate gating state separate from the fully open state that has reduced permeability to divalent cations yet has the same relative monovalent selectivity and pore dimensions as the fully open channel. Furthermore, this intermediate state should exist only when the cGMP binding sites are partially but not fully saturated.

directly record the reversal potential from single triply liganded heteromeric $\alpha\beta$ channels in the presence of 10mM Ca^{++} or 20mM Sr^{++} , which is extremely difficult since divalent cations at these concentrations strongly block the channel in a flickery manner. On theoretical grounds, however, a simple model of two conducting states (triply-liganded and fully saturated) each with different divalent cation selectivities cannot fully explain our results. This is due to the fact that a two conducting-state model with four total binding sites predicts that divalent cation selectivity as a function of cGMP concentration should show much lower cooperativity than we observe here since only one binding event differentiates these two states. Thus, a more complex mechanism must be occurring.

Intermediate gating states have been studied in voltage-gated K^+ channels as well. Chapman et al. (1997) have observed subconductance states during activation of the Kv2.1 voltage-gated K^+ channel. However, as they pointed out, subconductance states do not necessarily represent states with altered pore structures. It is possible that they represent times when the channel rapidly opens and closes, which upon filtering yields the appearance of subconductance states. Recently, however, Zheng and Sigworth (1997) have shown, at least in the mutant Shaker K^+ channel they examined, the subconductance state must indeed have an altered pore structure since its selectivity among monovalent cations is different from that of the fully open state.

What types of cGMP-induced structural changes in the pore might give rise to changes in the divalent cation permeability? Our observation that the relative permeabilities of the bulky organic monovalent cations methylammonium and dimethylammonium do not change as a function of cGMP suggests that the proposed intermediate state has the same physical pore dimensions as the fully open state. Differences in selectivity between the intermediate state and the open state are therefore suggestive of differences in the detailed positioning of the divalent cation selectivity filter within the pore. E363 has been shown to be an integral part of this filter since removing this negative charge substantially reduces calcium block and permeation (Root and

MacKinnon, 1993; Eismann et al., 1994). The suggestion that this residue might be changing its position during the gating structural transitions (Fodor et al., 1997) leads to the possibility that this may be part of the explanation for the reduced divalent cation permeability of the intermediate state. However, channels made from the α subunit alone, with which most of the investigations of structural transitions in the pore have been made, do not show cGMP-dependent shifts in divalent cation permeability. It is possible that the same structural changes occur in the pores of both α and $\alpha\beta$ channels but that actual changes in selectivity only occur in the context of the $\alpha\beta$ pore. Alternatively, the $\alpha\beta$ pore may undergo cGMP-dependent structural changes distinct from those of the α pore.

While the stoichiometry of retinal heteromeric $\alpha\beta$ channels has not yet been determined, olfactory $\alpha\beta$ channels have been shown to exist in a 2:2 stoichiometry (Shapiro and Zagotta, 1998). If this were true for retinal channels as well, then half of the pore is constructed from the β P region, which is very different in sequence when compared with α . One particular notable difference is the glycine rather than glutamate at position 363 in the β sequence. A better understanding of how these sequence differences relate to the observed functional differences will be obtained by doing detailed chimeric analysis.

We find, as have others (Colamartino et al., 1991; Karpen et al., 1992), that Ca^{++} block of native rod cGMP-gated channels is cGMP-dependent, though in some cases this is a small effect. This could be due either to direct effects on gating (as is the case for Ni^{++}), or it could be due to a structural changes in the pore. There is no way to distinguish between these two mechanisms from data presented here since both effects lead to the other. Ca^{++} modulation via calmodulin or an endogenous modulator cannot explain the effect since it is reversible (data not shown) and since we specifically removed this modulation by washing the patch in a solution containing 1mM EDTA and 1mM EGTA prior to all experiments. If it were due to the same pore structural change

that alters divalent cation permeability, the cGMP-dependence of the two effects should be the same. We find that the extent of Ca^{++} block does indeed have the same cGMP-dependence as Ca^{++} permeability, which is suggestive but not proof that this effect may be due to an alteration in pore structure.

cGMP-dependent changes in Ca^{++} permeability should give rise to cGMP-dependent changes in the fractional Ca^{++} current through the channel. We have recently found that this is indeed the case, at least for the native rod channel (this thesis, chapter IV). In these experiments, a rod outer segment is placed under whole-cell voltage clamp and loaded with the calcium sensitive fluorescent dye fura-2 and caged cGMP. A xenon flash lamp is then used to release cGMP into the cytoplasm, which rapidly opens cGMP-gated channels, causing a current and a fluorescence change, both of which are measured. The fluorescence change per unit charge carried through the channel (the integral of the current measurement) reveals a quantity proportional to the fractional Ca^{++} current through the channel. Flashing the same cell with different light intensities (to release different concentrations of cGMP) reveals that the fractional Ca^{++} current increases as a function of cGMP concentration, as expected from the results presented here.

What physiological role might cGMP-dependent changes in Ca^{++} permeability play in photoreceptor function? Since photoreceptor physiology occurs at very low cGMP concentrations, one consequence of these observations is that the channel spends most of its time in intermediate gating states with significantly lower Ca^{++} permeability than the more typically studied fully open state. However, since the Ca^{++} permeability appears to reach a minimum (non-zero) value at very low cGMP concentrations, we would not expect the Ca^{++} permeability to change significantly during the normal physiology of a photoreceptor cell. If any effect does occur, it will cause the calcium current to decrease slightly more than expected as the channels close during a light stimulus, possibly extending the range of light-adaptation. In other types of cells where CNG channels are

present, however, cGMP (or cAMP) may reach much higher concentration levels, resulting in more significant physiological effects of cGMP-dependent Ca^{++} permeability.

Cone CNG channels are known to be more permeable to Ca^{++} than rod channels (Picones and Korenbrot, 1995; Frings et al., 1995; Haynes, 1995a). In particular, Picones and Korenbrot (1995) have shown that cone channels are 2.4-fold more Ca^{++} -permeable. It has been suggested that this difference partially accounts for the functional differences between the two cell types (Korenbrot, 1995). At saturating cGMP concentrations, we find that cone channels are 3.3-fold more Ca^{++} permeable than rod channels, consistent within experimental error with previous measurements. However, at cGMP concentrations more relevant to physiology, we find cone channels to have 7.4-fold greater Ca^{++} permeability, significantly larger since cone channels show smaller cGMP-dependent changes in divalent cation permeability than rod channels.

Reference List

- Bradley, J., Li, J., Davidson, N., Lester, H. A., and Zinn, K. (1994) Heteromeric olfactory cyclic nucleotide-gated channels: a subunit that confers increased sensitivity to cAMP. *Proc Natl Acad Sci USA* 91: 8890-4
- Butler, J. N. (1968) The thermodynamic activity of calcium ion in sodium chloride-calcium chloride electrolytes. *Biophys J* 8: 1426-33
- Chapman, M. L., VanDongen, H. M., and VanDongen, A. M. (1997) Activation-dependent subconductance levels in the drk1 K⁺ channel suggest a subunit basis for ion permeation and gating. *Biophys J* 72: 708-19
- Chen, T. Y., Peng, Y. W., Dhallan, R. S., Ahamed, B., Reed, R. R., and Yau, K. W. (1993) A new subunit of the cyclic nucleotide-gated cation channel in retinal rods. *Nature* 362: 764-767
- Cobbs, W. H., Barkdoll, A. E. 3d, and Pugh, E. N. Jr (1985) Cyclic GMP increases photocurrent and light sensitivity of retinal cones. *Nature* 317: 64-6
- Cobbs, W. H. and Pugh, E. N. Jr (1987) Kinetics and components of the flash photocurrent of isolated retinal rods of the larval salamander, *Ambystoma tigrinum*. *J Physiol* 394: 529-72
- Colamartino, G., Menini, A., and Torre, V. (1991) Blockage and permeation of divalent cations through the cyclic GMP-activated channel from tiger salamander retinal rods. *J Physiol* 440: 189-206
- Eismann, E., Muller, F., Heinemann, S. H., and Kaupp, U. B. (1994) A single negative charge within the pore region of a cGMP-gated channel controls rectification, Ca²⁺ blockage, and ionic selectivity. *Proc Natl Acad Sci USA* 91: 1109-13
- Fain, G. L., Lamb, T. D., Matthews, H. R., and Murphy, R. L. (1989 Sep) Cytoplasmic calcium as the messenger for light adaptation in salamander rods. *J Physiol* 416: 215-43
- Fodor, A. A., Black, K. D., and Zagotta, W. N. (1997) Tetracaine reports a conformational change in the pore of cyclic nucleotide-gated channels. *J Gen Physiol* 110: 591-600
- Frings, S., Seifert, R., Godde, M., and Kaupp, U. B. (1995) Profoundly different calcium permeation and blockage determine the specific function of distinct cyclic nucleotide-gated channels. *Neuron* 15: 169-79
- Furman, R. E. and Tanaka, J. C. (1990) Monovalent selectivity of the cyclic guanosine monophosphate-activated ion channel. *J Gen Physiol* 96: 57-82
- Hackos, D. H. and Korenbrot, J. I. (1997) Calcium modulation of ligand affinity in the cyclic GMP-gated ion channels of cone photoreceptors. *J Gen Physiol* 110: 515-528
- Hanke, W., Cook, N. J., and Kaupp, U. B. (1988) cGMP-dependent channel protein from photoreceptor membranes: single-channel activity of the purified and reconstituted protein. *Proc Natl Acad Sci USA* 85: 94-8

- Haynes, L. W. (1995a) Permeation and block by internal and external divalent cations of the catfish cone photoreceptor cGMP-gated channel. *J Gen Physiol* 106: 507-23
- Haynes, L. W. (1995b) Permeation of internal and external monovalent cations through the catfish cone photoreceptor cGMP-gated channel. *J Gen Physiol* 106: 485-505
- Haynes, L. W., Kay, A. R., and Yau, K. W. (1986) Single cyclic GMP-activated channel activity in excised patches of rod outer segment membrane. *Nature* 321: 66-70
- Hestrin, S. and Korenbrot, J. I. (1990) Activation kinetics of retinal cones and rods: response to intense flashes of light. *J Neurosci* 10: 1967-73
- Hille, B. (1992) *Ionic Channels of Excitable Membranes*. 2nd Ed. Sinauer Associates, Inc. Sunderland, MA.
- Ildefonse, M. and Bennett, N. (1991) Single-channel study of the cGMP-dependent conductance of retinal rods from incorporation of native vesicles into planar lipid bilayers. *J Membr Biol* 123: 133-47
- Karpen, J. W., Loney, D. A., and Baylor, D. A. (1992) Cyclic GMP-activated channels of salamander retinal rods: spatial distribution and variation of responsiveness. *J Physiol* 448: 257-74
- Koch, K. W., Cook, N. J., and Kaupp, U. B. (1987) The cGMP-dependent channel of vertebrate rod photoreceptors exists in two forms of different cGMP sensitivity and pharmacological behavior. *J Biol Chem* 262: 14415-21
- Korenbrot, J. I. (1995) Ca^{2+} flux in retinal rod and cone outer segments: differences in Ca^{2+} selectivity of the cGMP-gated ion channels and Ca^{2+} clearance rates. *Cell Calcium* 18: 285-300
- Korenbrot, J. I. and Miller, D. L. (1986) Calcium ions act as modulators of intracellular information flow in retinal rod phototransduction. *Neurosci Res Suppl* 4: S11-34
- Korschen, H G, Illing, M, Seifert, R, Sesti, F, Williams, A, Gotzes, S, Colvilee, C, Muller, F, Dose, A, Godde, M, Molday, L, Kaupp, U B, and Molday, R S (1995) A 240 kDa protein represents the complete β subunit of the cyclic nucleotide-gated channel from rod photoreceptors. *Neuron* 15: 627-636
- Lagnado, L., Cervetto, L., and McNaughton, P. A. (1992) Calcium homeostasis in the outer segments of retinal rods from the tiger salamander. *J Physiol* 455: 111-42
- Lewis, C. A. (1979) Ion-concentration dependence of the reversal potential and the single channel conductance of ion channels at the frog neuromuscular junction. *J Physiol* 286: 417-45
- Liman, E. R. and Buck, L. B. (1994) A second subunit of the olfactory cyclic nucleotide-gated channel confers high sensitivity to camp. *Neuron* 13: 611-21

- Liman, E. R., Tytgat, J., and Hess, P. (1992) Subunit stoichiometry of a mammalian K⁺ channel determined by construction of multimeric cDNAs. *Neuron* 9: 861-71
- Liu, D. T., Tibbs, G. R., and Siegelbaum, S. A. (1996) Subunit stoichiometry of cyclic nucleotide-gated channels and effects of subunit order on channel function. *Neuron* 16: 983-90
- Matthews, H. R., Fain, G. L., Murphy, R. L., and Lamb, T. D. (1990) Light adaptation in cone photoreceptors of the salamander: a role for cytoplasmic calcium. *J Physiol* 420: 447-69
- Menini, A. (1990) Currents carried by monovalent cations through cyclic GMP-activated channels in excised patches from salamander rods. *J Physiol* 424: 167-85
- Miledi, R. and Parker, I. (1984) Chloride current induced by injection of calcium into *Xenopus* oocytes. *J Physiol* 357: 173-83
- Miller, J. L. and Korenbrot, J. I. (1993a) In retinal cones, membrane depolarization in darkness activates the cGMP-dependent conductance. A model of Ca²⁺ homeostasis and the regulation of guanylate cyclase. *J Gen Physiol* 101: 933-60
- Miller, J. L. and Korenbrot, J. I. (1993b) Phototransduction and adaptation in rods, single cones, and twin cones of the striped bass retina: a comparative study. *Vis Neurosci* 10: 653-67
- Miller, J. L. and Korenbrot, J. I. (1994a) Differences in calcium homeostasis between retinal rod and cone photoreceptors revealed by the effects of voltage on the cGMP-gated conductance in intact cells. *J Gen Physiol* 104: 909-40
- Miller, J. L., Picones, A., and Korenbrot, J. I. (1994b) Differences in transduction between rod and cone photoreceptors: an exploration of the role of calcium homeostasis. *Curr Opin Neurobiol* 4: 488-95
- Nakatani, K. and Yau, K. W. (1988a) Calcium and light adaptation in retinal rods and cones. *Nature* 334: 69-71
- Nakatani, K. and Yau, K. W. (1988b) Calcium and magnesium fluxes across the plasma membrane of the toad rod outer segment. *J Physiol* 395: 695-729
- Perry, R. J. and McNaughton, P. A. (1991) Response properties of cones from the retina of the tiger salamander. *J Physiol* 433: 561-87
- Picco, C. and Menini, A. (1993) The permeability of the cGMP-activated channel to organic cations in retinal rods of the tiger salamander. *J Physiol* 460: 741-58
- Picones, A. and Korenbrot, J. I. (1995) Permeability and interaction of Ca²⁺ with cGMP-gated ion channels differ in retinal rod and cone photoreceptors. *Biophys J* 69: 120-7
- Picones, A. and Korenbrot, J. I. (1992) Permeation and interaction of monovalent cations with the cGMP-gated channel of cone photoreceptors. *J Gen Physiol* 100: 647-73
- Robinson, R. A. and Stokes, R. H. (1959) *Electrolyte Solutions*. Putterworth & Co. (Publishers) Ltd., London, England.

- Root, M. J. and Mackinnon, R. (1993) Identification of an external divalent cation-binding site in the pore of a cGMP-activated channel. *Neuron* 11: 459-66
- Ruiz, M. L. and Karpen, J. W. (1997) Single cyclic nucleotide-gated channels locked in different ligand-bound states [see comments]. *Nature* 389: 389-92
- Shapiro, M. S. and Zagotta, W. N. (1998) Subunit stoichiometry and arrangement of cloned heteromultimeric olfactory cyclic nucleotide-gated channels. Biophysical Society Meeting, Kansas City, MO.
- Sun, Z. P., Akabas, M. H., Goulding, E. H., Karlin, A., Siegelbaum, S. A., Sun, Z. P., Akabas, M. H., Goulding, E. H., Karlin, A., and Siegelbaum, S. A. (1996) Exposure of residues in the cyclic nucleotide-gated channel pore: P region structure and function in gating. Exposure of residues in the cyclic nucleotide-gated channel pore: P region structure and function in gating. *Neuron* 16: 141-9. 141-9
- Tanaka, J. C. (1993) The effects of protons on 3',5'-cGMP-activated currents in photoreceptor patches. *Biophys J* 65: 2517-23
- Tanaka, J. C., Furman, R. E., Cobbs, W. H., and Mueller, P. (1987) Incorporation of a retinal rod cGMP-dependent conductance into planar bilayers. *Proc Natl Acad Sci USA* 84: 724-8
- Torre, V., Matthews, H. R., and Lamb, T. D. (1986) Role of calcium in regulating the cyclic GMP cascade of phototransduction in retinal rods. *Proc Natl Acad Sci USA* 83: 7109-13
- Torre, V., Straforini, M., Sesti, F., and Lamb, T. D. (1992) Different channel-gating properties of two classes of cyclic GMP-activated channel in vertebrate photoreceptors. *Proc R Soc Lond B Biol Sci* 250: 209-15
- Wells, G. B. and Tanaka, J. C. (1997) Ion selectivity predictions from a two-site permeation model for the cyclic nucleotide-gated channel of retinal rod cells. *Biophys J* 127-40
- Zheng, J. and Sigworth, F. J. (1997) Selectivity changes during activation of mutant Shaker potassium channels. *J Gen Physiol* 110: 101-17
- Zimmerman, A. L. and Baylor, D. A. (1992) Cation interactions within the cyclic GMP-activated channel of retinal rods from the tiger salamander. *J Physiol* 449: 759-83
- Zimmerman, A. L. and Baylor, D. A. (1986) Cyclic GMP-sensitive conductance of retinal rods consists of aqueous pores. *Nature* 321: 70-2

Chapter IV

Direct Measurement of Fractional Calcium Current through Rod and Cone Photoreceptor cGMP-gated Channels

Abstract

Cyclic nucleotide-gated ion channels mediate the electrical response to light in both rod and cone vertebrate photoreceptor cells. These channels allow both monovalent and divalent cations to permeate under physiological conditions. Ca^{++} ions entering the cell through these channels modulates the gain and kinetics of the photoresponse and is essential for the process of adaptation. While the total current through the cGMP-gated channels is easily measured in an active photoreceptor cell, the fraction of this current that is carried by Ca^{++} has not previously been measured directly. In this study, we make the first direct measurements of fractional Ca^{++} current through native photoreceptor channels under physiological conditions. This is done by simultaneously measuring total current via whole-cell voltage clamp and Ca^{++} influx using fura-2 fluorescence immediately after rapidly activating the channels by photolysing caged 8-bromo cGMP. These measurements are calibrated by doing similar experiments under nonphysiological conditions where Ca^{++} is the only permeant cation present. We find that the fractional Ca^{++} current is 20-25% in rods and essentially 100% in cones when the channels are activated with physiological (low) cGMP concentrations. Surprisingly, we find that the fractional Ca^{++} current in rods is a function of [cGMP], and increases to a value of 33.9% at high cGMP concentrations. In contrast, the fractional Ca^{++} current in cones decreases as a function of [cGMP] – possibly due to the depletion of Ca^{++} in the disc-like membrane invaginations present only in cones. The observation that under physiological conditions the fractional Ca^{++} current is significantly larger in cones than in rods may offer an explanation of the much faster Ca^{++} dynamics in cones.

Keywords: retina, phototransduction, calmodulin, rod photoreceptor, fish

Introduction

Rod and cone photoreceptors of the vertebrate retina generate the electrical response to light by closure of ion channels gated by cGMP in the outer segment membrane (Fesenko et al., 1985; Haynes and Yau, 1990). This closure results in a hyperpolarization of the photoreceptor membrane, which leads to reduced secretion of neurotransmitter at the synapse. The photoreceptor cGMP-gated channel is also the major entrance pathway for calcium ions into the outer segment cytoplasm. Therefore, when these channels close during the response to light, calcium influx decreases while calcium efflux through the outer segment Na,Ca-K exchange pump remains the same, resulting in a light-dependent decline in the cytoplasmic free calcium concentration.

Intracellular calcium acts as a second messenger communicating information about the number of open channels to the internal biochemical machinery, affecting and gain and kinetics of the photoresponse (Korenbrod and Miller, 1986; Torre et al., 1986). If cytoplasmic Ca^{++} concentrations are prevented by manipulation of the solution bathing the cells, the process of light adaptation is blocked (Nakatani and Yau, 1988; Fain et al., 1989; Matthews et al., 1990). Several outer segment calcium binding proteins have been identified that modulate key parts of the phototransduction pathway (for review, Polans et al., 1996). Guanylyl cyclase activating protein (GCAP) binds calcium to activate guanylyl cyclase, which is involved in the resynthesis of cGMP during recovery and adaptation (Gorczyca et al., 1994; Palczewski et al., 1994), recoverin modulates the rate of rhodopsin phosphorylation and inactivation in a calcium-dependent manner (Dizhoor et al., 1991; Lambrecht and Koch, 1991; Kawamura et al., 1993), calmodulin (or a similar molecule) binds the cGMP-gated channel itself, altering its sensitivity to cGMP (Hsu and Molday, 1993; Gordon et al., 1995), and a fourth calcium-sensitive factor may be involved in modulating the gain of the activation cascade (Lagnado and Baylor, 1994).

Phototransduction in cones is fundamentally similar to that in rods. Many of the proteins involved in cone phototransduction has been identified as isoforms of the respective proteins in rods. However, cones are much less sensitive to light than rods, have much faster photoresponse kinetics, and show more robust adaptation features than rods. The detailed molecular differences that give rise to these physiological differences are not well understood, but it has been proposed that these differences, at least in part, are due to differences in calcium homeostasis between the two cell types (Miller and Korenbrot, 1994; Miller et al., 1994). Specifically, cGMP-gated channels of cones have a greater permeability to calcium than rod channels (Perry and McNaughton, 1991; Picones and Korenbrot, 1995; Frings et al., 1995), and the efflux of Ca^{++} through the exchanger is much faster in cones (Nakatani and Yau, 1989; Hestrin and Korenbrot, 1990; Perry and McNaughton, 1991). In addition, some of the Ca^{++} -sensitive elements of the cone phototransduction machinery may be better tuned to respond to physiological changes in Ca^{++} in cones than the respective proteins in rods (Koutalos et al, 1996; Hackos and Korenbrot, 1997; Rebrik and Korenbrot, 1997).

Given the extreme importance of calcium dynamics in the photoresponse, it is of great interest to define precisely how intracellular Ca^{++} concentration is controlled by the cGMP-gated channel. While the total current through the channels in the dark is easily measured in both rods and cones, the percentage of this current carried by calcium has not been directly measured. Indirect estimates have been made by examining the multiexponential decay of the exchange current following a bright light flash, which causes all the channels to close. This decay curve is then extrapolated back to the point where half of the channels have closed. Because of the fact that the exchanger has a fixed stoichiometry of 1 Ca^{++} ion per unit charge carried across the membrane, a calculation of the exchange current immediately after the channel closure allows an estimation of the calcium efflux through the outer segment membrane. Since the influx and efflux of calcium must be the same at equilibrium, the fractional calcium current through the

channel can be derived. Measurements of the fractional Ca^{++} flux through photoreceptor cGMP-gated channels using this technique have been made in both rods (18%; Nakatani and Yau, 1986) and cones (21%; Perry and McNaughton, 1991).

In this study, we make the first direct determinations of the fraction of current carried by calcium (Pf) through both the rod and cone cGMP-gated channels under physiological conditions. Using the fluorescent Ca^{++} indicator dye fura-2, we are able to directly measure Ca^{++} flux while simultaneously measuring ion current through the channel, providing us with a direct means to determine Pf under a variety of conditions. Furthermore, we show that Pf, at least in the rod channel, increases as a function of cGMP.

Materials and Methods

Materials. We obtained striped bass (*Morone saxatilis*) from Professional Aquaculture Services (Chico, CA) and tiger salamanders (*Ambystoma tigrinum*) from Charles Sullivan (Memphis, TN). Fura-2 was obtained from Molecular Probes, Inc. (Eugene, OR). Caged 8-bromo cGMP was kindly provided by Dr. Volker Hagen (Forschungsinstitut für Molekulare Pharmakologie, Berlin, Germany).

Photoreceptor Isolation. Methods of cell isolation are described in detail elsewhere (Miller and Korenbrot, 1993b,1994). Animals were dark adapted and retinas were isolated under infrared illumination. Single cones were obtained by mechanical dissociation of Striped Bass retinas maintained in a Ringer's solution consisting of (mM): 143 NaCl, 2.5 KCl, 5 NaHCO₃, 1 Na₂HPO₄, 1 CaCl₂, 1MgCl₂, 5 pyruvate, 10 HEPES, pH 7.5, osmotic pressure 309 mOsM. Rod outer segments were isolated by mechanical dissociation of tiger salamander retinas maintained in a Ringer's solution composed of (mM): 100 NaCl, 2 KCl, 5 NaHCO₃, 1 Na₂HPO₄, 1 CaCl₂, 1 MgCl₂, 5 pyruvate, 10 HEPES, pH 7.5, osmotic pressure 227 mOsM.

Solitary photoreceptors were then firmly attached to a glass coverslip (which made the bottom of the recording chamber) derivitized with either wheat germ agglutinin or concanavalin A (Picones and Korenbrot, 1992). Cells were visualized with an inverted microscope equipped with DIC optics and operated under infrared light. A suspension of photoreceptors in pyruvate Ringer's was placed on the coverslip and the cells were allowed to settle down and attach for 5 min. The bath solution was then exchanged with a Ringer's solution of the same composition, but in which pyruvate was isosmotically replaced with glucose.

Photometry. The single-cell microfluorimeter used in these experiments is illustrated in fig. 1. The instrument is basically an inverted microscope that operates under infrared illumination (830-900 nm), uses video cameras to visualize the cells, and is equipped with DIC optics (Differential Interference Contrast) to enhance contrast. Fura-2 fluorescence was excited with UV light produced by a 150 W xenon arc lamp. Clean 380nm light was obtained by passing this light through two cold mirrors followed by 10cm of 2M CuSO₄ (to remove infrared and red light) and the following filters: WG280, WG295T, 2xWG360, 7-51, and a 380nm interference bandpass filter. In addition, the excitation light was passed through a coiled, 1 mm core diameter silica fiber optic cable to “scramble” the fluorescence excitation light to achieve a more uniform and homogenous illumination of the cell being studied despite the use of an inherently inhomogenous arc lamp source {Ellis, 1985}. This light was then presented to a cell (which had previously been selected and placed into whole-cell voltage clamp) using a Nikon epi-fluorescence system and a Nikon UV-40 objective lens.

In conventional epi-fluorescence microscopes, the fluorescence light is collected with the same microscope objective used to observe the cell. This multifunction requires the use of several dichroic mirrors and beamsplitters, first to combine and then to separate the various optical beams required in the measurement. This is inefficient because a large fraction of the photons (> 80%) are lost due to reflection or refraction at each of these various elements. Combined with the unavoidable inefficiency due to the fact that fluorescence-emitted photons are scattered over a 2π solid angle, conventional epi-fluorescence microscopes use a very bright source to collect generally very dim images. We optimized the instrument (by improving the efficiency of collection of the emitted photons) to be able to use a dim fluorescence excitation light as possible in order to avoid premature uncaging of the caged cGMP necessary for these experiments. This was done by collecting the emitted light with a highly efficient custom-made water immersion three-lens compound objective (N.A. = 0.65) with a working distance of 2.8 mm. Since

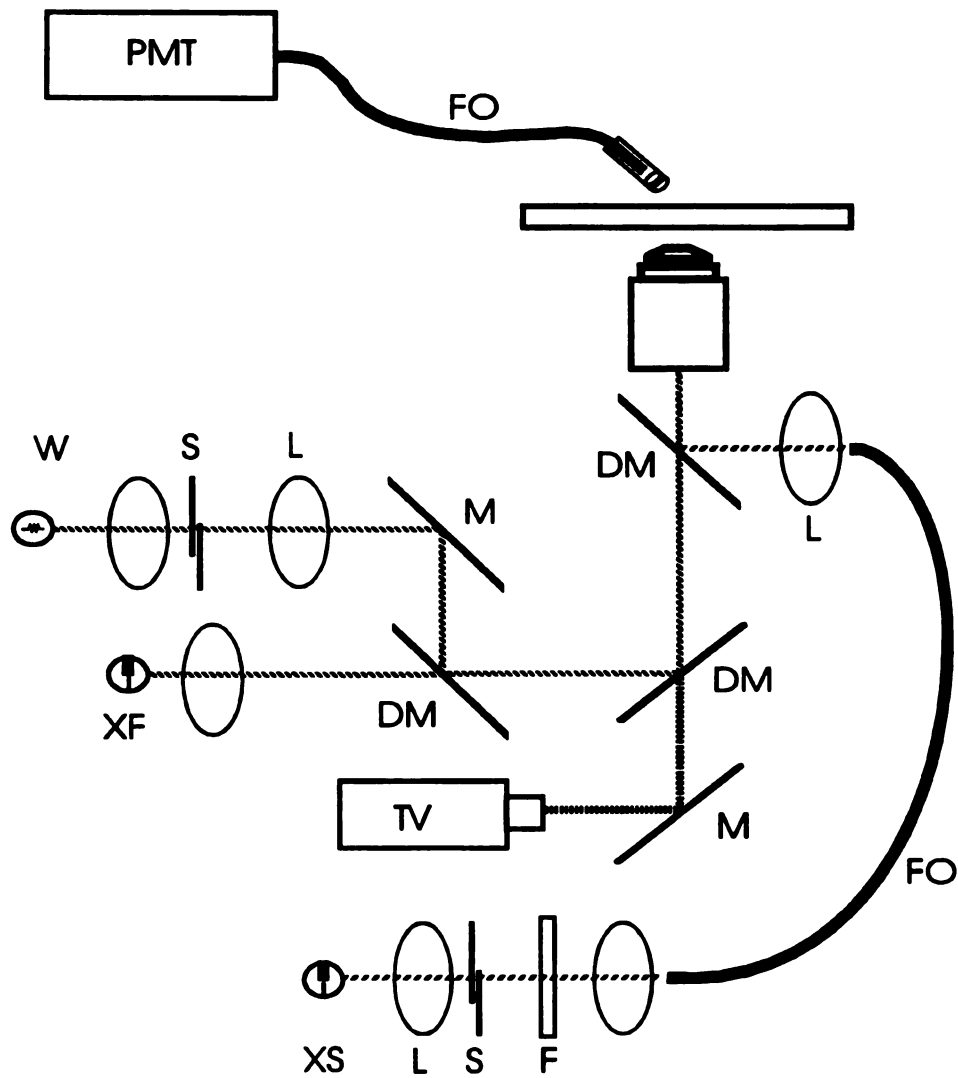


Figure 1. Schematic illustration of single cell microfluorometer. Three optical paths combine through mirrors (M) and dichroic mirrors (DM) to converge onto the microscope objective. The pathways bring light from any one of three sources: Tungsten (W), Xenon flash (XF), or Xenon steady (XS) source. Shutters (S), filters (F) and apertures in the optical paths select wavelengths and control presentation of light to the photoreceptor cells. The XS source that excites fluorescence is scrambled by a fiber optic (FO) to achieve homogeneous illumination. Fluorescence light emitted from the single cells is collected by a water immersion lens and transferred through a fiber optic (FO) to the photomultiplier tube (PMT). Cells are observed through the microscope objective with the aid of a TV camera.

this lens has a low magnification (2.5x), its light transmittance is higher than the 40x objective lens we used for imaging. The light from this lens is coupled directly onto the end of a single fiber optic (360 μm core diameter, N.A. = 0.47) which brings the light to a highly sensitive cooled (-20°C) photomultiplier tube (PMT) (Hamamatsu R943-02). Precise positioning of the collection lens was accomplished by directing light from an infrared laser diode back through the lens and imaging this light with the main oil-immersion objective. Light from a 200J xenon flash lamp (Strobex Model 278; Chadwick-Helmuth Co., El Monte, CA) required for photolysing caged-cGMP was also focusing by the 40x objective lens onto the cell. In order to prevent damage to the PMT during the 0.3 msec flash from the flash lamp, a high-speed shutter was placed in front of the PMT. The closure of this shutter was precisely timed by a microprocessor-controlled circuit which verified that the shutter closed correctly (by monitoring the PMT signal) before permitting the discharge of the flash lamp. The signal from the PMT was obtained by photon counting using a 50 msec counting window and calibrated against a fluorescence bead standard (Fluoresbrite carboxy BB 4.5 micron microspheres; Polysciences, Warrington, PA) to obtain fluorescence measurements in bead units (B.U.).

Electrical Recordings and Ionic Solutions. Tight-seal electrodes were made from aluminosilicate glass (1724; Corning Glass Works, Corning, NY) (1.5 x 1.0 mm, o.d. x i.d). We measured whole-cell membrane currents under voltage clamp at room temperature with a patch clamp amplifier (Axopatch-1D; Axon Instruments, Foster City, CA). Analog signals were low pass filtered below 200 Hz with an eight pole Bessel filter and were digitized on line simultaneously with the PMT signal at 100 Hz (FastLab; Indec, Capitola, CA).

Ionic Solutions. For rod experiments, we used the following intracellular pipette-filling solution (mM): 58 K-gluconate, 20 K-aspartate, 20 KCl, 20 NaCl, 0.5 MgCl_2 , 15 MOPS, pH 7.25, 228 mOsM osmotic pressure. We will refer to this solution as TSIS (tiger salamander intracellular solution). For the cone experiments, the following intracellular

solution was used (mM): 105 K-gluconate, 20 K-aspartate, 10 KCl, 20 NaCl, 0.5 MgCl₂, 15 MOPS, pH 7.25, 303 mOsM osmotic pressure. This solution will be referred to as FIS (fish intracellular solution). Generally, 2mM fura-2 and 50 μ M caged 8-bromo cGMP was added to these solutions immediately before starting the experiments. Caged 8-bromo cGMP solubilized in DMSO to make a 50mM stock solution, which was twice-serially diluted with intracellular solution and fura-2 in order to remove as much of the DMSO as possible since DMSO interfered with front-filling patch pipettes. This solution could be used within 3-4 hours before significant hydrolysis of the caged 8-bromo cGMP occurred.

Functions were fit to experimental data using least square minimization algorithms (Origin; MicroCal Software, Northampton, MA). Experimental errors are presented as standard deviations.

Results

Measurement of Calcium Flux through Rod Photoreceptor cGMP-gated Ion Channels

Rod cGMP-gated ion channels are highly permeable to calcium as well as other monovalent and divalent cations. While the total current can easily be determined, the fraction of the current carried by calcium has not been directly measured through channels of intact rods under physiological conditions. We chose to measure fractional calcium current (Pf) by simultaneously measuring both calcium influx using fura-2 fluorescence and total cGMP-dependent current using the whole-cell voltage clamp technique. After patch break-through, 5 min. was allowed for complete exchange of the intracellular solution with the solution inside the patch electrode, which contained 2 mM Fura-2 and 50 μ M caged 8-bromo cGMP. Since this solution did not contain ATP or GTP, any open cGMP-gated channels present in the dark closed with the timecourse of the solution exchange. Fura-2 was used at the high concentration of 2mM in order to eliminate the effects of any endogenous Ca⁺⁺ buffers that might be present in the outer segment.

The total fluorescence of a rod outer segment filled with 2mM Fura-2 at 380nm was found to be 3.48 ± 2.25 bead units (BU). A bright flash from the Xenon flash lamp released sufficient cGMP to generate a transient cGMP-dependent current of 400-1000 pA which activated within 5 msec of the flash and decayed exponentially with a timecourse of 5.4 ± 2.3 sec (fig. 2). To prevent damage to the photomultiplier tube (PMT), a shutter in front of the PMT was closed during the flash and immediately opened afterwards (see methods), introducing a short spike artifact into the fluorescence recording (fig. 2b). Once the channels were opened, the Fura-2 fluorescence at 380nm rapidly decreased to a minimum value within 2 sec, by which time the dye was completely saturated with Ca⁺⁺. This minimum fluorescence value is similar to the recorded fluorescence from a cell not loaded with Fura-2. Since the channels completely

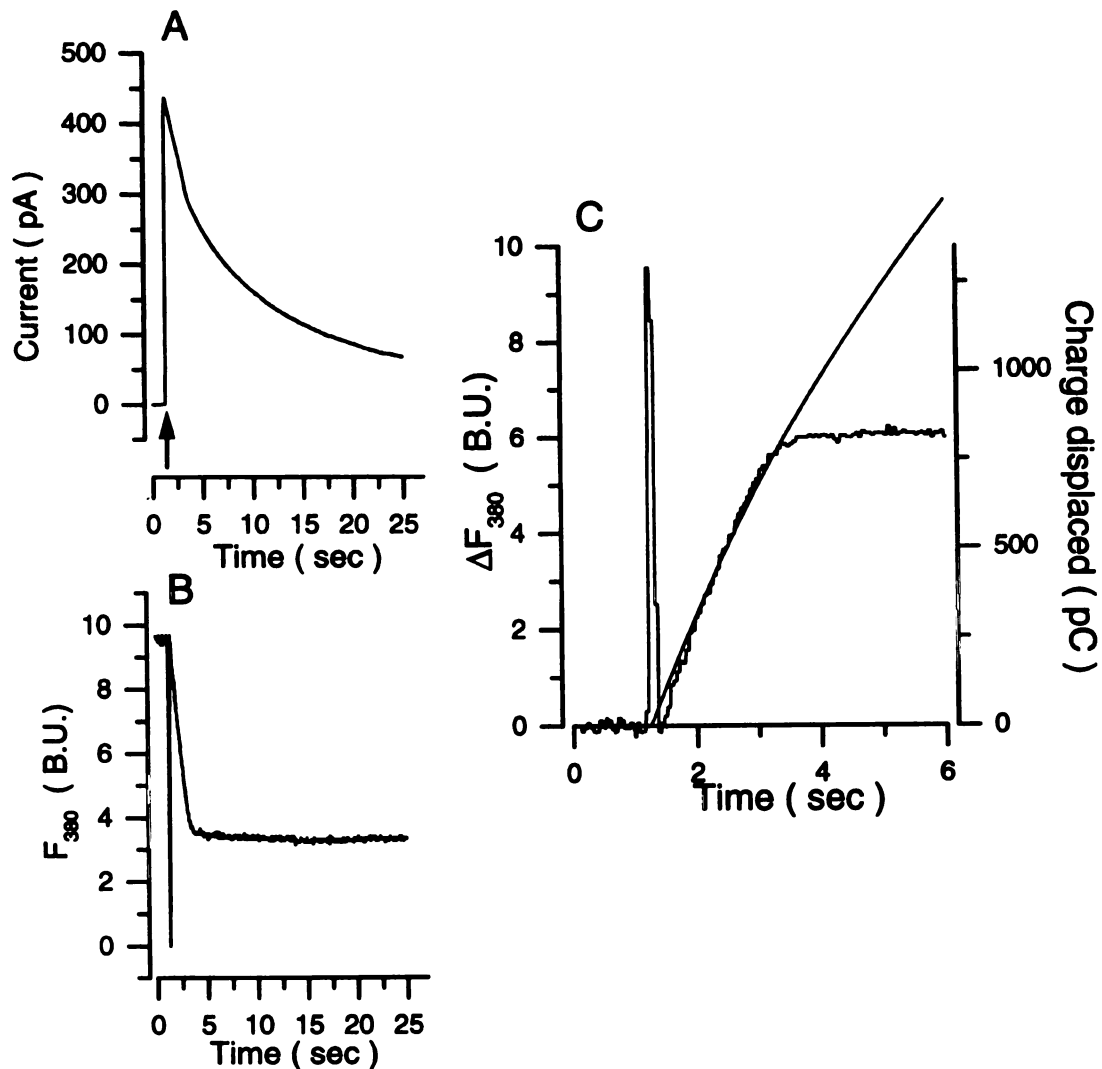


Figure 2. Measurement of Ca^{++} flux (f) through rod cGMP-gated channels. (A) A bright flash from a Xenon flash lamp is given at $t = 1.25$ sec., as indicated by arrow. Immediately after the flash, a large cGMP-dependent current (440 pA) is observed, which decays back to zero with an exponential timecourse of $\tau = 6.3$ sec. (B) Fluorescence measured at 380 nm is shown in bead units as a function of time. A shutter closes in front of the PMT immediately before the flash, causing the spike artifact at $t = 1.25$ sec. After the flash, Ca^{++} rapidly enters the cell, binds to fura-2, and causes the fluorescence at 380 nm to decrease. Fura-2 becomes completely saturated at 3.5 sec (2.25 sec after the flash). The remaining fluorescence after 3.5 sec is due to scatter of the fluorescence excitation light. (C) The change in fluorescence is plotted with the current integral (charge displaced across the membrane). Text equation 1 gives $f = 0.0074$ BU/pC for this dataset. Using the average f_{max} (see results), we find for this dataset $\text{Pf} = 65\%$.

closed within about 25 sec. after a flash, the Na,Ca-K exchange pump in the rod outer segment membrane was able to completely remove the Ca⁺⁺ from the cell within about 5 min., which enabled us to repeat the experiment on the same cell multiple times with identical results.

The interior of the cell acts as an integrator for the Ca⁺⁺ signal, while the measured whole-cell current reflects the instantaneous value the total current through the channel. To compare the two signals, we computed the integral of the whole-cell current and fit this function with the change in the fluorescence signal (fig. 2c) to obtain the proportionality constant f using the following equation:

$$f = \frac{\Delta F_{380}}{\int I_{total} dt} \quad (1)$$

where ΔF_{380} is the change in fluorescence over some time interval Δt , the I_{total} is the intergral over the same time interval of the total cGMP-dependent current. I_{total} itself is given by the equation:

$$I_{total} = I_{Ca} + I_{Mg} + I_{Na} + I_K \quad (2)$$

Recordings from x rods gave on average $f = 0.0038 \pm 0.00049$ B.U./pC (n=14). The quantity f is proportional to the fractional Ca⁺⁺ current shortly after the flash (while Fura-2 is a linear Ca⁺⁺ detector).

Calibration of the Calcium Flux Measurement in Rods

The actual value of the fractional Ca⁺⁺ current (Pf) is obtained only after calibration of the Ca⁺⁺ flux signal. We carried out this calibration measurement by doing the experiment under conditions where the whole-cell current was carried entirely by Ca⁺⁺. Under physiological conditions, Na⁺, K⁺, and Mg⁺⁺ permeate the channel in addition to Ca⁺⁺. Na⁺ was removed from both the intracellular and extracellular sides of the membrane and replaced with N-methyl D-glucamine (NMDG), which does not permeate either the rod or cone cGMP-gated channels (Stotz and Haynes, 1996). Since

replacing Na^+ with NMDG also interferes with the activity of the Na-K,Ca exchange pump, we exchanged the solutions immediately before (1-2 sec.) the flash using a perfusion system (see methods). An active exchange pump is necessary for these experiments since it removes any Ca^{++} that enters the cell through the leak current during the 5 min. internal exchange step. Mg^{++} was also removed from both sides of the membrane to eliminate Mg^{++} current. K^+ ions, however, could not be removed from the intracellular solution since this also interferes with the activity of the exchanger. Therefore, we used an intracellular solution containing 2.5 mM K^+ and an extracellular solution containing 10 mM K^+ , which defines a K^+ equilibrium potential of -35 mV (see methods). Under these conditions in the absence of extracellular Ca^{++} ions, the channel conducted no net current at -35 mV, as shown in fig. 3a. Therefore, the addition of 1 mM external Ca^{++} gave rise to a current carried entirely by Ca^{++} ions (fig. 3b). On average, this current was 230 ± 120 pA immediately following the flash, and decayed exponentially with a similar timecourse as the experiments done under physiological conditions (3.2 ± 1.8 sec.). Rapid Ca^{++} influx was also revealed by the fluorescence signal (fig. 3c). We then integrated the whole-cell current signal and fit this to the fluorescence signal to obtain the proportionality constant $fmax$ (fig. 3d) using the following equation:

$$fmax = \frac{\Delta F_{380}}{\int I_{Ca} dt} \quad (3)$$

The quantity $fmax$ represents the amount of fluorescence change caused by the influx of 1 pC of Ca^{++} ions. On average, we found $fmax = 0.0114 \pm 0.0012$ BU/pC ($n=5$). The fractional Ca^{++} current is obtained as $Pf = f/fmax$, which was found to be $33.9 \pm 4.3\%$ ($n=14$) for the rod cGMP-gated channel.

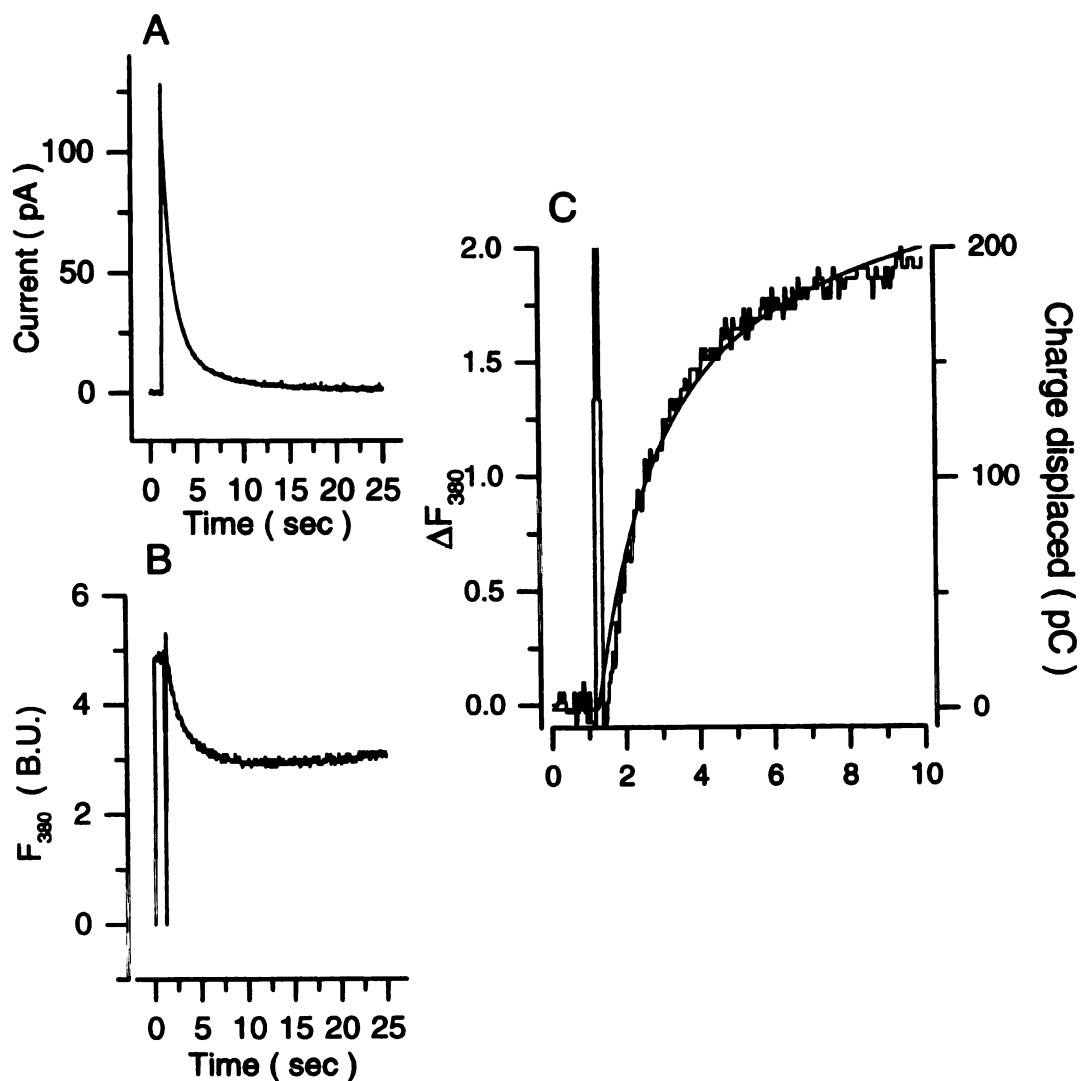


Figure 3. Calibration of the Ca²⁺ flux measurement in rods. Several seconds before the flash, a rod photoreceptor cell is bathed in a solution in which Ca²⁺ ions are the only permeable cations present. (A) At $t = 1.25$ sec., a flash from the Xenon flash lamp activates a cGMP-dependent current carried only by Ca²⁺. Immediately after the flash, this current is 127 pA, which rapidly decays with an exponential timecourse of $\tau = 1.8$ sec. (B) Fluorescence recorded at 380 nm. Immediately after the flash, fluorescence from fura-2 decreases as Ca²⁺ enters the cell. (C) The fluorescence change is plotted with the current integral. Eqn. 1 gives $f_{max} = 0.0101$ BU/pC for this dataset.

Fractional calcium current is a function of the cGMP concentration in rods.

Measurements in patches from rod outer segments membranes have revealed that the divalent cation permeability of these channels is dependent of the concentration of cGMP (this thesis, chapter III). To test whether this results in a cGMP-dependence of the fractional calcium current, we measured Pf as a function of flash intensity. The intensity of the Xenon flash lamp was varied by placing neutral density filters (0, 0.3, and 0.6 O.D.) immediately in front of the lamp. This allowed us to reduce the concentration of uncaged cGMP by either 50% (0.3 O.D.) or 75% (0.6 O.D.). The resulting flash-activated currents are shown in fig. 4a. The activation of these cGMP-dependent currents also resulting in a Ca⁺⁺ influx as shown in fig. 4b. The cGMP-dependent currents were integrated as a function of time and plotted with the fluorescence changes measured at 380 nm (fig. 4c). The change displaced axis was scales so that the 0 O.D. current integral fit the fluorescence change measured at that same flash intensity. Fluorescence changes recorded at either 0.3 or 0.6 O.D. were consistently below the current integral curves calculated at these flash intensities. This indicates that at low cGMP concentration (low flash intensity), the fractional Ca⁺⁺ current was significantly less than when the channel was under conditions of high (0 O.D.) cGMP concentrations. Using eqn. 1, we find on average $f_{0.O.D.} = 0.0038 \pm 0.00049$ BU/pC (n=14) (as before), $f_{0.3O.D.} = 0.0031 \pm 0.00042$ BU/pC (n=11), and $f_{0.6O.D.} = 0.0025 \pm 0.00045$ BU/pC (n=7). By applying eqn. 2 with a value for $f_{max} = 0.0114 \pm 0.0012$ BU/pC (n=5) (as calculated before), we find that $P_{f0.O.D.} = 33.9 \pm 4.3\%$, $P_{f0.3O.D.} = 27.4 \pm 3.7\%$, and $P_{f0.6O.D.} = 22.4 \pm 3.9\%$. Therefore, the fractional Ca⁺⁺ current in rods decreases as the cGMP concentration is lowered.

Measurement of Ca⁺⁺ flux through the cone cGMP-gated channel

Perry and McNaughton (1991) have shown by extrapolating the decay of the exchange current that the fractional Ca⁺⁺ current through the cone channel is 21%. Relative permeability measurements in excised patches have revealed that cone channels are 2.5-8

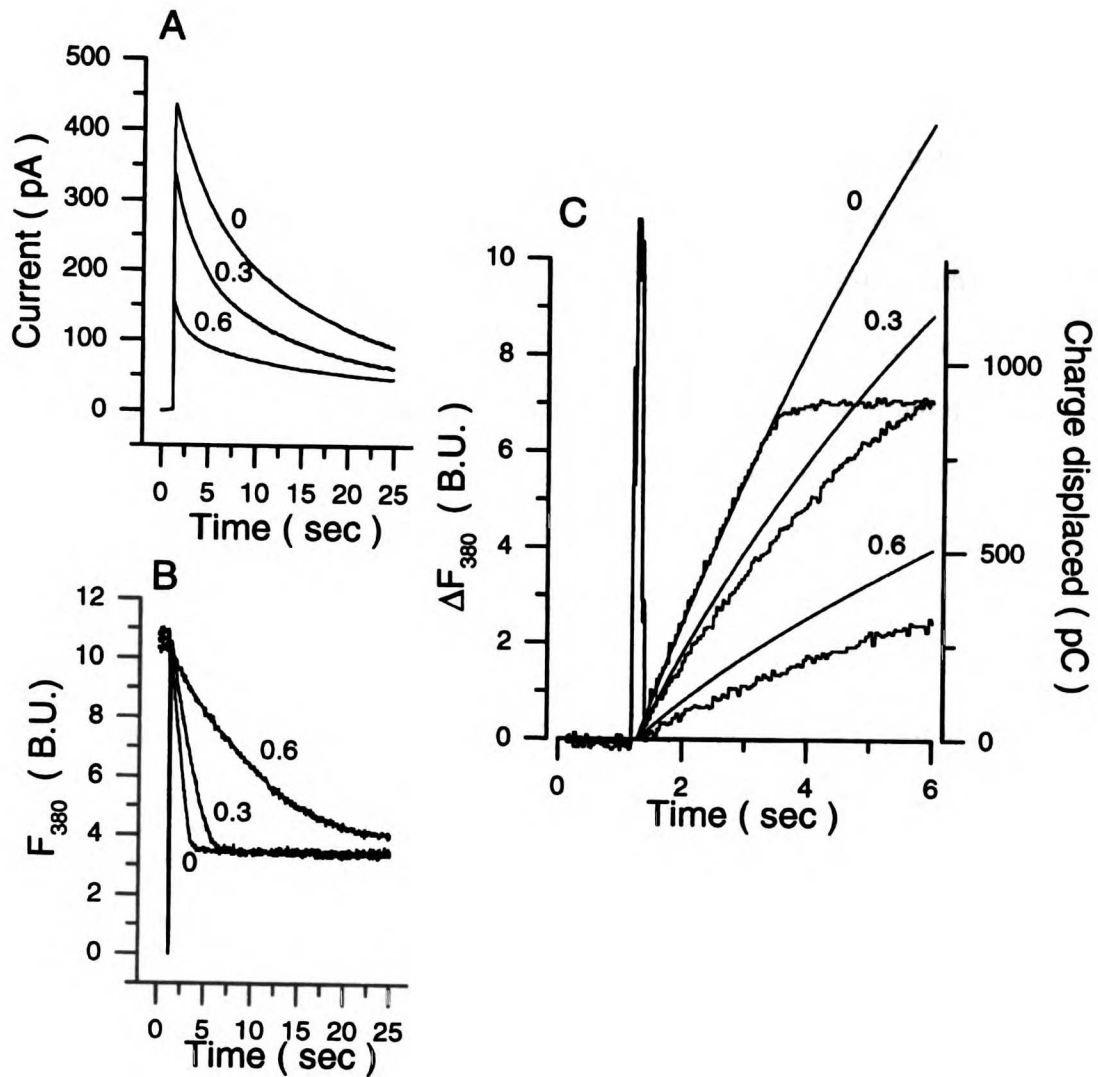


Figure 4. Dependence of Pf on flash intensity (cGMP concentration). (A) Flashes of different intensity (0 O.D., 0.3 O.D., or 0.6 O.D.) were successively applied to the same rod photoreceptor cell. The cell was allowed to recover for 3 min. after each flash. (B) Fluorescence measurements at 380 nm following flashes of different intensities (as indicated). As expected, Ca^{++} enters the cell more slowly when fewer cGMP-gated channels are opened. (C) Fluorescence changes plotted with current integrals (flash intensities are indicated in O.D.). The current integrals are scaled so that the 0 O.D. curve fits the fluorescence measured at 0 O.D. Fluorescence changes measured at either 0.3 O.D. or 0.6 O.D. are consistently smaller than expected from the current integrals. For this dataset, we find $\text{Pf}_{0\text{OD}} = 68\%$; $\text{Pf}_{0.3\text{OD}} = 60\%$; $\text{Pf}_{0.6\text{OD}} = 49\%$.

fold more Ca^{++} permeable than rod channels (Picones and Korenbrot, 1995; Frings et al., 1995; Haynes, 1995; this thesis, chapter III). In order to verify that cone channels have a greater Pf for Ca^{++} than rod channels, we chose to measure this quantity directly by recording fura-2 fluorescence and whole-cell current simultaneously from a single striped bass cone following an uncaging flash from a Xenon flash lamp. As in the rod experiments, cones were placed into whole cell voltage clamp and filled with 2mM fura-2 and 50mM caged 8-bromo cGMP. After waiting 5 min. to allow the cell's endogenous intracellular solution to become completely replaced with the pipette solution, the Xenon flash lamp was discharged, resulting in a rapid current increase (fig. 5a) and a subsequent decrease in the fura-2 fluorescence as measured at 380 nm (fig. 5b). We then integrated the current recording and scaled it with the change in fluorescence (fig. 5c). To obtain this match, the average scaling constant $f = 0.0019 \pm 0.00017$ BU/pC (eqn. 1).

These Ca^{++} flux measurements were then calibrated by doing similar flux measurements in the absence of Na^+ . As with rods, we replaced Na^+ on both sides of the membrane with NMDG. Since intracellular K^+ is necessary for the activity of the Na-Ca,K exchange pump (which kept intracellular Ca^{++} as low as possible before and between flashes), we added 10mM K^+ to the intracellular NMDG solution. Adding 2.5 mM K^+ to the extracellular solution and using a -35 mV holding potential prevented any net K^+ current through the channel (as was done in the rod experiments). Normal Ringer's was used as the extracellular solution until a few seconds before the flash, when this solution was rapidly exchanged with the NMDG extracellular solution. Under these conditions, the measured whole-cell cGMP-dependent current is only carried by Ca^{++} (fig. 6a). Using eqn. 3, we obtained on average $f_{\text{max}} = 0.0035 \pm 0.0019$ BU/pC for the cone channel. Thus, we find that $\text{Pf} = 55.1 \pm 5.0\%$ for the cone channel, which is larger than the rod Pf (measured using 0 O.D. flash intensity) by a factor of 1.63.

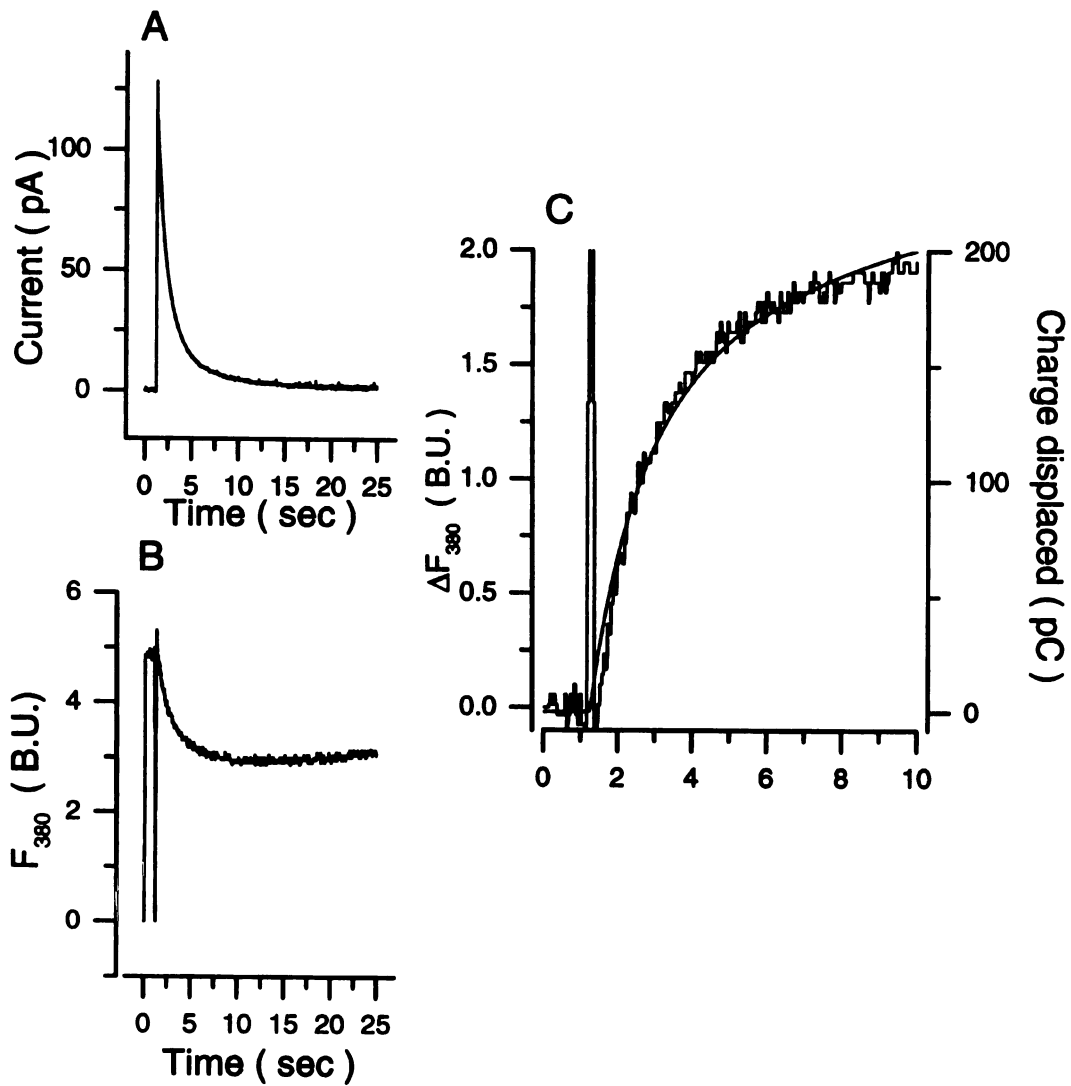


Figure 5. Measurement of Ca^{++} flux through cone cGMP-gated channels. (A) A flash from the Xenon flash lamp is applied to a cone photoreceptor at $t = 1.25$ sec. This activates a cGMP-dependent current of 425pA, which decays back toward zero with an exponential timecourse of $t = 1.4$ sec. (B) Fluorescence recorded at 380 nm during and after the flash. As Ca^{++} enters the outer segment, the fluorescence decreases and eventually starts to recover due to the much faster Na-Ca,K exchange pump in the cone outer segment membrane. (C) Change in fluorescence plotted with current integral. For this dataset, $f = 0.0016$ BU/pC.

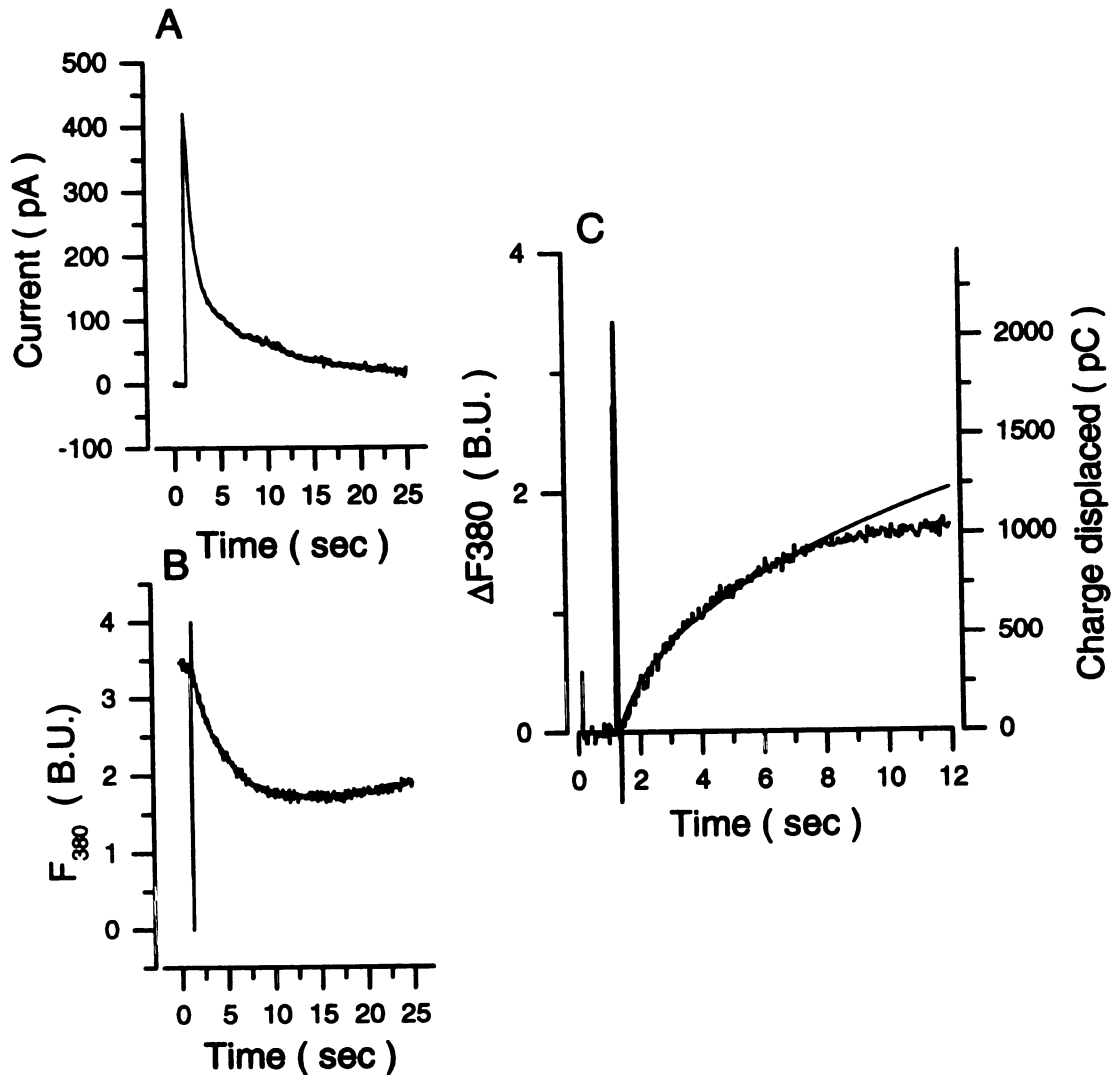


Figure 6. Calibration of the Ca²⁺ flux measurement in cones. This measurement was done with NMDG replacing all the permeant cations except for Ca²⁺. (A) The flash in this case activates a current carried only by Ca²⁺ ions (in this patch 61pA). This current rapidly decays with an exponential timecourse of $t = 0.56$ sec. (B) Fluorescence recording measured at 380 nm, showing the influx of Ca²⁺ into the outer segment. (C) Fluorescence changes plotted with current integral. Using eqn. 3 gives $f_{max} = 0.0036$ BU/pC for this patch.

Fractional calcium current decreases as a function of cGMP concentration in cones

While the permeability of Ca^{++} relative to Na^+ is a function of cGMP in patches excised from the cone outer segment membrane (this thesis, chapter III), the extent of this dependence is 1.55 fold, significantly lower than the extent of the cGMP-dependence in rods (3.42 fold). A consequence of this difference is that the cone channel is as much as 7.5-fold more permeable to Ca^{++} compared to the rod channel at low cGMP concentrations. To test whether of cone Pf is dependent on [cGMP] as it is in rods and to determine the difference between the rod and cone Pf at physiological cGMP concentrations, we determined the Pf at several different flash intensities. To vary the flash intensity, we placed different neutral density filters (0, 0.3, 0.5, 0.6 O.D.) in front of the Xenon flash lamp. Fig. 7a shows cGMP-dependent currents opened after flashes of different intensity and fig. 7b shows the resulting change in the fluorescence measured at 380 nm, indicating a Ca^{++} influx through the channels. We then determined the charge influx by integrating the current data, which was scaled with ΔF_{380} so that the current integral and ΔF curves measured with 0 O.D. flashes match each other (at times shortly after the flash), and plotted as a function of time (fig. 7c). Fluorescence curves for less intense flashes (0.3 and 0.6 O.D.) consistently showed larger than expected changes. This indicates that in cones, fractional calcium current increases as cGMP concentration is decreased, with is opposite in direction as seen in rod cells (fig. 4) and opposite in direction as expected from excised patch recordings of calcium permeability. We find on average $f_{0\text{O.D.}} = 0.0019 \pm 0.00017$ BU/pC (as before), $f_{0.3\text{O.D.}} = 0.0031 \pm 0.00063$ BU/pC, and $f_{0.6\text{O.D.}} = 0.0038 \pm 0.0011$. By applying eqn. 3 with a value for $f_{max} = 0.0035 \pm 0.0019$ BU/pC (as calculated before), we find that $\text{Pf}_{0\text{O.D.}} = 55.1 \pm 5.0\%$ (n=22), $\text{Pf}_{0.3\text{O.D.}} = 89.1 \pm 18\%$ (n=12), and $\text{Pf}_{0.6\text{O.D.}} = 110 \pm 31\%$ (n=3).

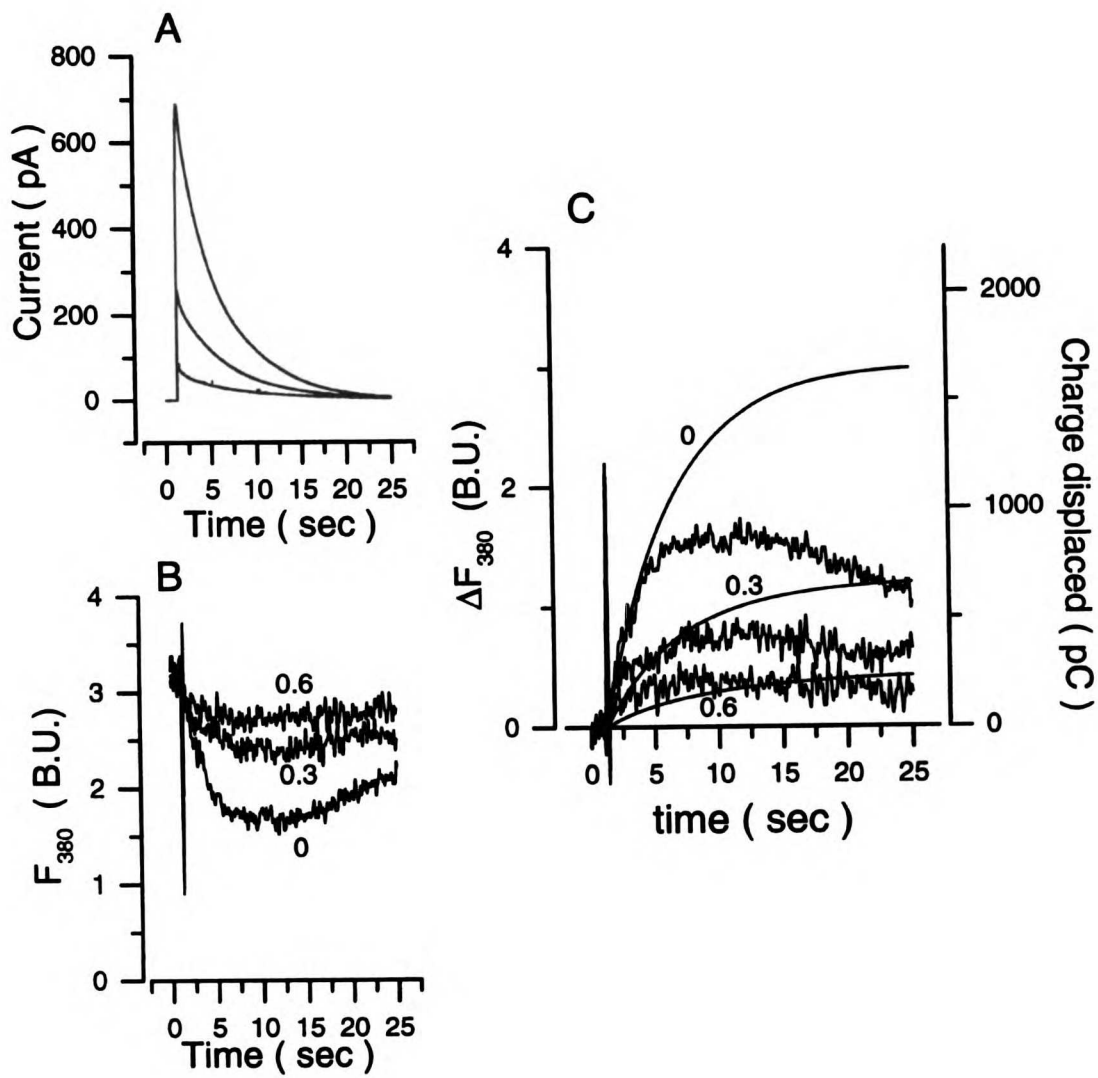


Figure 7. Dependence of Pf on flash intensity in cone photoreceptors. (A) Flashes of varying intensity (0 O.D., 0.3 O.D., 0.6 O.D.) from the Xenon flash lamp activate different amounts of cGMP-dependent current. (B) Fluorescence measured at 380 nm decreases after the flash, indicating Ca^{++} flowing into the cell. (C) Fluorescence changes plotted with current integrals. The current integrals are scaled so that the 0 O.D. curve fits the fluorescence measured at 0 O.D. Fluorescence changes measured at either 0.3 O.D. or 0.6 O.D. are consistently larger than expected from the current integrals. For this dataset, we find $Pf_{0OD} = 52\%$; $Pf_{0.3OD} = 74\%$; $Pf_{0.6OD} = 94\%$.

Discussion

We present here the first direct measurements of the fractional Ca^{++} flux through the rod and cone photoreceptor cGMP-gated channels. These measurements were done under physiological ionic conditions by measuring both the whole-cell current and calcium influx (by fura-2 fluorescence) simultaneously immediately after photolysing caged 8-bromo cGMP. We calibrated the measurements by doing additional experiments under conditions where the only possible net current was that carried by Ca^{++} . In this way, we determined the effective fluorescence change per unit charge transferred. From these data, we determined the fractional Ca^{++} current (Pf) for both channels. Furthermore, we found that Pf for both rod and cone channels varied with flash intensity (cGMP concentration). The Pf for the rod channel increased with [cGMP], as expected from measurements of Ca^{++} permeability as a function of [cGMP] (this thesis, chapter 2). In contrast, the cone Pf decreased with [cGMP], in opposite direction as expected from the permeability measurements.

Several conditions must be met in order to accurately determine the fractional Ca^{++} current using this technique (Neher, 1995). First, all of the Ca^{++} entering the cell must cause a fluorescence change. This must be true in both the f and f_{max} measurements. Specifically, each Ca^{++} ion that enters the cell is assumed to bind to a fura-2 molecule and add to the fluorescence signal in a linear manner. Any Ca^{++} ions that are either bound by intracellular Ca^{++} buffers or transported out of the cell through the Na-Ca,K exchange pump or through open cGMP-gated channels will not be counted in the fluorescence signal and will lead to an error in the value of the measured Pf. Furthermore, as fura-2 starts to become partially saturated, some of the Ca^{++} ions will remain free upon entering the cell, and will not be counted. We solved these potential problems by using a very high concentration of fura-2 (2mM), which out-competes the endogenous Ca^{++} buffer and lengthens the time before the dye becomes saturated. Before the dye is saturated, we assume that the free Ca^{++} concentration is very low (<100nM),

which also effectively prevents Ca^{++} efflux through the exchange pump. To verify that 2mM fura-2 was sufficient to solve these problems, we used 4mM fura-2 for several f_{max} measurements ($n = 6$) with identical results (data not shown). The point when the current integral diverges from the ΔF_{380} curve was taken as the time when fura-2 becomes partially saturated. Only data measured before this occurs was used in f and f_{max} calculations.

A second condition that must be met to obtain accurate Pf measurements is that the fluorescence from all fura-2 molecules in the cell must be measured with equal efficiency. This means that the fluorescence excitation and detection windows must be homogenous, a condition not always met in fluorescence microscopes. Part of this problem is due to the non-homogenous wandering image of the arc in the Xenon lamp. We solved this problem by passing the excitation light through coiled fiber optic to scramble the image of the arc (Ellis, 1985). In addition, we measured the intensity of a standard fluorescent bead (see methods) at different positions within the detection window, verifying that the efficiency of detection varied by $< 5\%$ within this window.

We found that the 8-bromo cGMP-dependent current following the discharge of the flash lamp was transient in nature, decaying to zero within several seconds (fig. 1). This can either be due to a decline in the sensitivity of the channel to 8-bromo cGMP or a rapid removal of 8-bromo cGMP from the outer segment cytoplasm. Experiments with photoreceptor cGMP-gated channels in excised patches indicate that the channel should not deactivate or desensitize within the timecourse of these experiments. However, the cGMP-sensitivities of rod and cone channels are known to be modulated by Ca^{++} and a calmodulin-like protein (Gordon et al., 1995; Hackos and Korenbrot, 1997). Therefore, a possible mechanism for the transient nature of the currents in these experiments is that upon entering the cell through the channel, Ca^{++} ions interact with the channel to cause a decrease in sensitivity to cGMP (resulting in a time-dependent closure of the channels).

However, we have found that the inactivation of the current after a flash occurs even in the absence of extracellular Ca^{++} (Hackos and Korenbrot, unpublished observations).

A more likely explanation is that 8-bromo cGMP is being removed in a time dependent manner from the cytoplasm. There are several ways that this could happen. One possibility is that the released 8-bromo cGMP is rapidly hydrolyzed of the cGMP phosphodiesterase (PDE) present in the outer segment. This, however, is very unlikely since the rate of hydrolysis of 8-bromo cGMP by this PDE is extremely slow (about 4000-fold slower than cGMP hydrolysis). We find that the rate of the time-dependent inactivation of the current following a flash is only slightly slower after 8-bromo cGMP release than after cGMP release. Another possibility is that 8-bromo cGMP, which is moderately membrane permeable, rapidly leaks out of the photoreceptor cell. We find, however, that the time-dependent inactivation occurs even in the presence of $50\mu\text{M}$ 8-bromo cGMP in the extracellular media. We believe that the inactivation is due to the presence of high concentrations of cGMP buffer within the outer segment. Cote and Brunnock (1993) have shown that rod photoreceptor outer segments have two classes of cGMP buffers, one of which is high affinity (60nM) with a capacity of $30\mu\text{M}$, and the other which is lower affinity ($6.6\mu\text{M}$) with a capacity of $78\mu\text{M}$. Thus, the total buffering capacity should be $108\mu\text{M}$. Since we are releasing subsaturating concentrations of 8-bromo cGMP (the rod channel's $K_{1/2}$ for 8-bromo cGMP is about $3\mu\text{M}$), we expect that at most $2\text{-}5\mu\text{M}$ is released per flash. This is much lower than the capacity of the cGMP buffers, and therefore at equilibrium should be essentially completely bound by the buffers, as we observe. This technique should allow the kinetic parameters of these buffers to be determined.

We find that the fractional Ca^{++} current in rods increases as a function of cGMP concentration (see fig. 8a). This is consistent with previous observations of relative divalent cation permeability in excised rod outer segment patches (this thesis, chapter III). In cones, however, Pf decreases as a function of [cGMP], which is in the opposite

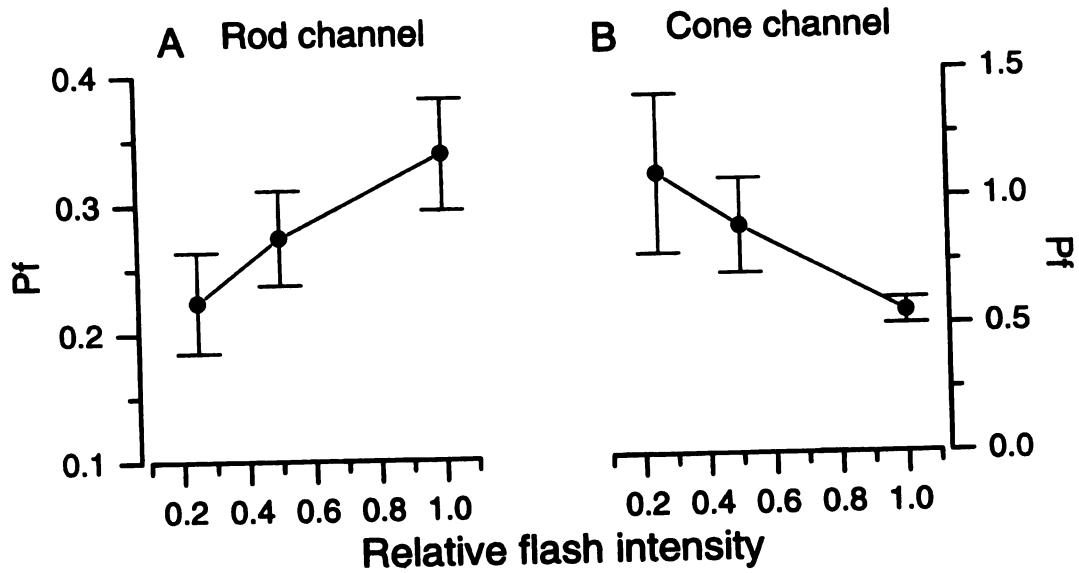


Figure 8. Average fractional calcium currents (Pf) through the cGMP-gated channel measured in either rod or cone photoreceptor cells at different flash intensities. The Pf of the rod channel is found to increase with flash intensity, while the cone Pf decreases as a function of flash intensity. Error bars indicate S.E.M.

direction as is seen in excised patches (fig. 8b). One possible explanation of this is that Ca^{++} may be rapidly depleted from the extracellular surface of the membrane. Even small amounts of Ca^{++} depletion would be expected to have large effects since Pf decreases very steeply with decreasing extracellular Ca^{++} (Frings et al., 1995). The greater the flash intensity, the greater the amount of Ca^{++} depletion will occur, giving rise to a cGMP-dependent decrease in Pf. This is expected to be a much larger problem in cones since the outer segment membrane is continuous with disc-like membrane invaginations, whereas in rods, and outer segment membrane is separate from the disc membranes. Therefore, the cone channel is expected to exist within the invaginations, where the diffusion of Ca^{++} is highly restricted. Thus, a local Ca^{++} depletion will occur in cones.

Under physiological conditions (at low cGMP concentrations), however, the outer segment current is only 50-100 pA, which may be too small for Ca^{++} depletion to occur. In these conditions, we find that in rods, Pf = 23% and in cones, Pf = 110%. Therefore, cone channels, which are effectively Ca^{++} channels, allow about 4-fold higher fractional Ca^{++} currents than rod channels. Our values of Pf for both rod and cone channels are larger than previous indirect measurements (rods 18%; Nakatani and Yau, 1986 and cones 21%; Perry and McNaughton, 1991). These discrepancies are most likely due to an underestimation of the exchange current following a bright flash stimulus. This is particularly true for cones since the fast part of the exchange timecourse may be almost as fast as the rate of inactivation of the channel, making it difficult to detect. The much larger Ca^{++} flux rate in cones may explain part of the physiological differences between rod and cone photoreceptor cells.

References

- Balasubramanian, S.; Lynch, J. W., and Barry, P. H. (1996) Calcium-dependent modulation of the agonist affinity of the mammalian olfactory cyclic nucleotide-gated channel by calmodulin and a novel endogenous factor. *J Membr Biol* 152: 13-23
- Chen, C. K.; Inglese, J.; Lefkowitz, R. J., and Hurley, J. B. (1995) Ca^{2+} -dependent interaction of recoverin with rhodopsin kinase. *J Biol Chem* 270: 18060-6
- Cote, R. H. and Brunnock M. A. (1993) Intracellular cGMP concentration in rod photoreceptors is regulated by binding to high and moderate affinity cGMP binding sites. *J Biol Chem* 268: 17190-8
- Dizhoor, A. M.; Ray, S.; Kumar, S.; Niemi, G.; Spencer, M.; Brolley, D.; Walsh, K. A.; Philipov, P. P.; Hurley, J. B., and Stryer, L. (1991) Recoverin: a calcium sensitive activator of retinal rod guanylate cyclase. *Science* 251: 915-8
- Ellis, G. W. (1985) Microscope illuminator with fiber optic source integrator. *J Cell Biol* 101: 83a
- Fain, G. L.; Lamb, T. D.; Matthews, H. R., and Murphy, R. L. (1989) Cytoplasmic calcium as the messenger for light adaptation in salamander rods. *J Physiol* 416: 215-43
- Fesenko, E E; Kolesnikov, S S, and Lyubarski, A L. (1985) Induction by cyclic GMP of cationic conductance in plasma membrane of retinal rod outer segments. *Nature* 313: 310-13
- Frings, S.; Seifert, R.; Godde, M., and Kaupp, U. B. (1995) Profoundly different calcium permeation and blockage determine the specific function of distinct cyclic nucleotide-gated channels. *Neuron* 15: 169-79
- Gorczyca, W. A.; Polans, A. S.; Surgucheva, I. G.; Subbaraya, I.; Baehr, W., and Palczewski, K. (1995) Guanylyl cyclase activating protein. A calcium-sensitive regulator of phototransduction. *J Biol Chem* 270: 22029-36
- Gordon, S. E.; Downing-Park, J., and Zimmerman, A. L. (1995) Modulation of the cGMP-gated ion channel in frog rods by calmodulin and an endogenous inhibitory factor. *J Physiol* 486: 533-46
- Gorodovikova, E. N.; Senin, I. I., and Philippov, P. P. (1994) Calcium-sensitive control of rhodopsin phosphorylation in the reconstituted system consisting of photoreceptor membranes, rhodopsin kinase and recoverin. *Febs Letters* 353: 171-2

- Hackos, D H and Korenbrot, J I. (1997) Calcium modulation of ligand affinity in the cGMP-gated ion channels of cone photoreceptors. *J Gen Physiol* 110: 515-28
- Haynes, L W and Yau, K.-W. (1990) Single channel measurement from the cGMP-activated conductance of catfish retinal cones. *J Physiol* 429: 451-81
- Haynes, L. W. (1995) Permeation and block by internal and external divalent cations of the catfish cone photoreceptor cGMP-gated channel. *J Gen Physiol* 106: 507-23
- Hestrin, S and Korenbrot, J I. (1990) Activation kinetics of retinal cones and rods: response to intense flashes of light. *J Neurosci* 10: 1967-1973
- Hsu, Y. T. and Molday, R. S. (1993) Modulation of the cGMP-gated channel of rod photoreceptor cells by calmodulin. *Nature* 361: 76-9
- Kawamura, S. (1993) Rhodopsin phosphorylation as a mechanism of cyclic GMP phosphodiesterase regulation by S-modulin. *Nature* 362: 855-7
- Korenbrot, J. I. and Miller, D. L. (1986) Calcium ions act as modulators of intracellular information flow in retinal rod phototransduction. *Neurosci Res Suppl* 4: S11-34
- Koutalos, Y. and Yau, K. W. (1996) Regulation of sensitivity in vertebrate rod photoreceptors by calcium. *Trends Neurosci* 19: 73-81
- Lagnado, L and Baylor, D A. (1994) Calcium controls light-triggered formation of catalytically active rhodopsin. *Nature* 367: 173-177
- Lambrecht, H. G. and Koch, K. W. (1991) A 26 kd calcium binding protein from bovine rod outer segments as modulator of photoreceptor guanylate cyclase. *EMBO* 10: 793-8
- Matthews, H. R.; Fain, G. L.; Murphy, R. L., and Lamb, T. D. (1990) Light adaptation in cone photoreceptors of the salamander: a role for cytoplasmic calcium. *J Physiol* 420: 447-69
- Miller, J. L. and Korenbrot, J. I. (1993) Phototransduction and adaptation in rods, single cones, and twin cones of the striped bass retina: a comparative study. *Vis Neurosci* 10: 653-67
- Miller, J. L. and Korenbrot, J. I. (1994) Differences in calcium homeostasis between retinal rod and cone photoreceptors revealed by the effects of voltage on the cGMP-gated conductance in intact cells. *J Gen Physiol* 104: 909-40

- Miller, J. L.; Picones, A., and Korenbrot, J. I. (1994) Differences in transduction between rod and cone photoreceptors: an exploration of the role of calcium homeostasis. *Curr Opin Neurobiol* 4: 488-95
- Nakatani, K. and Yau, K. W. (1986) Calcium and Magnesium fluxes across the plasma membrane of the toad rod outer segment. *J Physiol* 395: 695-729
- Nakatani, K. and Yau, K. W. (1988) Calcium and light adaptation in retinal rods and cones. *Nature* 334: 69-71
- Nakatani, K. and Yau, K. W. (1989) Sodium-dependent calcium extrusion and sensitivity regulation in retinal cones of the salamander. *J Physiol* 409: 525-48
- Neher, E. (1995) The use of fura-2 for estimating Ca buffers and Ca fluxes. *Neuropharm* 34: 1423-42
- Palczewski, K.; Subbaraya, I.; Gorczyca, W. A.; Helekar, B. S.; Ruiz, C. C.; Ohguro, H.; Huang, J.; Zhao, X.; Crabb, J. W.; Johnson, R. S., and et al. (1994) Molecular cloning and characterization of retinal photoreceptor guanylyl cyclase-activating protein. *Neuron* 13: 395-404
- Perry, R J and McNaughton, P A. (1991) Response properties of cones of the retina of the tiger salamander. *J Physiol* 433: 561-587
- Picones, A. and Korenbrot, J. I. (1992) Permeation and interaction of monovalent cations with the cGMP-gated channel of cone photoreceptors. *J Gen Physiol* 100: 647-73
- Picones, A. and Korenbrot, J. I. (1995) Permeability and interaction of Ca²⁺ with cGMP-gated ion channels differ in retinal rod and cone photoreceptors. *Biophys J* 69: 120-7
- Polans, A.; Baehr, W., and Palczewski, K. (1996) Turned on by Ca²⁺! The physiology and pathology of Ca(2+)-binding proteins in the retina. *Trends Neurosci* 19: 547-54
- Rebrik, T. and Korenbrot, J.I. (1997) cGMP-gated conductance in intact outer segments of cone photoreceptors with an electropermeabilized inner segment. *Investig. Ophthalmol Vis Sci* 38: S722 (Abst.).
- Schnapf, J. L.; Kraft, T. W.; Nunn, B. J., and Baylor, D. A. (1988) Spectral sensitivity of primate photoreceptors. *Vis Neurosci* 1: 255-61
- Stotz, S. C. and Haynes, L. W. (1996) Block of the cGMP-gated cation channel of catfish rod and cone photoreceptors by organic cations. *Biophys J* 71: 3136-47

Torre, V.; Matthews, H. R., and Lamb, T. D. (1986) Role of calcium in regulating the cyclic GMP cascade of phototransduction in retinal rods. *Proc Nat Acad Sci USA* 83: 7109-13

Chapter V
Summery and Conclusions

Rod and cone photoreceptor cells differ in their physiological roles and properties. Rods are designed for low level light detection, and therefore sacrifice response kinetics for enhanced sensitivity. Cones, in contrast, are designed to be able to rapidly detect contrast differences in an image despite large amounts of background light. Cones are therefore much less sensitive to light, have faster response kinetics, and have much more robust adaptation abilities than rods. Understanding what molecular differences between the two cell types give rise to these important physiological differences has been the motivation for this thesis work.

While the basic mechanism for phototransduction is thought to be the same in cones as in rods, the detailed molecular properties of the enzymes involved in cone phototransduction have proved very difficult to determine. This is mostly due to the difficulty of obtaining biochemical quantities of the cone enzymes due to the lack of a good biochemical preparation of cone outer segments. Patch clamp technology, however, allows the investigation of a subset of the cone molecules at the single-cell level. In particular, the cone cGMP-gated channel can be readily studied.

I've chosen to make a detailed comparison between the rod and cone photoreceptor cGMP-gated channels in the hopes of finding functional differences that might give rise to part of the physiological difference between the cell types. In particular, I have focused on the interaction between the channel and Ca^{++} ions, since differences in Ca^{++} homeostasis have been proposed to be important in defining rod-cone differences (Miller and Korenbrot, 1994; Miller et al., 1994). There are four aspects of the channel's interaction with Ca^{++} that I have examined in this thesis. 1) Ca^{++} -calmodulin modulation of the $K_{1/2}$ for cGMP binding (chapter II); 2) Relative Ca^{++} permeability (chapter III); 3) Voltage-dependent Ca^{++} block of the pore (chapter III); 4) Fractional Ca^{++} current through the channel under physiological conditions (chapter IV).

I have found that the cone channel, like the rod channel, is modulated by intracellular Ca^{++} (chapter II). This modulation is dependent on a small molecule that remains attached to the patch in the presence of Ca^{++} , but is rapidly released from the

Rod and cone photoreceptor cells differ in their physiological roles and properties. Rods are designed for low level light detection, and therefore sacrifice response kinetics for enhanced sensitivity. Cones, in contrast, are designed to be able to rapidly detect contrast differences in an image despite large amounts of background light. Cones are therefore much less sensitive to light, have faster response kinetics, and have much more robust adaptation abilities than rods. Understanding what molecular differences between the two cell types give rise to these important physiological differences has been the motivation for this thesis work.

While the basic mechanism for phototransduction is thought to be the same in cones as in rods, the detailed molecular properties of the enzymes involved in cone phototransduction have proved very difficult to determine. This is mostly due to the difficulty of obtaining biochemical quantities of the cone enzymes due to the lack of a good biochemical preparation of cone outer segments. Patch clamp technology, however, allows the investigation of a subset of the cone molecules at the single-cell level. In particular, the cone cGMP-gated channel can be readily studied.

I've chosen to make a detailed comparison between the rod and cone photoreceptor cGMP-gated channels in the hopes of finding functional differences that might give rise to part of the physiological difference between the cell types. In particular, I have focused on the interaction between the channel and Ca^{++} ions, since differences in Ca^{++} homeostasis have been proposed to be important in defining rod-cone differences (Miller and Korenbrot, 1994; Miller et al., 1994). There are four aspects of the channel's interaction with Ca^{++} that I have examined in this thesis. 1) Ca^{++} -calmodulin modulation of the $K_{1/2}$ for cGMP binding (chapter II); 2) Relative Ca^{++} permeability (chapter III); 3) Voltage-dependent Ca^{++} block of the pore (chapter III); 4) Fractional Ca^{++} current through the channel under physiological conditions (chapter IV).

I have found that the cone channel, like the rod channel, is modulated by intracellular Ca^{++} (chapter II). This modulation is dependent on a small molecule that remains attached to the patch in the presence of Ca^{++} , but is rapidly released from the

patch when Ca^{++} is brought below about 1 μM in concentration. Once this molecule is removed from the patch, purified calmodulin will cause a Ca^{++} -dependent modulation of the $K_{1/2}$ for cGMP, but not to the same extent (in cones) as the endogenous modulator. Ca^{++} modulation of rod and cone channels is similar, except that in rods, a much lower Ca^{++} concentration is required to release the modulator (Gordon et al., 1995).

Cone cGMP-gated channels have a larger relative Ca^{++} permeability than rod channels (Picones and Korenbrot, 1995; Haynes, 1995; Frings et al., 1995). I have found that this difference is in fact 7.5-fold, much larger than has previously been measured since other investigators did not take into account cGMP-dependent changes in Ca^{++} permeability (chapter III). The observation that Ca^{++} permeability is cGMP-dependent also reveals interesting information about the gating mechanism of cGMP-gated channels. While divalent cation permeability was found to change as a function of [cGMP], the permeabilities of several monovalent cations of different sizes (Cs^+ , NH_4^+ , methylammonium, and dimethylammonium) were found to be independent of cGMP concentration. Furthermore, while recombinant bovine rod cGMP-gated channels made from both α and β subunits showed cGMP-dependent Ca^{++} permeability, channels made from only α subunits showed no cGMP-dependence of its Ca^{++} permeability. These results suggest that in native cGMP-gated channels, there must be an intermediate gating state present at low cGMP concentrations that has low divalent cation permeability, but the same interactions with monovalent cations and overall pore dimensions as the fully open state.

While the observation that the relative Ca^{++} permeability of the cone channel is much larger than that of the rod channel is suggestive of an important rod-cone difference, the quantity that is most important for the physiology of the cell is the actual Ca^{++} current through the channel. Since cones and rods have similar outer segment membrane currents in the dark, if cones have a larger Ca^{++} current than rods, then they must have a larger fractional Ca^{++} current. I have found that this is indeed the case (chapter IV). By making the first direct measurements of fractional Ca^{++} current (Pf) in

both rod and cone photoreceptors using simultaneous whole-cell current and single-cell fluorescence measurements, I find that in rods, $P_f = 23\%$, and in cones, $P_f = 110\%$. Thus, the cone cGMP-gated channel is essentially a Ca^{++} channel under physiological conditions.

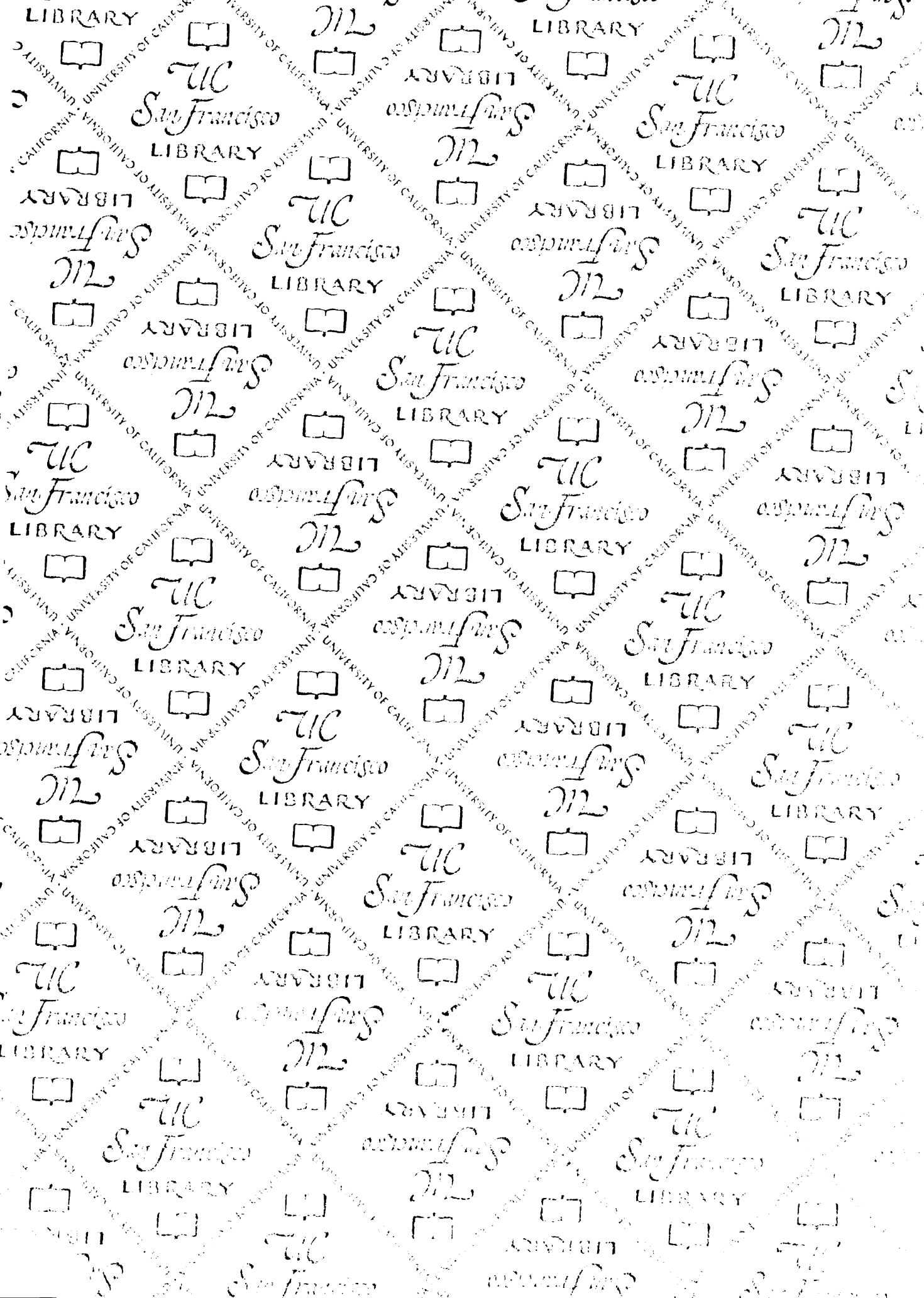
Taking my results together suggests that differences between the rod and cone cGMP-gated channels may indeed play a role in defining the physiological differences between the two cell types. A greater Ca^{++} flux through the cone channel means that light-dependent changes in intracellular Ca^{++} will be faster and larger in cones than in rods. This should lead to a faster photoresponse timecourse (since guanylyl cyclase will become activated more rapidly), and to greater adaptation abilities in cones, as is observed. Also, the fact that the cone channel is more readily modulated by Ca^{++} (since the Ca^{++} -dependence of this modulation is closer to the physiological range of Ca^{++} concentrations) may further enhance the cones adaptation abilities.

However, mathematical modeling of the rod and cone photoresponses indicates that differences between the rod and cone cGMP-gated channels cannot fully explain the known physiological differences. Therefore, other molecular differences must be present, such as a greater rate of transducin inactivation. Eventually, the technology will become available to study the activities of all the phototransduction components in cones, enabling a better understanding of the molecular mechanisms that give rise to the rod-cone differences.

References

- Frings, S.; Seifert, R.; Godde, M., and Kaupp, U. B. (1995) Profoundly different calcium permeation and blockage determine the specific function of distinct cyclic nucleotide-gated channels. *Neuron* 15: 169-79
- Gordon, S. E.; Downing-Park, J., and Zimmerman, A. L. (1995) Modulation of the cGMP-gated ion channel in frog rods by calmodulin and an endogenous inhibitory factor. *J Physiol* 486: 533-46
- Haynes, L. W. (1995) Permeation and block by internal and external divalent cations of the catfish cone photoreceptor cGMP-gated channel. *J Gen Physiol* 106: 507-23
- Miller, J. L. and Korenbrot, J. I. (1994) Differences in calcium homeostasis between retinal rod and cone photoreceptors revealed by the effects of voltage on the cGMP-gated conductance in intact cells. *J Gen Physiol* 104: 909-40
- Miller, J. L.; Picones, A., and Korenbrot, J. I. (1994) Differences in transduction between rod and cone photoreceptors: an exploration of the role of calcium homeostasis. *Curr Opin Neurobiol* 4: 488-95
- Picones, A. and Korenbrot, J. I. (1995) Permeability and interaction of Ca^{2+} with cGMP-gated ion channels differ in retinal rod and cone photoreceptors. *Biophys J* 69: 120-7

UNIVERSITY OF CALIFORNIA LIBRARY



For reference

Not to be taken from the room.

